UNIVERSITY OF TRENTO - Italy

International PhD Program in Biomolecular Sciences

Centre for Integrative Biology

XXVII Cycle

Investigation of the Structural and Molecular Substrate of Atrial Fibrillation

Tutor

Prof. Michela Alessandra Denti

Centre for Integrative Biology (CIBIO)

Advisor

Dr. Flavia Ravelli

Department of Physics - University of Trento

Ph.D. Thesis of

Laura Avogaro

Centre for Integrative Biology (CIBIO)

Academic Year 2014-2015

Declaration of authorship

I confirm that this is my own work and the use of all material from other sources has been properly and fully acknowledged.

Signed 

“You never know how strong you are…
until being strong is the only choice you have”

TABLE OF CONTENTS

LIST OF ABBREVIATIONS 6

ABSTRACT 8

CHAPTER 1. INTRODUCTION 11

Atrial Fibrillation: an overview 11
Mechanisms of AF 13
Basis of the cardiac action potential 13
Pathophysiology of AF 13
Atrial remodeling 15
Electrical remodeling 15
Structural remodeling 17
Genetic contributors to atrial fibrillation 18
Atrial fibrosis & Atrial fibrillation 21
Molecular mechanisms leading to atrial fibrosis 22
Extracardiac factors involved in atrial fibrosis 24
Extracellular matrix remodeling in atrial fibrosis: the collagen fibers network 26
The collagen fibers network of the heart: structural architecture 26
The collagen fibers network of the heart: synthesis, composition and regulation 27
MiRNAs & Atrial Fibrillation 30
Biogenesis and biological action of miRNAs 30
MiRNAs expression profile in the heart 32
Functions of miRNAs in AF 32
MiRNAs involved in electrical remodeling 32
MiRNAs involved in structural remodeling 34

AIM OF THE STUDY 37

BIBLIOGRAPHY 39

CHAPTER 2. STRUCTURAL CHARACTERIZATION 58

2.1 Quantification of collagen content and intramural distribution in human atrial tissue samples by Picrosirius red staining 60

Materials and methods 60
Human tissue collection and processing 60
Picrosirius red staining 60
Imaging and quantification of fibrosis 61
Statistical analysis 62
Results 63
Intramural profile of fibrotic content in the whole population 63
Comparison of the intramural profile in AF and SR patients 65
Discussion 67
Bibliography 70

2.2 Quantification of collagen fiber orientation and scale dimension in human atrial tissue samples by Non-linear Optical imaging 74

Materials and methods……74
Human tissue collection and preparation…..……..... 74
Non-linear Optical imaging.....74
Image processing and spectral analysis.....76
Statistical analysis.....78
Results..... 79
Properties of collagen network in AF compared to SR patients…….……..79
Depth-profile in the sub-epicardial layers in AF compared to SR patients..81
Discussion..... 84
Bibliography 86

CHAPTER 3. MOLECULAR CHARACTERIZATION 87

3.1 Determination of the most suitable reference genes for miRNAs' data normalization……..…….……...89

Materials and methods 89
Patient sample..…….……..……...…….……89
Human tissue processing and RNA isolation..…….....…….……..89
Selection of candidate reference genes.....…….....…..…….……....90
Reverse transcription qRT-PCR (RT-qPCR)..…..……90
Data analysis and software-based selection of endogenous reference gene…91
Results.....93
Quantity and integrity…. ……. …..……..……...93
Expression stability of the candidate reference genes-determination of the most suitable reference genes..…....……..……..93
Discussion.....99
Bibliography…..……..102

3.2 MiRNAs expression profiles in AF compared to SR patients..... 106

Materials and methods ..... .106
Patient samples…..…..…….……..……106
Human tissue processing and RNA isolation.…..……106
Selection of AF-related miRNAs..…….……..……...106
Reverse transcription qRT-PCR (RT-qPCR).…..……107
Histological correlates…….……..……...107
Data analysis and statistical analysis.…..…….108
Results..... 109
MiRNAs expression profiles in the overall population of patients..….109
Correlation between steady state fibrosis and miRNAs expression…..111
Discussion..... 112

LIMITATIONS OF THE STUDY…….……115

GENERAL DISCUSSION AND CONCLUSION 116

Future perspectives……118

BIBLIOGRAPHY 120

APPENDIX 123

ACKNOWLEDGEMENTS..... 127

LIST OF ABBREVIATIONS

AF	Atrial Fibrillation
ACC	American College of Cardiology
ADP	Action potential duration
AERP	Atrial effective refractory period
AHA	American Heart Association
Ang II	Angiotensin II
AP	Action potential
AP-1	Activator protein I
AT1R	Angiotensin type I receptor
AT2R	Angiotensin type II receptor
ATR	Atrial tachycardia remodeling
CCN	cyr61, ctgf, nov
CFs	Cardiac fibroblasts
CHF	Congestive Heart Failure
CTGF	Connective tissue growth factor
DA	Degree of anisotropy
DADs	Delayed afterdepolarizations
DAG	Diacylglycerol
DW	Dominant wavelenght
EADs	Early afterdepolarizations
ECM	Extracellular matrix
ERK	Extracellular signal-related kinase
ESC	European Society of Cardiology
FFT	Fast Fourier Transform
GWAS	Genome wide association studies
IP3	Inositol 1,4,5-trisphosphate
JNK	c-Jun N-terminal kinase
MAPK	Mitogen-activated protein kinases
MMPs	Matrix metalloproteinases
myoFBs	Myofibroblasts
NCX	Na^{+},Ca^{2+} -exchanger
NFAT	Nuclear factor of activated T-cells
NF-kB	Nuclear factor-kB
NLO	Non-linear optical microscopy
PDGF	Platelet-Derived Growth Factor
PIP_2	Phosphoinositol bisphosphate
PKC	Protein kinase C
PP2A	Protein phosphatase 2A
PTPs	Phosphotyrosine phosphatase
RAAS	Renin-angiotensin-aldosterone system
RISC	RNA-induced silencing complex
RyR2	Ryanodine receptor 2
SERCA	SR Ca^{2+}-ATPase
SHG	Second harmonic generation
SNPs	Single nucleotide polymorphisms

SPRY1	Sprouty-1
SR	Sarcoplasmic reticulum
SR	Sinus rhythm
TGFR-2	Transforming growth factor receptor 2
TGF-β	Transforming growth factor β
TGF-β1	Transforming Growth Factor β1
THRAP1	Thyroid hormone-associated protein 1
TIMPs	Tissue inhibitor of metalloproteinases
TPEF	Two photon excited fluorescence
TRPC3	Transient receptor potential channel channel 3

ABSTRACT

Atrial fibrillation (AF) is the most common sustained arrhythmia worldwide and a frequent cause of hospitalization. Moreover, it represents one of the most frequent complication following cardiac surgery with an incidence of around 30% and an important predictor of patient morbidity. The exact pathophysiological mechanisms responsible for the onset and perpetuation of AF are not completely understood. However, clinical and experimental insights on the factors causing AF have suggested that atrial fibrillation is a multi-factorial phenomenon. Atrial fibrillation is characterized by a highly complex and irregular electrical activation of the atrial tissue, which is the manifestation of diverse abnormalities (electrical, structural, metabolic, neurohormonal, and/or molecular alterations) in diverse pathological conditions. In particular, it has been shown that fibrosis, a phenomenon in which extracellular matrix (ECM) components, mainly fibrillar collagen, accumulate between cardiomyocytes, leads to the inhomogeneous atrial electrical conduction typical of fibrillation. Recent studies have suggested that the deregulation of gene expression may act as a molecular mechanism of arrhythmogenesis. In particular, miRNAs, a new class of non-coding RNAs have rapidly emerged as one of the key players in the gene expression regulatory network, so variations in their expression levels may constitute a pathway for the arrhythmia-induced atrial remodeling.

The present study aims to investigate the structural and molecular features of atrial tissue, with particular attention to fibrosis, which may be involved in the formation of a pro-arrhythmic substrate. By using both histological and advanced microscopy techniques, intramural fibrotic content and 3D collagen network properties were determined in atrial samples, collected during cardiac surgery in patients who developed or not AF. The quantitative analysis indicated a general decrease of collagen content from the outer (the epicardium) to the inner (the endocardium) myocardial wall, in the overall patient population. However, AF patients presented higher fibrotic values compared to sinus rhythm (SR) patients in the deeper myocardial layers, thus supporting the hypothesis that an accumulation of fibrotic tissue within the myocardial wall may represent an important structural contributor in the pathophysiology of AF. In addition to a quantitative assessment, collagen properties such as fibers orientation (degree and anisotropy) and scale dimension, were determined by non-linear optical microscopy techniques. The analysis revealed that in SR patients collagen network showed a fine architecture characterized by thin fibrils with changing angles and

directions compared to AF, where fibers tended to pack-up in larger bundles of defined directions. A quantitative analysis of the 3D collagen network features, throughout the atrial wall, revealed that fibers orientation and scale dimension changed along tissue depth in both SR and AF patients, with larger values of orientation and fiber changes in AF tissues. These results highlight the spatial rearrangement and thickening of the 3D collagen network in AF patients, suggesting its possible role in the maintenance of the arrhythmia.

Numerous evidence indicated that also an altered regulation of gene expression may play an important role in the mechanisms of atrial remodeling which underlie AF. In this perspective, the expression pattern of some miRNAs known to target different genes involved in diverse mechanisms that underlie AF was evaluated. A panel of miRNAs (miR-1, miR-133a/b, miR-30c, miR-29a/b, miR-208a/b, miR-328, miR-499, miR-590 and miR-21), principally involved in the formation of a pro-arrhythmic substrate, was selected after an accurate review of the literature and analyzed by RT-qPCR, in AF patients versus SR individuals. To accurately determine the levels of analyzed miRNAs, their expression data are usually normalized relatively to endogenous and/or exogenous reference genes. To date, no general agreement between different normalization strategies has been found, in particular in cardiac tissue, for the study of AF. For these reasons, a preliminary study aiming to establish the best endogenous reference genes for miRNAs data normalization was performed. Specifically, different well-established analysis tools such as NormFinder, GeNorm, BestKeeper and ΔCt method, were applied on five commonly used endogenous reference transcripts such as 5S, U6, SNORD48, SNORD44 and miR-16. The suitable reference gene obtained, SNORD48, was applied for miRNAs data normalization. Our findings revealed that miRNAs expression levels were different in AF compared to SR patients. MiR-208a and miR-208b displayed statistically significant differences between the two populations. To investigate possible relationships between miRNAs expression levels and the fibrotic content a correlation measurement was also performed. Our analysis revealed that miR-21 and miR-208b were close to a significant correlation with fibrosis. In conclusion, this work introduced new techniques and implemented new methods of analysis for the study of the substrate of AF. In particular, the results obtained with this multiscale approach, from structural to molecular level, exacerbated the role of fibrosis as a critical contributor in the formation of a pro-arrhythmic substrate. Nonetheless, further studies are needed for a better understanding of the ways

in which structural, molecular and also cellular remodeling may alter the impulse propagation in the myocardium.

CHAPTER 1. INTRODUCTION

Atrial Fibrillation: an overview

Atrial fibrillation (AF) constitutes the most frequent arrhythmia worldwide as well as the most frequent complication following cardiac surgery, which contributes significantly to patient morbidity and mortality. AF is associated with hemodynamic instability, prolonged hospital stay, an increased risk of stroke and congestive heart failure (CHF), leading to elevated costs for healthcare and medical treatments.

AF is a multi-factorial disorder (Maesen *et al*., 2012). The mechanisms underlying AF occurrence and maintenance are complex and poorly understood. Despite this, during the last decades, numerous progresses have been made in understanding its pathophysiology (Nattel, 2002; Iwasaki *et al*., 2011; Wakili *et al*., 2011). Epidemiological data evidenced a rising global incidence of AF, thereby posing this condition as an epidemic burden (Chugh *et al*., 2014). In 2010, the estimated number of individuals globally affected by AF was 33.5 million, with 5 million of new cases per year (Chugh *et al*., 2014). AF is increasing with the age of the population, ranges from 0,1% in the under 55 to 9% in the population aged 80 or older (Go *et al*., 2001). AF incidence resulted higher in man than in women, in particular in the developed countries (Kannel *et al*., 1998; Chugh *et al*., 2014). The American College of Cardiology (ACC) in collaboration with the American Heart Association (AHA) and the European Society of Cardiology (ESC), proposed a classification system for AF in order to simply and clarify its heterogeneous clinical features (Fuster *et al*., 2006). According to this system AF is classified in three main forms: paroxysmal, persistent and permanent. The paroxysmal form occurs periodically and it is able to self-terminate within 7 days. Persistent AF usually lasts for more than 7 days and medical treatments are needed to terminate the arrhythmia. In permanent AF, which is irreversible, the sinus rhythm cannot be sustained by pharmacology or cardioversion but it needs further medical treatments. AF occurrence usually initiates as paroxysmal. It may subsequently evolve into persistent or permanent forms (de Vos *et al*., 2010) through a process known as *remodeling*, which implicates electrical and structural changes in the atrial tissue (Nattel & Harada, 2014). AF is frequently underestimated because it may occur in asymptomatic form. Conversely, patients who manifest AF usually present symptoms as palpitations, weakness, fainting, fatigue, dizziness, breath shortness, angina (Fuster *et al*., 2006). The factors which lead to AF may be classified as acute factors, which usually derived by the surgical intervention, and chronic factors, which

are related to the structure of the heart (Maesen *et al*., 2012). Among the numerous factors predisposing to AF, it is also possible to distinguish between genetic determinants, extra-cardiac factors and underlying heart diseases (Wakili *et al*., 2011).

Several strategies are currently available to treat AF, all of which aim to restore the normal sinus rhythm, controlling the ventricular rate and preventing thromboembolism and stroke (Prystowsky, 2000). Different approaches are usually applied to treat AF. They may be divided in two main categories: pharmacological and non-pharmacological. Pharmacological treatments refer to class I and class III anti-arrhythmic drugs, digitalis, β-blockers and Ca^{2+} antagonists. On the other side, non-pharmacological treatments include a series of procedures as catheter ablation, pacing, the application of implantable devices as well as different surgery procedures ("*Maze*" procedure or left atrial appendectomy). Pharmacological approaches are generally preferred due to their non-invasive properties and are considered first-line intervention in AF management. However, they are still a matter of concern due to their side effects (Dobrev & Nattel, 2010).

Over the last decades, the management of cardiac arrhythmias has advanced enormously due to the numerous efforts in clinical research and biomedical technologies. Genetics and molecular biology studies have identified mutations, gene variants and new proteins (Mahida *et al*., 2011; Sinner *et al*., 2011; Tucker & Ellinor, 2014) involved in the occurrence of AF, opening new possibilities for the treatment of arrhythmia. Medical technologies have improved new imaging systems as well as non-invasive diagnostic tools; new pharmacological molecules, as well as biological therapies, have been discovered and developed in order to minimize pro-arrhythmic risks, thus increasing efficacy and safety (Nattel *et al*., 2014). All these approaches may offer many advantages, firstly improving the quality of life and also the economic outcomes. Nonetheless, it is well accomplished that any intervention in the treatment of AF has to be accurately designed, taking into consideration the underlying clinical situation for each patient examined.

Mechanisms of AF

Basis of the cardiac action potential

The classical electrophysiological behaviour of the heart consists in the propagation of the electrical impulses in an orderly way, causing rapid depolarization and slow polarization. These phenomena are able to generate action potentials in cardiac cells. Cardiac action potential reflects the modifications of transmembrane potentials which are determined by the inward (depolarizing) and outward (repolarizing) currents.

In normal condition cardiac action potential (AP) lasts from 200 to 400 hundred milliseconds and consist of five phases: Phase 0, Phase 1, Phase 2, Phase 3, and Phase 4. During phase 0 a rapid depolarization occurs due to a massive inward current carried by voltage-gated sodium channels (I_{Na}). This phase is followed by the inactivation of I_{Na} as well as the activation of the transient outward potassium current (I_{to}), which cause an early repolarization (Phase 1). During phase 2 the repolarization process continues. During this stage, the inward L-type calcium current (I_{CaL}) counteracts with a gradually increasing the outward repolarizing potassium currents, which are mainly composed of the rapid delayed rectifier potassium current (I_{Kr}). This phase represents the classical "plateau" in the cardiac AP. During phase 3 both I_{Kr} and slow delayed rectifier potassium current (I_{Ks}) contribute to terminate the repolarization. Subsequently, cardiac cells return to resting potential (Phase 4).

Pathophysiology of AF

AF is a complex phenomenon, so to better understand the underlying mechanisms it is necessary to illustrate its pathophysiological context.

It is well recognized that atrial ectopic activity, as well as the formation of single or multiple reentry circuits, represent the main pathophysiological mechanisms of AF occurrence and maintenance. Normal atrial cells action potential stays at the resting phase after repolarization. In some circumstances Na^+ or Ca^{2+} inward currents may increase over the time, thus depolarizing cardiac cells; on the other side, K^+ currents may also decrease causing cell repolarization. In this context, cells that reach threshold potential may be fired producing atrial automaticity. An ectopic atrial activation is the result of an automatic firing that occurs before a normal beat. Delayed afterdepolarizations (DADs) represents the most important mechanism of focal atrial arrhythmias. They result from an abnormal diastolic leak of Ca^{2+} from the sarcoplasmic

reticulum (SR), the main cardiomyocytes Ca^{2+} storage organelle. Ca^{2+} enters cardiomyocytes by voltage-dependent Ca^{2+} channels (phase 2), which in turn triggers Ca^{2+} release through the SR via ryanodine receptors 2 (RyR2). After action potential repolarization Ca^{2+} is removed from the cytosol to the SR by the pump SR Ca^{2+}ATPase (SERCA), thus diastolic relaxation occurs. DADs represent the consequence of an excessive diastolic leak of Ca^{2+} from the SR to the cytoplasm through RyR2 (Dobrev *et al.*, 2011). The excess of diastolic Ca^{2+} is handled by the Na^{+}, Ca^{2+}-exchanger (NCX) which transports three Na^{+} ions into the cell per single Ca^{2+} ion extruded. In this case, a depolarizing current is produced causing DADs. DADs that reach potential threshold cause ectopic firing. Another mechanism that generates ectopic atrial activation is represented by early afterdepolarizations (EADs), which is due to inward Ca^{2+} currents during ADP prolongation. Reentry circuits require a trigger and a vulnerable "substrate" for the initiation. A trigger is generally represented by a premature ectopic beat, while the substrate is characterized by electrical and structural alterations of the cardiac tissue architecture. Cardiac tissue presents a discrete refractory period (an interval during which the tissue is not excitable until the second stimulus). If an ectopic beat reaches a still refractory region it will not be able to propagate throughout the tissue; on the contrary, if enough time has gone for the recovery of the excitability region, the impulse can re-enter causing the activation of the tissue. It is accomplished that shorter refractory period (allowing faster recovery of excitability) and/or slower conduction velocity (gaining more time for the non-refractory region to regain excitability) may favor the maintenance of reentry. Reentry may manifest either as single or multiple-circuit form.

Atrial Remodeling

To date, several experimental and clinical studies have demonstrated that during AF occurrence the properties of the cardiac tissue change over time, thus increasing the likelihood of ectopic or reentrant activities which sustained AF itself (Nattel & Harada, 2014). Collectively these changes referred to the phenomenon of *atrial remodeling* (Allessie *et al*., 2002; Nattel *et al*., 2008).

Electrical remodeling

AF modifies the electrophysiological properties of the atrial tissue by altering ion channels/transporters expression and/or their functions (Schotten *et al*., 2011). The abbreviation of the atrial effective refractory period (AERP) accompanied with the loss of the physiological rate adaptation, represent the major consequences of this phenomenon which is termed *electrical remodeling* (Wijffels *et al*., 1995; Brundel *et al*., 2001). AF-induced electrical remodeling has been recently indicated as *atrial tachycardia remodeling* (ATR).

The reduction of the L-type Ca^{2+} current (I_{CaL}) and the enhancement of the inward rectifier K^+ currents, such as the background current (I_{K1}) and the constitutively acetylcholine-regulated K^+ current (I_{KACh}) (Cha *et al*., 2006; Dobrev *et al*., 2001; Dobrev *et al*., 2005), are the main components of the electrical remodeling. In addition, an abnormal expression and distribution of the gap junction connexin hemichannels, has also been observed (Nattel & Harada, 2014).

The rapid increase of the atrial rate (tachycardia) with the onset of AF causes a massive Ca^{2+} influx into cardiomyocytes. To prevent potentially cytotoxic effects, cardiomyocytes respond by reducing the inward Ca^{2+} current I_{CaL} which causes ADP and wavelength shortening, thus creating a substrate for AF maintenance (Nattel, 2002). At the initial phase, the ADP reduction is a consequence of I_{caL} inactivation. On the contrary, when AF is sustained, the decrease of I_{CaL} may result by the downregulation of the pore-forming Ca^{2+} channels subunit (α-subunit) (Yue *et al*., 1999) and also by posttranslational mechanisms, such as protein dephosphorylation and breakdown (Christ *et al*., 2004; Brundel *et al*., 2002). It has also been demonstrated that an impairment in intracellular Ca^{2+} handling may cause loss of ADP rate dependence, thus predisposing to AF occurrence (Kneller *et al*., 2002).

Some investigators have demonstrated that ATR reduces the expression of Cav1.2 α-subunit (Brundel *et al*., 2001; Yue *et al*., 1999) whereas others have not observed any

modification. In addition, other studies indicated a reduction in the expression of β_1, β_{2a}, β_{2b}, β_3 and $\alpha_{2\delta2}$ accessory I_{CaL} subunits (Christ *et al*., 2004; Gaborit *et al*., 2005; Greiser *et al*., 2007; Schotten 2003). It has also been observed that due to a reduction in the endogenous expression of glutathione (Carnes *et al*., 2007), Cav1.2 *S*-nitrosylation resulted increased in AF. This highlight the importance of the oxidative stress in I_{caL} changes. In addition, it has been observed an increase in the expression of ZnT-1 (a protein associated with Zn homeostasis) in ATR, resulting in I_{caL} suppression (Beharier *et al*., 2007). Nonetheless, I_{CaL} dysregulation may derived by an impairment in tyrosine kinases activities (Greiser *et al*., 2007).

The resting membrane potential of cardiomyocytes is maintained by K^+ currents (inward rectifiers), which becomes more negative during AF. In particular, I_{K1}, which is composed primarily of Kir2.1 subunits, has been indicated as one of the most important determinants of AF-maintaining reentry (Pandit *et al*., 2005) and it is up-regulated in AF (Wakili *et al*., 2011). Another important inward-rectifier K^+ current is represented by I_{KACh}, which mediates cardiac vagal effects. The release of acetylcholine from the vagal nerve endings activates I_{KACh}, causing the abbreviation of the ADP and the cell-membrane hyperpolarization (Nattel *et al*., 2008). The increase of vagal activity may promote AF by stabilizing reentry circuits (Kneller *et al*., 2002). ATR modifies the I_{KACh} system in a way that agonist-stimulated I_{KACh} (vagal activation) is decreased, while its constitutively form $I_{KACh,c}$ is increased (Cha *et al*., 2006; Dobrev *et al*., 2005; Ehrlich *et al*., 2004; Voigt *et al*., 2008). Some studies indicate that the enhancement of $I_{KACh,c}$ derived by an increase in single-channel open probability, is a consequence of slowed channel closure (Voigt *et al*., 2008). In this regard, some investigators observed that in ATR models (Ehrlich *et al*., 2004; Voigt *et al*., 2008) mRNA and protein levels of Kir3 subunits (which underlying I_{KACh}) remained unvaried; on the contrary, in human patient with chronic AF they were decreased (Dobrev *et al*., 2005). It has also observed that during AF there is an up-regulation of protein kinase C (PKC) (Voigt *et al*., 2007), suggesting that an increase in PKC-mediated phosphorylation may play an important role in $I_{KACh,c}$ enhancement. Some studies have also demonstrated that the blockage of $I_{KACh,c}$ suppresses the ADP abbreviation, decreasing AF occurrence (Cha *et al.*, 2006), thus placing $I_{KACh,c}$ among the important players of arrhythmias.

A consistent reduction of the transient outward K^+ current (I_{to}) has been observed in ATR (Nattel *et al.*, 2007). Despite the functional consequences of its down-regulation remain to be clarified, it is accomplished that I_{to} activation is fast and produces an outward current which opposes the inward Na^+ current during the initial phase of the

cardiac action potential. As a consequence, I_{to} downregulation may affect wave propagation by increasing the action potential amplitude.

It has been observed that the decrease of I_{to} parallels the downregulation of the pore forming Kv4.3 α-subunits, both at mRNA and protein expression level (Yue *et al.,* 1999). In this regard, the activation of Ca^{2+}-dependent protein phosphatase calcineurin (Rossow *et al.,* 2006) as well as the proteolytic activity mediated by calpains (Brundel *et al.,* 2002; Goette *et al.,* 2002), may have a significant role in suppressing Kv4.3 gene transcription and protein degradation, respectively.

The information regarding I_{Kur} modifications during AF occurrence result inconsistent (Nattel *et al.,* 2007). However, it is accomplished that its role in atrial repolarization is strongly dependent on the action potential morphology (Courtemanche *et al.,* 1999). Nevertheless, due to its atrial specificity, I_{Kur} still remains an attractive therapeutic target for AF treatment (Nattel, 2002).

I_{Kr} and I_{Ks} delayed-rectifier currents resulted unchanged in ATR experimental models, while in humans there is a lack of information in the field due to experimental technical difficulties (Yue *et al.,*1996).

Structural remodeling

Numerous evidence indicate that structural remodeling represents an important contributor to the formation of the AF substrate (Burstein & Nattel, 2008).

Structural remodeling is a slower process compared to electrical remodeling, which comprises numerous morphological changes of the atrial myocardial tissue structure and architecture (Corradi *et al*., 2008; Nattel *et al*., 2008). In this regards, it has been demonstrated that a combination of atrial enlargement with atrial fibrosis, creates longer potential conduction pathways for reentry, slows conduction and also imposes conduction barriers, leading to the formation of reentry circuits that sustained AF itself (Nattel *et al*., 2008). The exact regulatory mechanisms underlying atrial extracellular matrix (ECM) remodeling as well as the precise signaling pathways which lead to structural changes, have not been completely elucidated. Despite this, it is well accomplished that several secreted factors are involved in the profibrotic process, many of which act both at a single level and synergistically (Katz, 2002).

Genetic contributors to atrial fibrillation

AF mechanisms include also a genetic component, characterized by a complex background that involves numerous pathways (Mahida & Ellinor, 2012). The way to unravel the genetic basis of AF has progressed from the identification of genes associated with familial AF to clinical observational studies, thus demonstrating its hereditability. In addition, over the last decade, genome-wide association studies (GWAS) have identified hundreds of new genetic association, involving common single nucleotide polymorphisms (SNPs).

Despite the complex and aging-related clinical risk factors AF is hereditable. In this context, the Framingham study indicated that parental AF increased the risk of AF in offspring (Fox *et al.,* 2004). In addition, a study performed by Ellinor and coworkers reported that lone AF (without apparent structural heart diseases) increases the risk of AF in family members (Ellinor *et al.,* 2005).

Linkage studies and candidate gene searches allowed for the identification of numerous ion channel gene mutations. In this context, mutations in the potassium channel (e.g. in *KCNQ1*, *KCNE2*, *KCNH2*, *KCNJ2*, *KCNA5*) (Das *et al.,* 2009; Hong *et al.,* 2005; Makiyama *et al.,* 2008; Xia *et al.,* 2005; Yang *et al.,* 2004) and in the sodium channel (in *SCN5A* and *SCN4B*) (Benito *et al.,* 2008; Li *et al.,* 2013) have been associated with familial AF. Several non-ion channel genes have also been associated with familial monogenic AF. Among these genes *PRKAG*, that is associated with familial Wolff-Parkinson-White syndrome and AF (Gollob *et al.,* 2001) and *NPPA,* that encodes for atrial natriuretic peptide (Hodgson-Zingman *et al.,* 2008, Disertori *et al.,* 2016), have been found. Additionally, some developmental genes, such as genes encoding transcription factors involved in cardiogenesis from the GATA family (Posch *et al.,* 2010; J. Wang *et al.,* 2012; Wang *et al.,* 2013) and NKX2-5, have been implicated in AF (Huang *et al.,* 2013). Structural genes, such as *GJA5,* which encode for connexin 40, and RYR2, which encodes for the ryanodine receptor releasing intracellular stores of calcium, have also been associated with familial AF (Gollob *et al.,*2006; Kazemian *et al.,* 2011). Further, some genes encoding nuclear membrane-associated proteins, such as *LMNA*, which encodes for lamin expressed in the inner nuclear lamina (Beckmann *et al.,* 2010) and NUP155, which encodes for a nucleoporin (Zhang *et al.,* 2008), have been linked to familial AF.

Despite the studies about familial AF have greatly improved the understanding of genes associated with AF monogenic forms, they constitute only a fraction of the global

burden. Complex diseases, such as AF, follow the "common disease common variant" hypothesis, which predicts that common variants with small effects appear to be responsible for a majority of the heritability of the traits (Manolio *et al.,* 2009).

In this context, GWAS allowed for the identification of 14 AF-associated genetic loci to date, thus overcoming possible biases deriving from candidate gene analysis (Deshmukh *et al.,* 2015; Ellinor *et al.,* 2012; Sinner *et al.,* 2014). In particular, the first GWAS study, performed in 2007, identified a susceptibility locus at chromosome 4q25 in a population of European descent as well as in an Asian population (Gudbjartsson *et al.,* 2007). The region around the 4q25 locus has been defined as a 'genetic desert', with the closest gene (*PITX2*) located 150000 base pairs upstream. *PITX2* encodes for the paired-like homeodomain transcription factor 2 with 3 different isoforms. Importantly, the *PITX2c* isoform is the major expressed in the heart (Franco *et al.,* 2012). *PITX2* is involved in the embryonic cardiogenesis, where it is crucial to right–left asymmetry, in terms of the suppression of the formation of a sinus node in the left atrium and the formation of the myocardial sleeves in the pulmonary veins (Mommersteeg *et al.,* 2007). Studies on knockout and haploinsufficient *PITX2* mice, have revealed a predisposition to atrial arrhythmias (Wang *et al.,* 2010) and AF (Kirchhof *et al.,* 2011). In humans and mice, it has been observed that the depletion of *PITX2c* reduces the levels of mRNA encoding sodium and potassium channel protein subunits, suggesting this gene as an upstream transcriptional regulator of atrial electrical function (Chinchilla *et al.,* 2011; Tao *et al.,* 2014).

GWAS studies have also identified numerous other loci associated with transcription factors that seem to be important for cardiac development. Specifically, *ZFHX3* which is located on chromosome 16q22, intronic to the zinc finger homeobox 3 gene, is known to be involved in the regulation of growth and differentiation of skeletal muscle and neuronal tissues (Benjamin *et al.,* 2009). *ZFHX3* is necessary for the transcriptional activation of the gene POU class I homeobox 1 (*POU1F1*), that interacts with *PITX2*, allowing DNA binding and transcriptional activity (Liu *et al.,* 2012). Another GWAS study described the gene *PRRX1*, that encodes for a homeodomain transcription factor present in the connective tissue in the developing heart (Ellinor *et al.,* 2012). In particular, knockout animal models of *PRRX1* have shown impairments in the pulmonary vasculature (Ihida-Stansbury *et al.,* 2004).

Hitherto, two loci in ion channel genes have been significantly associated with AF in GWAS. First, a locus was identified on chromosome 1q22 within an intron of the

KCNN3 gene, that encodes for the calcium-activated potassium SK3 (Ellinor *et al.*, 2010). Second, a locus was described on chromosome 15q24, within an intron on the hyperpolarization-activated cyclic nucleotide-gated 4 (*HCN4*) gene (Ellinor *et al.*, 2012). *HCN4* is present in the sinoatrial node and regulates the I_f current, which is responsible for the pacemaker current in nodal myocytes. Mutations of this channel may cause diminished action potential frequency and delayed after depolarizations, thus leading to AF (Macri *et al.*, 2014).

A meta-analysis of GWAS performed in 2010 identified numerous new AF loci, including three within/close to genes that are involved in cellular structural components. In particular, a locus on chromosome 7q31 within an intron of the gene *CAV1*, that encodes caveolin-1, was associated with AF (Ellinor *et al.*, 2012). *CAV1* is co-expressed with a potassium channel gene (*KCNH2*), which is involved in the repolarization phase of the action potential. The risk allele and AF are associated with decreased expression of *CAV1* (Martin *et al.*, 2015). In addition, caveolin-1 has been postulated as an anti-fibrotic factor in atrial tissue, since down-regulation of *Cav-1* results in an increase of TGF-β1, leading to the activation of the Smad signal pathway and to the production of collagen (Yi *et al.*, 2014).

A SNP located within an intron of the *SYNE2* gene, that encodes for nesprin-2, a protein that anchors nuclei to the cytoskeleton, has also been associated with AF. A wide meta-analysis of GWAS performed by Ellinor and colleagues identified a susceptibility locus on chromosome 10, between *SYNPO2L* and *MYOZ1* genes, and another locus in an open-reading frame on chromosome 9 (*C9orf3*) (Ellinor *et al.*, 2012). *MYOZ1* encodes for a protein which is involved in stabilizing the sarcomere, while *C9orf3* is associated with three coding genes (including *FBP1* and *FBP2*), that are involved in gluconeogenesis (Ellinor *et al.*, 2012).

Atrial fibrosis & Atrial Fibrillation

Although not exclusively related to AF, fibrosis constitutes a common feature in AF representing one of the most important contributors to arrhythmogenesis (Schotten *et al.*, 2011). Atrial fibrosis has been observed in lone AF (Boldt *et al.*, 2004; Frustaci *et al.*, 1997) as well as in other pathological conditions associated with AF, such as congestive heart failure (Burstein *et al.*, 2009; Li *et al.*,1999), rheumatic heart disease (Xiao *et al.*, 2010), valvular disease (Anné *et al.*, 2005), dilated and hypertrophic cardiomyopathy (Ohtani *et al.*, 1995; Prinz *et al.*, 2011) and senescence (Gramley *et al.*, 2009). However, some experimental and clinical studies have demonstrated beneficial effects both in AF stability and in atrial structural remodeling by the administration of compounds with known anti-fibrotic effects, as Angiotensin II type 1 receptor blocker (Kumagai *et al.*, 2003), statins (Li *et al.*, 2001; Shiroshita *et al.*, 2007) and omega-3 polyunsaturated fatty acids (Sakabe *et al.*, 2007). Collectively, this evidence suggest an association between atrial fibrosis and AF. In addition, it is well accomplished that AF itself may promote atrial fibrosis, which in turn sustains AF (Burstein & Nattel, 2008; Yue *et al.*, 2011).

Atrial fibrosis is a complex phenomenon, which is characterized mainly by an excessive accumulation of ECM proteins, secreted primarily by myofibroblasts (myoFBs) (the activated form of cardiac fibroblasts, under pathological conditions)(Burstein & Nattel, 2008; Yue *et al.*, 2011). Fibrosis can be a reparative or a reactive process. During reparative fibrosis, the cardiac tissue architecture is maintained by the replacement of dead cardiomyocytes. On the contrary, under pathological conditions, reactive fibrosis causes the accumulation of ECM components leading to interstitial expansion and muscle bundles separation (Burstein *et al.*, 2008; Yue *et al.*, 1999). The resultant fibrotic tissue creates a barrier that interferes with the normal electrical impulse propagation, leading to conduction abnormalities as arrhythmogenesis (Li *et al.*, 1999).

Molecular mechanisms leading to atrial fibrosis

The exact molecular mechanisms underlying atrial fibrosis, in particular regarding the ECM formation, remain to be clarified. Nonetheless, a growing body of evidence has indicated that numerous factors (secreted both by cardiomyocytes and cardiac fibroblasts**)** and signaling pathways are involved in this process (Burstein & Nattel, 2008) (**Figure A**).

Angiotensin II (Ang II) is considered one of the most potent pro-fibrotic molecules and has been demonstrated to have an important role in AF (Ehrlich *et al*., 2006). Ang II binds to two distinct receptor subtypes: angiotensin type I (AT1R) and angiotensin type II (AT2R) receptors. Both receptors present different signaling cascades with opposite effects. The activation of AT1R by Ang II stimulates fibroblasts proliferation, cardiomyocytes hypertrophy and apoptosis (Burstein & Nattel, 2008). The AT1R, through the Shc/GRb2/SOS adapter-protein complex, activates the GTPase protein RAS that initiates a series of mitogen-activated protein kinase phosphorylation cascades, which are important in the remodeling process (Hunyady & Catt, 2006). The mitogen activated protein kinases ERK (extracellular signal-related kinase) -1 and -2, JNK (c-Jun N-terminal kinase) and p38, activate transcription factors as Elk-1, c-jun and c-fos that modulate gene expression. The activation of AT1R also stimulates phospholipase C, which breaks down the membrane phosphoinositol bisphosphate (PIP2) into diacylglycerol (DAG) and inositol 1,4,5-trisphosphate (IP3). DAG, by the activation of the PKC, and IP3, by increasing intracellular Ca^{2+} release, promote remodeling. In addition, the signal occurs through the JAK/STAT pathway that activates transcription factors, such as the activator protein 1 (AP-1) and the nuclear factor-kB (NF-kB).

The activation of AT2R inhibits mitogen-activated protein kinases (MAPK) (Hunyady & Catt, 2006) by phosphotyrosine phosphatase (PTPs) and protein phosphatase 2A (PP2A), leading to anti-proliferative effects. The balance between ATR1 and ATR2 could have important implications for the treatment of AF.

Transforming Growth Factor β1 (TGF-β1) is a molecule secreted by both cardiomyocytes and fibroblasts which may be considered the primary downstream mediator of Ang II, either in autocrine and paracrine modes. Ang II induces TGF-β1 synthesis, which stimulates fibroblasts activity. In turn, TGF-β1 enhances Ang II and the production of other pro-fibrotic factors creating a positive feedback (Rosenkranz, 2004). TGF-β1 also stimulates fibroblast activation and collagen deposition via SMAD

protein (Attisano & Wrana, 2002). Some studies revealed that cardiac overexpression of constitutively active TGF-β1 causes selective atrial fibrosis and atrial conduction heterogeneity, thus predisposing to AF (Verheule *et al*., 2004). Platelet-Derived Growth Factor (PDGF) is one of the numerous growth factors which stimulates fibroblasts proliferation and differentiation. After the binding of the ligand, the PDGF receptors dimerize leading to the activation of a tyrosine kinase, which in turn forms part of the receptor itself. This tyrosine kinase phosphorylates intracellular domains of the PDGF receptor. The autophosphorylation activates the PDGF receptors, leading to the activation of a signaling pathway via mitogen-activated protein kinase JAK/STAT and phospholipase C (shared with TGF-β1 and Ang II). In addition, also PDGF seems to underlie fibroblast hyperresponsiveness, thus explaining the higher susceptibility of the atria with respect to the ventricles in the fibrotic remodeling process (Burstein *et al*., 2008). CTGF belongs to the CCN (cyr61, ctgf, nov) protein family and it is known to be the major downstream effector of the TGF-β1 in the fibrotic process. CTGF directly activates fibroblasts (Ahmed *et al*., 2004) and it is up-regulated by both Ang II (Ahmed *et al.*, 2004) and TGF-β1 (Chen *et al.*, 2000).

The process of cardiac structural remodeling comprises numerous factors involved not only in the synthesis of the ECM components but also in their degradation. In this context, matrix metalloproteinases (MMPs) and their inhibitors (TIMPs) play a critical role in the maintenance of the ECM homeostasis (Kakkar & Lee, 2010). MMPs represent a family of zinc-dependent endopeptidases, which are responsible for ECM degradation. An anomalous increase in MMPs activity causes the degradation of matrix proteins (D'Armiento, 2002; Li *et al.*, 2000; Thomas *et al.*, 1998), while TIMPs inhibit the proteolytic activity of MMPs by establishing tight-binding complexes (Gomez *et al.*,1997). It has been observed that both the expression and the activity of cardiac MMPs increase in numerous pathological conditions, including heart failure and myocardial infarction (Cleutjens, 1995; Spinale *et al.*, 2000; Sutton & Sharpe, 2000). Recently, many evidence in humans and animal models have shown an unbalance between MMPs and TIMPs expression in atrial fibrillation. Specifically, matrix metalloproteinase-9 was found up regulated and TIMP-1 was down-regulated in dogs with atrial fibrillation, compared to the controls (Zhang *et al.*, 2008). In addition, another study performed on canine animal models revealed an increase of the activity of

MMP-9 (~50%), paralleling a decrease of TIMP-4 (~50%), after rapid atrial pacing-induced heart failure (Hoit *et al.*, 2002).

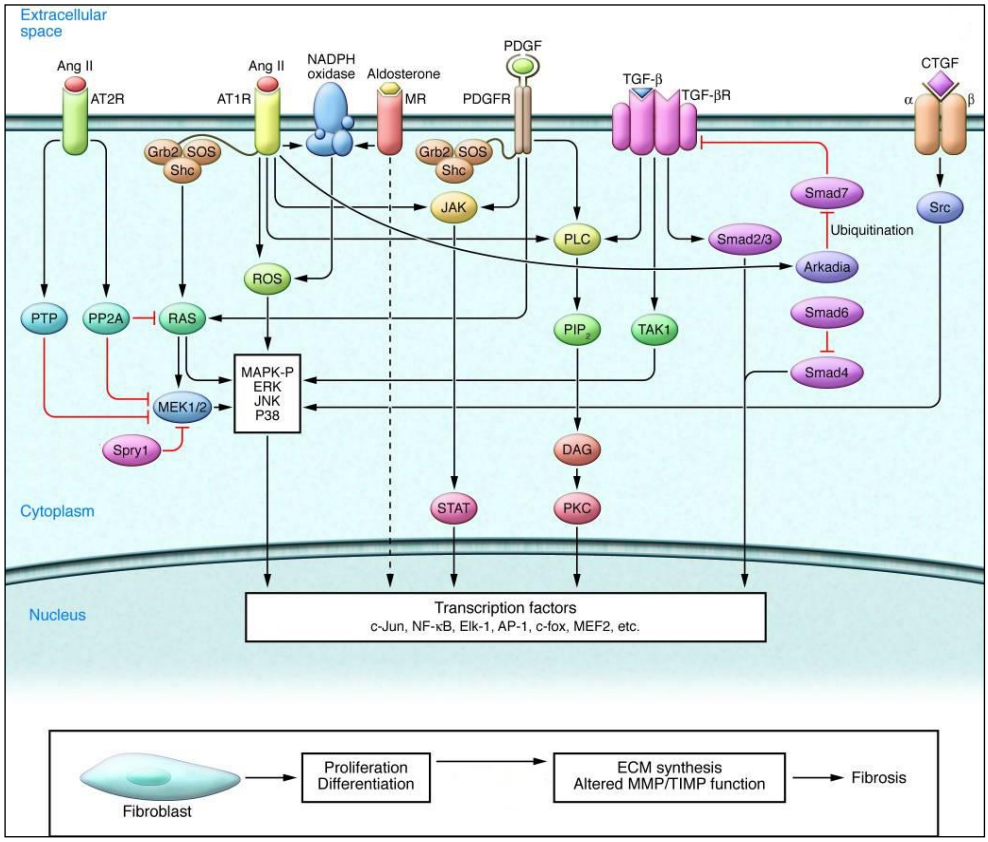

Figure A: Molecular mechanisms leading to atrial fibrosis. Major profibrotic signaling pathways involved in fibrosis (modified from Wakili *et al.*, 2011).

Extracardiac factors involved in atrial fibrosis

Several extracardiac factors have been indicated to predispose to fibrosis in AF. Diabetes, obesity, metabolic syndrome, systemic inflammation, obstructive and central sleep apnea, athlete's heart, hyperthyroidism and the use of toxic substances, have all been demonstrated to affect the myocardium (Schoonderwoerd *et al.*, 2008). Diabetes, which is known to be associated with cardiomyopathy and cardiac fibrosis, has been recently indicated to triple the risk of AF in obese individuals (Grundvold *et al.*, 2015). Obesity causes electrical and structural modifications of the myocardium, leading to delay and heterogeneity in atrial conduction, inflammation and fibrosis. The pathways underlying these processes comprised TGF-β_1 signaling activation, oxidative stress and the up-regulation of PDGF and endothelin (Abed *et al.*, 2013). Obstructive and central sleep apnea are also associated with atrial remodeling and AF (Matassini *el al.*, 2015). In this context, animal studies of obstructive

sleep apnea showed a substantial down-regulation of connexin43 associated with an altered expression of ion channels proteins, resulting in shortening of the atrial refractory period, slowing conduction, cardiomyocytes apoptosis and cardiac fibrosis (Iwasaki *et al.*, 2014).

Extracellular matrix remodeling in atrial fibrosis: the collagen fibers network

The cardiac ECM represents the three-dimensional scaffold that defines the geometry and the muscular architecture of the cardiac chambers. It is an active system able to respond to different mechanical stresses and numerous external stimuli, as neuroendocrine activation, growth factors and cytokines.

The formation and redistribution of connective tissue fibers modulate the geometry of the myocardium in order to adapt to the physiological conditions, thus preventing (or attenuating) the effects of new electrical, mechanical and chemical stimuli.

Collagen fibers, the major components of the cardiac ECM, are normally associated with the maintenance of the tissue structure architecture. A large number of cardiovascular disorders, including myocardial infarction, hypertension, and heart failure are related to alterations in the amount, type, stability and organization of collagen fibers (Ju & Dixon, 1996). In addition, it has been shown that during pathological conditions collagen fibers undergo both qualitative and quantitative modifications, leading to an excessive accumulation either in regions of cardiomyocytes loss (as in reparative fibrosis) or diffusely (as in dilated cardiomyopathy and reactive fibrosis)(Tarone *et al.*, 2014).

The global accumulation of collagen fibers impairs the mechanical properties of the myocardium causing an increase in the wall stiffness, resulting in less compliant chambers which may predispose to arrhythmogenesis.

The collagen fibers network of the heart: structural architecture

Myocardial ECM is composed primarily of a complex network of fibrillar collagen (Caulfield & Borg, 1979). The spatial organization of collagen in the heart has been described by the detailed organization of layers that surround and interconnect both individual and groups of cardiomyocytes (Robinson *et al.*, 1983). Specifically, from the outer to the inner side it is possible to find: the *epimysium*, the *perimysium* and the *endomysium*, respectively. The epimysium is the connective tissue that surrounds all of the cardiomyocytes bundles in the myocardium. The perimysium represents the sheath of connective tissue that surrounds and interconnects groups of cardiomyocytes, in a particular orientation. The endomysium constitutes the inner matrix element that surrounds individual cardiomyocytes, within each bundle. While the epimysium and the

perimysium are composed primarily of fibrillar collagen, the endomysium represents a complex network of collagen and elastin. The general content and structure of these elements are believed to be involved in the maintenance of the shape and distensibility of the cardiac chambers (Weber *et al.,* 1994; Weber, 1989). It has been shown that the fibrillar collagen network forms a structural continuum with the fibrous skeleton of the entire heart, including cardiac valves, chordate tendinae and the perivascular matrix. The perimysium may have a great impact on cardiac performance due to the property to interconnect all the contractile elements of the myocardium (Robinson *et al.,* 1983). The orientation of the perimysium results altered by the loading conditions of the heart, assuming a coiled configuration when relaxed and a linear configuration when stretched (Robinson *et al.,* 1988). The fibers that constitute the perimysium are normally oriented along the long-axis of the muscle bundles. In addition, they also provide extensive branching patterns that link cardiomyocytes all through the myocardium by an organized network of fibrillar collagen (Robinson *et al.,* 1987, 1983, 1988). The connectivity of the fibrillar collagen network may play an important role in the coordination of the whole myocardial contraction. Studies in this field have been shown that the myocardium of mammals due to its numerous matrix interconnections, can generate a more powerful cardiac contraction compared to a myocardium with poorly interconnected perimysial fibers as observed in frog hearts (Factor & Robinson, 1988).

Collectively, this evidence suggests that the contractile ability of the myocardium represents an example of biological engineering, made possible by its three-dimensional architecture primarily based on the content and organization of the fibrillar collagen network.

The collagen fibers network of the heart: synthesis, composition and regulation

Collagen is produced by CFs as a precursor, procollagen. It is subsequently converted into its mature form by a series of proteolytic reactions (Kagan & Trackman, 1991; Prockop & Kivirikko, 1995) followed by post-translational modification, leading to intermolecular cross-linking formation between adjacent fibers. Collagen fibers are then assembled together, forming larger fibers that are resistant to degradation (Bishop & Laurent, 1995).

The human heart is primarily composed of types I and types III collagen, accounting for the 85% and 15%, respectively. However, collagen types IV, V, VI are also present but in a low percentage (Manabe *et al.*, 2002; Weber *et al.*, 1988; Medugorac & Jacob, 1983). Collagen type I has been associated with thicker perimysial fibers, which play an important role in withstanding shear stresses and in coordinating the whole contraction (Weber, 1989). On the contrary, collagen type III, which has been associated with thinner perimysial fibers, is less rigid and may confer elasticity to the myocardium. Despite their exact functional role in the myocardium has never been clearly demonstrated, some evidence indicates that the ratio of collagen isoforms may influence myocardial compliance and diastolic relaxation (Burgess *et al.*, 1996). In particular, some studies indicated an altered proportion of collagen type I respect to collagen type III in AF patient, after cardiac surgery (Grammer *et al.*, 2005). The content of cardiac collagen in the normal myocardium is around 2-4% (Brower *et al.*, 2006) with a relatively high turnover, ranging from 1 to 6% per day (Bishop & Laurent, 1995; Laurent, 1987; Weber & Brilla, 1991). Normally, at the steady state condition collagen synthesis and degradation are comparable. Several molecules such as growth factors, hormones and cytokines, are involved in the modulation of collagen synthesis. Among these, the *β*-adrenergic system, the renin-angiotensin-aldosterone system (RAAS) and the transforming growth factor-β (TGF-*β*) are indicated to be the most important. The *β*-adrenergic system (Calderone *et al*., 1998) and the RAAS system (Sun *et al*., 2001) increase cardiac collagen synthesis via G-protein-coupled signaling pathways (Meszaros *et al*., 2000). TGF-*β* acts by stimulating SMAD and Rho/ROCK signaling cascades, resulting in the activation of ECM genes and increasing the expression and secretion of growth factors (as connective tissue growth factor, CTGF).

Prior to assembly, about 50% of the fibrillar collagen is degraded inside the cell. Fibrillar collagen and other ECM components are normally broken down by MMPs, which are released mainly by CFs and also by inflammatory cells and cardiomyocytes (Spinale, 2007). Collagenases (MMP-1, MMP-8, MMP-13), gelatinases (MMP-2, MMP-9) and stromelysins (MMP-3), are indicated to be responsible for ECM degradation (Porter & Turner, 2009). The expression of MMPs is influenced by growth factors (such as TGF-*β*) and cytokines, while their inhibition is mediated by Angiotensin II. Despite the importance of biochemical signaling pathways in collagen synthesis and degradation, a pivotal role is also determined by mechanical loading which is able to modulate myocyte growth as well as the three-dimensional architecture

of the ECM. Studies on different tissue samples such as tendon (Canty & Kadler, 2005), skin (Armstrong & Ferguson, 1995) and heart valve leaflet (Driessen *et al.*, 2003), indicated that load bearing fibrillar collagen align with local directions of principal stress. It is also known that the post-natal development growth of myocyte and nonmyocyte components (Bernardo et al., 2010), is accompanied by the spatial arrangement of collagen fibers network, thus preserving ECM architecture and function. During pathological conditions, mechanical stimuli as pressure overload, lead to the remodeling of both cellular and acellular myocardial components, thus indicating that the myocardium has the capability to sense and respond to differences in mechanical loading. As indicated by *in vitro* studies, fibroblasts (with different tissue origins) exposed to mechanical stimulation, increase their proliferation rate, collagen production, altered MMPs expression, growth factors and cytokines levels (Thampatty & Wang, 2008). Another study indicated that cyclic mechanical deformation of CFs gave rise to an increase in collagen production, albeit affected by other matrix component and serum growth factors (Butt & Bishop 1997; Carver *et al.*, 1991). The exact mechanisms that underlie the mechano-transduction in the ECM are not fully elucidated. However, it is accomplished that there are numerous deformation sensors coupled to signaling cascades, as stretch-activator ion channels, integrins, cytoskeletal structures (Berenji *et al.*, 2005; Ross & Borg, 2001; Thampatty & Wang, 2008), which are able to stimulate different ECM components.

In summary, the cardiac ECM constitutes the scaffold for the three-dimensional organization of cardiac cells, as well as for the transmission of forces across the entire heart wall. Nonetheless, it represents an active system with the capability to sense differences in mechanical loading and consequently, it is also able to adapt to them.

MicroRNAs & Atrial Fibrillation

MicroRNAs (miRNAs) represent an evolutionarily conserved class of small (~22 nucleotides) non-coding RNAs (Ambros, 2004; Gan *et al.*, 2013) first discovered in the nematode *Caenorhabditis elegans* (Ruvkun & Giusto, 1989; Ruvkun *et al.*, 1989).

Virtually expressed in all organisms, miRNAs represent a fundamental component of the genetic regulation, suggesting a key role in biological processes (Latronico & Condorelli, 2008; Thum *et al.*, 2008). MiRNAs are considered negative regulators of gene expression at the post-transcriptional level. They inhibit protein translation and/or promote mRNA degradation by base-pairing to complementary sequences within mRNA transcripts (Van Rooij & Olson, 2012).

To date, more than 2,500 mature miRNAs have been identified in the human genome (www.miRbase.org, Release 21) and over 60% of protein-coding genes have been found to be regulated by miRNAs (Friedman *et al.*, 2009). The physiological importance of miRNAs has been well documented in numerous biological processes such as cellular proliferation, differentiation (Brás-Rosário *et al.*, 2013), tissue remodeling (Orenes-Piñero *et al.*, 2013; Xu *et al.*, 2013), tumorigenesis (Dvinge *et al.*, 2013; Song *et al.*, 2013) and also in cardiovascular diseases (Small *et al.*, 2010).

Several studies have also indicated an involvement of miRNAs in AF-related remodeling processes, suggesting a key role of these small non-coding RNAs in the regulation of many signaling mechanisms underlying atrial fibrosis and AF.

Biogenesis and biological action of miRNAs

The maturation process of miRNAs comprises different steps (Bartel, 2004; Cullen, 2004) that start with the transcription operated by RNA polymerase II of single-stranded non-coding RNAs (**Figure B**). According to the genomic location of the primary coding sequences, it is possible to define different types of miRNAs: *intergenic* miRNAs, which are located between genes, and *intragenic* miRNAs, that are generated by the processing of introns in protein-coding genes. Transcription of intergenic miRNAs leads to the formation of primary precursors (pri-miRNAs) with a characteristic hairpin or "stem-loop" like structure (Denli *et al.*, 2004). The pri-miRNA is subsequently processed by an endonucleolytic cleavage into ~70 nucleotide hairpin-shaped precursor miRNA (pre-miRNA). The processing of pre-miRNAs from intergenic genomic sequences is mediated by the nuclear RNase III *Drosha*, while the processing of

intragenic miRNAs needs additional splicing enzymes. The unique exception is represented by one subtype of intronic miRNA (*mirtron*), which produces its pre-miRNA by using only a splicing enzyme, in a Drosha-independent manner (Berezikov, 2011). Pre-miRNAs are then transported by the protein *Exportin-5* from the nucleus to the cytoplasm (Lund *et al.,* 2004), where they are further process into a mature miRNA duplex of ~22 nucleotide length by the RNase III enzyme *Dicer* (Kim *et al.,* 2009). The mature miRNA is then incorporated into the RNA-induced silencing complex (RISC) to form miRISC (Gregory *et al.,* 2005). The two miRNA strands, the "passenger" and the "guide" strand, are then separated leaving only the guide strand assembled into the miRISC complex. The miRISC complex binds to the complementary sequence of the target mRNA, usually in the 3'-untranslated region (3'-UTR) (Carthew *et al.,* 2009). Despite most miRNA-mRNA binding interactions are not fully complementary, a perfect match between the miRNA "seed region" (2-8 nucleotides in the 5'-end) and the target mRNA is believed to be required for miRNA action. Possibly according to the degree of complementarity between miRNAs and their target mRNAs, miRNAs can inhibit the translation of the encoded proteins or lead to mRNA degradation.

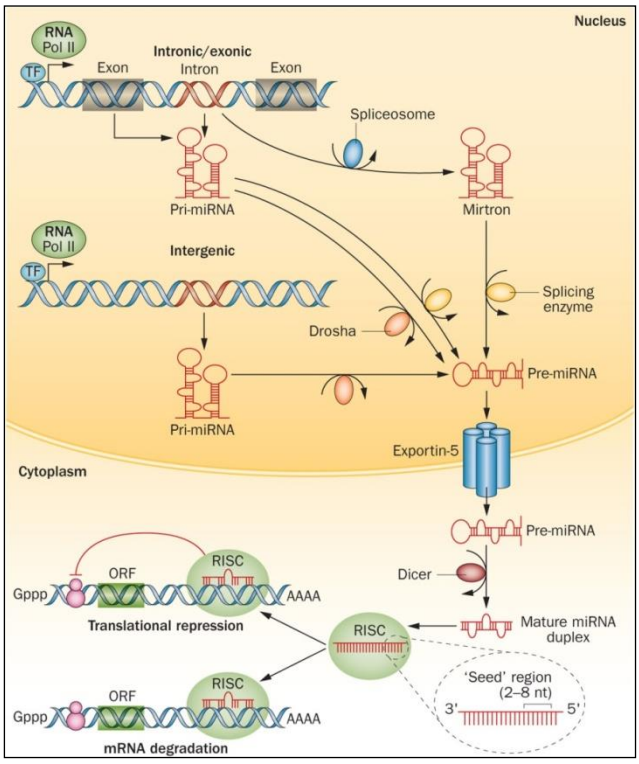

Figure B: Biogenesis and action of miRNAs (Luo *et al.*, 2015).

MiRNAs expression profile in the heart

The normal myocardium presents a distinct pattern of miRNAs, which is different from other organs (Liang *et al.,* 2007). Studies revealed that the top 20 most abundant miRNAs expressed in the human heart are: miR-1, miR-133a/b, miR-26a/b, miR-125a/b, let-7a/b/c/f/g, miR-16, miR-100, miR-126, miR-145, miR-195, miR-199, miR-20, miR-21, miR-23, miR-24, miR-29a/b, miR-27a/b, miR-30a/b/c, miR-92a/b, and miR-99 (Liang *et al.,* 2007). The majority of these miRNAs are also expressed in different organs, apart for miR-1 and miR-133a/b that are preferentially expressed in cardiac and skeletal muscle (Chen *et al.,* 2006). In addition, other medium-expressed miRNAs such as miR-208a/b and miR-499, are found to be cardiac-specific (Van Rooij *et al.,* 2007).

Functions of miRNAs in AF

MiRNAs involved in electrical remodeling

As already mentioned, arrhythmogenesis is generally attributed to enhanced trigger activity, which may result in alterations in different ion channels as well as impairment in Ca^{2+} handling (Ter Keurs & Boyden, 2007) and modulation of the cardiac inwardly rectifying K+ current (I_{K1}) (Dhamoon & Jalife, 2005).

miRNAs play an important role in the functional control of ion channel genes during electrical remodeling (Luo *et al.,* 2010), thus contributing to AF progression (Figure C). Studies in the field, have shown an inverse correlation between the expression of miR-1 and the distribution of inward rectifying potassium channel (Kir2), in left atrial tissue patient with persistent AF. In particular, it has been observed a downregulation of miR-1 by 86% accompany with a high expression of Kir2, which represents an important factor in AF maintenance (Girmatsion *et al.,* 2009). miR-1 has also been suggested to have a mechanistic importance in AF pathophysiology, via targeting both I_{K1} and connexin43 (Girmatsion *et al.,* 2009; Yang *et al.,* 2007), that are considered key regulators of cardiac conduction. It has also been proposed an involvement of miR-1 in the modulation of Ca^{2+} handling. Specifically, miR-1 causes the hyperphosphorylation of RyR2, enhancing its activity, thus promoting arrhythmogenic SR Ca^{2+} release (Terentyev *et al.,* 2009). In a similar way, also miR-26 has been shown to repress I_{K1} (Luo *et al.,* 2013). The transcription of miR-26 is negatively controlled by the calcium/calmodulin/calcineurin-regulated nuclear factor of activated T-cells (NFAT)

pathway. An increase in NFAT translocation has been observed both in dogs and in humans with AF, according to a reduction of miR-26 (Luo *et al.*, 2013).

Experimental evidence has shown an up-regulation of miR-328 in AF patients and has identified CACNA1C and CACNB1 genes (which encode L-type Ca^{2+} channels subunits), as putative targets (Lu *et al.*, 2010). In this perspective, an up-regulation of miR-328 may reduce I_{CaL} density and shorten action potential duration (ADP), thus predisposing to an elevated risk of arrhythmia (Lu *et al.*, 2010).

More recently, a strong association between miR-499, that is up-regulated in AF atrial tissue samples, and the gene KCNN3, which encodes the small conductance Ca^{2+} activated K^{+} channel 3 (SK3) has been observed, suggesting a possible contribute to the electrical remodeling process (Ling *et al.*, 2013).

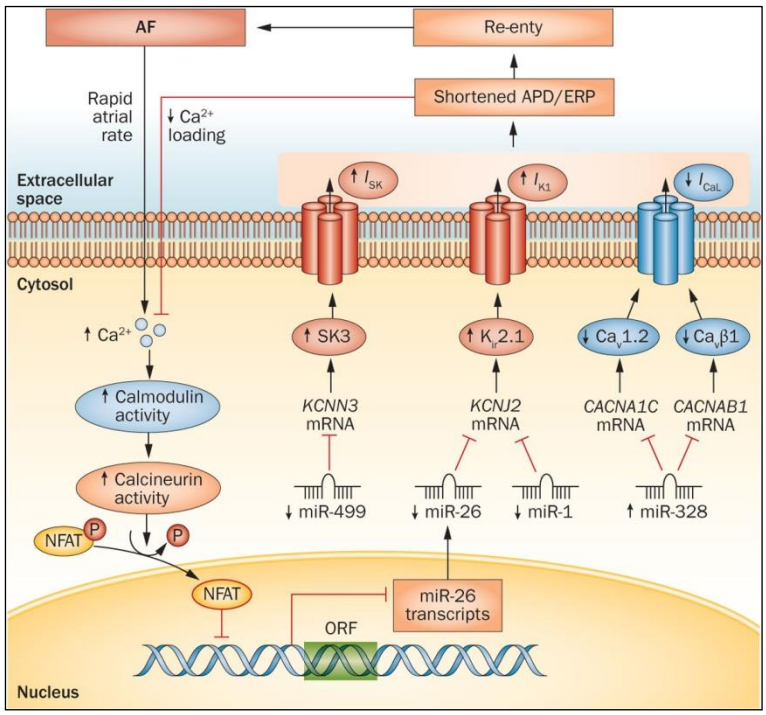

Figure C: miRNAs in AF-associated electrical remodeling (Luo *et al.*, 2015).

MiRNAs involved in structural remodeling

Structural remodeling represents a key component responsible for atrial structural changes occurred during the fibrotic process, that can be directly related to the onset of AF. Multiple miRNAs as miR-21, miR-29, miR-30 miR-133, miR-590 and miR-26 have been indicated as potential participants in the modulation of the fibrotic remodeling process during AF (**Figure D**).

miR-21, which is highly expressed in cardiac fibroblasts, targets and represses the translation of Sprouty-1 (SPRY1), which represents a negative regulator of the extracellular signal-regulated kinase ERK (a member of the mitogen-activated protein kinase family) pathway (Thum *et al.,* 2008). ERK activation promotes fibrosis, so its derepression via miR-21, which induces the downregulation of SPRY1, results pro-fibrotic. Experimental studies on animal models have shown that cardiac disfunction consequently to myocardial infarction, results in an enhanced susceptibility to AF (as a consequence of atrial fibrosis) and miR-21 up-regulation (Cardin *et al.,* 2012). The up-regulation of miR-21 was consistent with SPRY1 downregulation, and also with an increase in ERK phosphorylation. In addition, other studies demonstrated that miR-21 knockdown suppressed atrial fibrosis, preventing AF development in rats with myocardial infarction (Cardin *et al.,* 2012). It has also been observed that AF patients have increased levels of miR-21, as a result of the activation of the p21-Rac1/connective tissue factor (CTGF)/lysyl oxidase pathway (Adam *et al.,* 2012).

miR-29 has been recently suggested as a mechanistic contributor in AF, by regulating of numerous extracellular matrix genes, such as collagen, elastin and fibrillin. Experimental studies revealed a down-regulation of miR-29 in dogs with heart failure, as well as an increase in extracellular matrix proteins, predisposing to AF (Dawson *et al.,* 2013). In addition, some *in vivo* miR-29 knock-down studies have indicated an increase in collagen production, while a decrease in miR-29b expression has been observed in both atrial and blood samples from patient with AF (Dawson *et al.,* 2013).

Downregulation of miR-30 and miR-133 has been indicated to contribute to ventricular fibrosis during cardiac hypertrophy via CTGF derepression (Duisters *et al.,* 2009). Accordingly, an increase of miR-30 and miR-133 levels have been demonstrated to inversely correlate with CTGF expression in dogs with fibrosis and AF (Li *et al.,* 2012).

Some studies performed on canine models have revealed that the administration of nicotine, results in atrial fibrosis promoting AF (Shan *et al.,* 2009). In particular, TGF-β_1 and TGF-β receptor type-2 (TGFR-2) resulted upregulated in dogs treated with

nicotine, whereas the expression of miR-133 and miR-590 (which target TGF-β_1 and TGFR-2) was reduced (Shan *et al.,* 2009). Although the causal link has not been proven, the downregulation of miR-133 and miR-590 might be responsible for fibrogenesis in these animal models. This evidence suggests this mechanism a potential factor in the association between AF occurrence and cigarette smoking in humans (Andrade *et al.,* 2014).

miR-26, in addition to its role in electrical remodeling, might also contribute to atrial fibrotic remodeling by regulating the expression of the transient receptor potential channel 3 (TRPC3) (Harada *et al.,* 2012). TRPC3 is a nonselective cation channel that mediates Ca^{2+} entry in different cell types. Therefore, changes in its expression promote the activation of Ca^{2+}-dependent ERK signalling pathways, resulting in fibroblasts proliferation and differentiation which may contribute to atrial fibrosis (Harada *et al.,* 2012).

miR-208 is a highly conserved miRNA family which includes two members, miR-208a and miR-208b, that share similar nucleotide sequences. miR-208a and miR-208b (accompanied also with miR-499), are defined as "Myomirs" because they control muscle myosin content, myofiber identity, and muscle performance (van Rooij *et al.,* 2009). MiR-208 has indicated required for cardiomyocyte hypertrophy and fibrosis in response to stress and hypothyroidism (Van Roij *et al.,* 2007). Transgenic overexpression of miR-208a in the heart has demonstrated sufficient to induce hypertrophic growth in mice, as well as a pronounced repression of the miR-208 regulatory targets, such as thyroid hormone–associated protein 1 (THRAP1) and myostatin, which represent negative regulators of muscle growth and hypertrophy (Callis *et al.,* 2009). The therapeutic inhibition of miR-208a during hypertension-induced heart failure in rats have shown to prevents cardiac remodeling, improving cardiac function, overall health, and survival (Montgomery *et al.,* 2011).

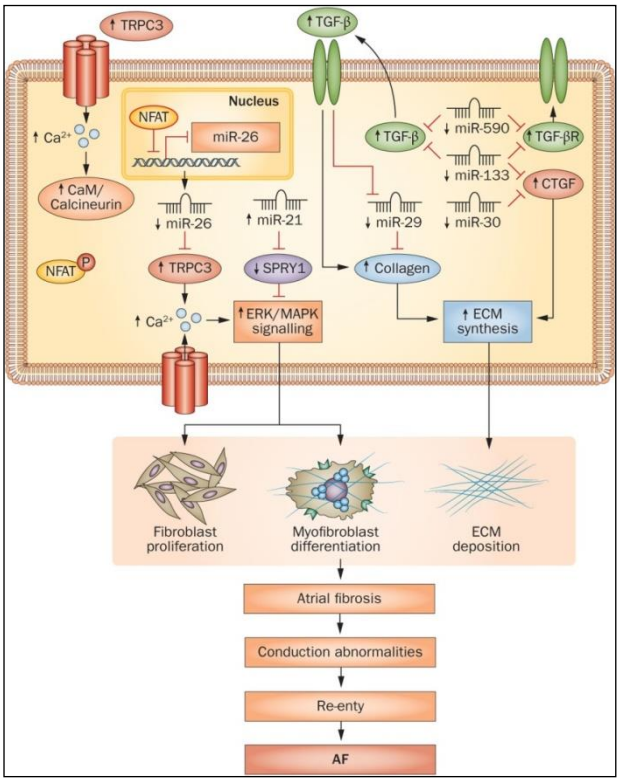

Figure D: miRNAs in AF-associated structural remodeling (Luo *et al.*, 2015).

AIM OF THE STUDY

A major advancement in the understanding of the pathogenesis of AF is the recognition that AF induces both structural and molecular alterations in the atria, which in turn promotes the recurrence and maintenance of AF (Nattel & Harada, 2014). A hallmark of structural remodeling is represented by atrial fibrosis (Allessie *et al.,* 2002; Li *et al.,* 1999), a phenomenon in which ECM components, primarily fibrillar collagen, accumulate between muscle fibers. The increase in interstital collagen influences both the mechanical and the electrical properties of the heart, increasing muscle stiffness and reducing coupling between adjacent cardiomyocytes (Weber *et al.,* 2013). A role for fibrotic tissue in wave break formation (Wu *et al.,* 1998), conduction delays and "zig-zag" course of conduction (de Bakker *et al.,* 2006; Kawara *et al.,* 2001), it is also exacerbate by the complex 3D structure of the atrium (Rodefeld *et al.,* 1997). In this perspective, a better knowledge of the fibrotic content within the myocardial tissue wall may provide novel insights of the structural features that characterize a pro-arrhythmic substrate. In particular, to date no information about the fibrotic content and the intramural distribution throughout the human atrial wall are available.

The first aim of the present study was to investigate the structural properties of the atrial tissue, which may contribute to the formation of a pro-arrhythmic substrate. By using both histological and advanced microscopy techniques, the collagen content and its 3D properties were determined in atrial tissue samples collected during cardiac surgery, in patients who developed or not AF. In particular, for the first time, the 3D intramural profile of fibrotic content was determined. In addition to a quantitative assessment, the 3D properties of collagen fibers as orientation (degree and anisotropy) and scale dimension, were evaluated by using non-linear optical microscopy techniques, such as two-photon microscopy and SHG.

In the recent years, a growing body of evidence has suggested that also an altered regulation of gene expression may play an important role in the mechanisms of atrial remodeling, which underlie AF (Kim *et al.,* 2005; Thijssen *et al.,* 2002). Nonetheless, the frequent mismatch between mRNA and protein levels of gene expression has promoted the investigation of the regulatory mechanisms, at the post-transcriptional level. In particular microRNAs, which are a class of small endogenous non-coding RNAs that negatively regulate gene expression, have shown to be involved in the control of the mechanisms governing AF, thus providing novel insights into the

molecular basis of the pathogenesis of AF (Luo *et al.*, 2015; Santulli *et al.*, 2014; Wang *et al.*, 2011).

The second aim of the study was to investigate the expression pattern of some miRNAs known to target different genes involved in diverse mechanisms that underlie AF and to correlate this with histological features, in order to find a possible relationship between the expression of miRNAs and the fibrotic content. MiRNAs expression levels were analyzed by RT-qPCR analysis of atrial tissue samples, collected from cardiac surgery patients in AF or in normal sinus rhythm. To accurately determine the levels of analyzed miRNAs, their expression data are usually normalized relatively to endogenous and/or exogenous reference genes. To date, no general agreement between different normalization strategies has been found. In addition, there is a lack of information regarding reliable housekeeping genes for miRNAs analysis in cardiac tissue, in particular for the study of AF. For these reasons, a preliminary study aiming to establish the best endogenous reference genes for miRNAs data normalization, was performed. Different well-established analysis tools were applied on five commonly used endogenous reference transcripts. The suitable reference gene thus obtained was applied to miRNAs' data normalization.

BIBLIOGRAPHY

Abed, H. S., Samuel, C. S., Lau, D. H., Kelly, D. J., Royce, S. G., Alasady, M., Mahajan, R., Kuklik, P., Zhang, Y., Brooks, A.G., Nelson, A.J., Worthley, S.G., Abhayaratna, W.P., Kalman, J.M., Wittert, G.A., Sanders, P. (2013). Obesity results in progressive atrial structural and electrical remodeling: Implications for atrial fibrillation. *Heart Rhythm: the official journal of the Heart Rhythm Society*, 10(1):90–100.

Adam, O., Löhfelm, B., Thum, T., Gupta, S. K., Puhl, S.-L., Schäfers, H.-J., Böhm, M., Laufs, U. (2012). Role of miR-21 in the pathogenesis of atrial fibrosis. *Basic Research in Cardiology*, 107(5):278.

Ahmed, M. S., Øie, E., Vinge, L. E., Yndestad, A., Andersen, G. Ø., Andersson, Y., Attramadal, T., Attramadal, H. (2004). Connective tissue growth factor - A novel mediator of angiotensin II-stimulated cardiac fibroblast activation in heart failure in rats. *Journal of Molecular and Cellular Cardiology*, 36(3):393–404.

Allessie, M., Ausma, J., Schotten, U. (2002). Electrical, contractile and structural remodeling during atrial fibrillation. *Cardiovascular Research*, 54(2):230–246.

Ambros, V. (2004). The functions of animal microRNAs. *Nature*, 431(7006):350–5.

Andrade, J., Khairy, P., Dobrev, D., Nattel, S. (2014). The clinical profile and pathophysiology of atrial fibrillation: Relationships among clinical features, epidemiology, and mechanisms. *Circulation Research*, 114(9):1453–1468.

Anné, W., Willems, R., Roskams, T., Sergeant, P., Herijgers, P., Holemans, P., Ector, H., Heidbüchel, H. (2005). Matrix metalloproteinases and atrial remodeling in patients with mitral valve disease and atrial fibrillation. *Cardiovascular Research*, 67(4): 655–666.

Anumonwo, J. M., Kalifa, J. (2014). Risk Factors and Genetics of Atrial Fibrillation. *Cardiology Clinics*, 32(4):485–494.

Armstrong, J. R., Ferguson, M. W. (1995). Ontogeny of the skin and the transition from scar-free to scarring phenotype during wound healing in the pouch young of a marsupial, Monodelphis domestica. *Developmental Biology*, 169(1):242–260.

Attisano, L., Wrana, J. L. (2002). Signal transduction by the TGF-beta superfamily. *Science (New York, N.Y.)*, 296(5573):1646–1647.

Bartel, D. P. (2004). MicroRNAs: genomics, biogenesis, mechanism, and function. *Cell*, 116(2):281–297.

Beckmann, B. M., Holinski-Feder, E., Walter, M. C., Haserück, N., Reithmann, C., Hinterseer, M., … Kääb, S. (2010). Laminopathy presenting as familial atrial fibrillation. *International Journal of Cardiology*, 145(2):394–396.

Beharier, O., Etzion, Y., Katz, A., Friedman, H., Tenbosh, N., Zacharish, S., Bereza, S., Goshen, U., Moran, A. (2007). Crosstalk between L-type calcium channels and ZnT-1, a new player in rate-dependent cardiac electrical remodeling. *Cell Calcium*, 42(1):71–82.

Benito, B., Brugada, R., Perich, R. M., Lizotte, E., Cinca, J., Mont, L., … Brugada, J. (2008). A mutation in the sodium channel is responsible for the association of long QT syndrome and familial atrial fibrillation. *Heart Rhythm*, 5(10):1434-1440.

Benjamin, E. J., Rice, K. M., Arking, D. E., Pfeufer, A., van Noord, C., Smith, A. V, … Witteman, J. C. M. (2009). Variants in ZFHX3 are associated with atrial fibrillation in individuals of European ancestry. *Nature Genetics*, 41(8):879-881.

Berenji, K., Drazner, M. H., Rothermel, B. A., Hill, J. A. (2005). Does load-induced ventricular hypertrophy progress to systolic heart failure? *American Journal of Physiology. Heart and Circulatory Physiology*, 289(1):H8–H16.

Berezikov, E. (2011). Evolution of microRNA diversity and regulation in animals. *Nature Reviews Genetics*, 12(12):846–860.

Bernardo, B. C., Weeks, K. L., Pretorius, L., McMullen, J. R. (2010). Molecular distinction between physiological and pathological cardiac hypertrophy: Experimental findings and therapeutic strategies. *Pharmacology and Therapeutics*, 128(1):191–227.

Bishop, J. E., Laurent, G. J. (1995). Collagen turnover and its regulation in the normal and hypertrophying heart. *European Heart Journal*, 16 Suppl C:38–44.

Boldt, A., Wetzel, U., Lauschke, J., Weigl, J., Gummert, J., Hindricks, G., Kottkamp, H., Dhein, S. (2004). Fibrosis in left atrial tissue of patients with atrial fibrillation with and without underlying mitral valve disease. *Heart (British Cardiac Society)*, 90(4):400–405.

Brás-Rosário, L., Matsuda, A., Pinheiro, A. I., Gardner, R., Lopes, T., Amaral, A., Gama-Carvalho, M. (2013). Expression profile of microRNAs regulating proliferation and differentiation in mouse adult cardiac stem cells. *PloS One*, 8(5): e63041.

Brower, G. L., Gardner, J. D., Forman, M. F., Murray, D. B., Voloshenyuk, T., Levick, S. P., Janicki, J. S. (2006). The relationship between myocardial extracellular matrix remodeling and ventricular function. *European Journal of Cardio-Thoracic Surgery*, 30(4):604–610.

Brundel, B. J., Van Gelder, I. C., Henning, R. H., Tieleman, R. G., Tuinenburg, A. E., Wietses, M., Grandjean, J. G., Van Gilst, W.H., Crijns, H. J. (2001). Ion channel remodeling is related to intraoperative atrial effective refractory periods in patients with paroxysmal and persistent atrial fibrillation. *Circulation*, 103(5):684–690.

Brundel, B. J., Ausma, J., van Gelder, I. C., Van der Want, J. J., van Gilst, W. H., Crijns, H. J., Henning, R. H. (2002). Activation of proteolysis by calpains and structural changes in human paroxysmal and persistent atrial fibrillation. *Cardiovascular Research*, 54(2):380–389.

Burgess, M. L., Buggy, J., Price, R. L., Abel, F. L., Terracio, L., Samarel, A. M., Borg, T. K. (1996). Exercise- and hypertension-induced collagen changes are related to left ventricular function in rat hearts. *The American Journal of Physiology*, 270(1 Pt 2):H151-159.

Burstein, B., Libby, E., Calderone, A., Nattel, S. (2008). Differential behaviors of atrial versus ventricular fibroblasts: A potential role for platelet-derived growth factor in atrial-ventricular remodeling differences. *Circulation*, 117(13):1630–1641.

Burstein, B., Nattel, S. (2008). Atrial Fibrosis: Mechanisms and Clinical Relevance in Atrial Fibrillation. *Journal of the American College of Cardiology*, 51(8):802–809.

Burstein, B., Comtois, P., Michael, G., Nishida, K., Villeneuve, L., Yeh, Y. H., Nattel, S. (2009). Changes in connexin expression and the atrial fibrillation substrate in congestive heart failure. *Circulation Research*, 105(12):1213–1222.

Butt, R. P., Bishop, J. E. (1997). Mechanical load enhances the stimulatory effect of serum growth factors on cardiac fibroblast procollagen synthesis. *Journal of Molecular and Cellular Cardiology*, 29(4):1141–1151.

Calderone, A., Thaik, C. M., Takahashi, N., Chang, D. L., Colucci, W. S. (1998). Nitric oxide, atrial natriuretic peptide, and cyclic GMP inhibit the growth-promoting effects of norepinephrine in cardiac myocytes and fibroblasts. *The Journal of Clinical Investigation*, 101(4):812–818.

Callis, T. E., Pandya, K., Hee, Y. S., Tang, R. H., Tatsuguchi, M., Huang, Z. P., … Wang, D. Z. (2009). MicroRNA-208a is a regulator of cardiac hypertrophy and conduction in mice. *Journal of Clinical Investigation*, 119(9):2772-2786.

Canty, E. G., Kadler, K. E. (2005). Procollagen trafficking, processing and fibrillogenesis. *Journal of Cell Science*, 118(Pt 7):1341-1353.

Cardin, S., Guasch, E., Luo, X., Naud, P., Le Quang, K., Shi, Y., Tardif, J.C., Comtois, P., Nattel, S. (2012). Role for MicroRNA-21 in atrial profibrillatory fibrotic remodeling associated with experimental postinfarction heart failure. *Circulation. Arrhythmia and Electrophysiology*, 5(5):1027–1035.

Carnes, C. A., Janssen, P. M. L., Ruehr, M. L., Nakayama, H., Nakayama, T., Haase, H., Bauer, J. A., Chung, M. K., Fearon, I. M., Gillinov, A. M., Hamlin, R. L., Van Wagoner, D. R. (2007). Atrial glutathione content, calcium current, and contractility. *Journal of Biological Chemistry*, 282(38):28063–28073.

Carthew, R. W., Sontheimer, E. J. (2009). Origins and Mechanisms of miRNAs and siRNAs. *Cell*, 136(4):642–655.

Carver, W., Nagpal, M. L., Nachtigal, M., Borg, T. K., Terracio, L. (1991). Collagen expression in mechanically stimulated cardiac fibroblasts. *Circulation Research*, 69(1):116–122.

Caulfield, J. B., Borg, T. K. (1979). The collagen network of the heart. *Laboratory Investigation; a journal of technical methods and pathology*, 40(3):364–372.

Cha, T. J., Ehrlich, J. R., Chartier, D., Qi, X. Y., Xiao, L., Nattel, S. (2006). Kir3-based inward rectifier potassium current: Potential role in atrial tachycardia remodeling effects on atrial repolarization and arrhythmias. *Circulation*, 113(14):1730–1737.

Chen, J. F., Mandel, E. M., Thomson, J. M., Wu, Q., Callis, T. E., Hammond, S. M., Conlon, F. L., Wang, D. Z. (2006). The role of microRNA-1 and microRNA-133 in skeletal muscle proliferation and differentiation. *Nature Genetics*, 38(2):228–233.

Chen, M. M., Lam, A., Abraham, J. A., Schreiner, G. F., Joly, A. H. (2000). CTGF expression is induced by TGF- beta in cardiac fibroblasts and cardiac myocytes: a potential role in heart fibrosis. *Journal of Molecular and Cellular Cardiology*, 32(10):1805–1819.

Chinchilla, A., Daimi, H., Lozano-Velasco, E., Dominguez, J. N., Caballero, R., Delpón, E., Tamargo, J., Cinca, J., Hove-Madsen, L., Aranega, A. E., Franco, D. (2011). PITX2 insufficiency leads to atrial electrical and structural remodeling linked to arrhythmogenesis. *Circulation. Cardiovascular Genetics*, 4(3):269–279.

Christ, T., Boknik, P., Wöhrl, S., Wettwer, E., Graf, E. M., Bosch, R. F., Knaut, M., Schmitz, W., Ravens, U., Dobrev, D. (2004). L-type Ca^{2+} current downregulation in chronic human atrial fibrillation is associated with increased activity of protein phosphatases. *Circulation*, 110(17): 2651–2657.

Chugh, S. S., Havmoeller, R., Narayanan, K., Singh, D., Rienstra, M., Benjamin, E. J., Gillum, R. F., Kim, Y. H., McAnulty, J. H. Jr., Zheng, Z. J., Forouzanfar, M. H., Naghavi, M., Mensah, G. A., Ezzati, M., Murray, C. J. (2014). Worldwide epidemiology of atrial fibrillation: A global burden of disease 2010 study. *Circulation*, 129(8):837–847.

Cleutjens, J. P., Kandala, J. C., Guarda, E., Guntaka, R. V., Weber K. T. (1995). Regulation of collagen degradation in the rat myocardium after infarction. *Journal of Molecular and Cellular Cardiology*, 27(6):1281–1292.

Corradi, D., Callegari, S., Maestri, R., Benussi, S., Alfieri, O. (2008). Structural remodeling in atrial fibrillation. *Nature Clinical Practice. Cardiovascular Medicine*, 5(12):782–796.

Corradi, D. (2014). Atrial fibrillation from the pathologist's perspective. *Cardiovascular Pathology*, 23(2):71–84.

Courtemanche, M., Ramirez, R. J., Nattel, S. (1999). Ionic targets for drug therapy and atrial fibrillation-induced electrical remodeling: Insights from a mathematical model. *Cardiovascular Research*, 42(2):477–489.

Cullen, B. R. (2004). Transcription and processing of human microRNA precursors. *Molecular Cell*, 16(6):861–865.

D'Armiento, J. (2002). Matrix metalloproteinase disruption of the extracellular matrix and cardiac dysfunction. *Trends in Cardiovascular Medicine*, 12(3):97-101.

Das, S., Makino, S., Melman, Y. F., Shea, M. A., Goyal, S. B., Rosenzweig, A., … Ellinor, P. T. (2009). Mutation in the S3 segment of KCNQ1 results in familial lone atrial fibrillation. *Heart Rhythm*, 6(8):1146-1153.

Dawson, K., Wakili, R., Ördög, B., Clauss, S., Chen, Y., Iwasaki, Y., Voigt, N., Qi, X. Y., Sinner, M. F., Dobrev, D., Kääb, S., Nattel S. (2013). MicroRNA29: A mechanistic contributor and potential biomarker in atrial fibrillation. *Circulation*, 127(14):1466–1475.

de Bakker, J. M., van Rijen, H. M. (2006). Continuous and discontinuous propagation in heart muscle. *Journal of Cardiovascular Electrophysiology*, 17(5):567-573.

De Vos, C. B., Pisters, R., Nieuwlaat, R., Prins, M. H., Tieleman, R. G., Coelen, R. J., van den Heijkant, A. C., Allessie, M. A., Crijns, H. J. (2010). Progression From Paroxysmal to Persistent Atrial Fibrillation. Clinical Correlates and Prognosis. *Journal of the American College of Cardiology*, 55(8):725–731.

Denli, A. M., Tops, B. B., Plasterk, R. H., Ketting, R. F., Hannon, G. J. (2004). Processing of primary microRNAs by the Microprocessor complex. *Nature*, 432(7014):231–235.

Deshmukh, A., Barnard, J., Sun, H., Newton, D., Castel, L., Pettersson, G., … Chung, M. K. (2015). Left atrial transcriptional changes associated with atrial fibrillation susceptibility and persistence. *Circulation: Arrhythmia and Electrophysiology*, 8(1):32-41.

Dhamoon, A. S., Jalife, J. (2005). The inward rectifier current (I_{K1}) controls cardiac excitability and is involved in arrhythmogenesis. *Heart Rhythm*, 2(3):316–324.

Disertori M, Masè M, Narula N, Mazzola S, dal Piaz EC, Quintarelli S, Cristoforetti A, Marini M, Ravelli F, Arbustini E. (2016) Atrial fibrillation and NPPA gene p.S64R mutation: are cardiologists helpless spectators of healthy mutation carriers? *J Cardiovasc Med (Hagerstown)*,17(3):177-180.

Dobrev, D., Friedrich, A., Voigt, N., Jost, N., Wettwer, E., Christ, T., Knaut, M., Ravens, U. (2005). The G protein-gated potassium current $I_{K,ACh}$ is constitutively active in patients with chronic atrial fibrillation. *Circulation*, 112(24):3697–3706.

Dobrev, D., Graf, E., Wettwer, E., Himmel, H. M., Hála, O., Doerfel, C., Christ, T., Schüler, S., Ravens, U. (2001). Molecular Basis of Downregulation of G-Protein-Coupled Inward Rectifying K^+ Current ($I_{K,ACh}$) in Chronic Human Atrial Fibrillation: Decrease in GIRK4 mRNA Correlates With Reduced $I_{K,ACh}$ and Muscarinic Receptor-Mediated Shortening of Action Potentials. *Circulation*, 104(21):2551–2557.

Dobrev, D., Nattel, S. (2010). New antiarrhythmic drugs for treatment of atrial fibrillation. *Lancet*, 375(9721):1212–1223.

Dobrev, D., Voigt, N., Wehrens, X. H. (2011). The ryanodine receptor channel as a molecular motif in atrial fibrillation: Pathophysiological and therapeutic implications. *Cardiovascular Research*, 89(4):734-743.

Driessen, N. J., Boerboom, R. A, Huyghe, J. M., Bouten, C. V, Baaijens, F. P. (2003). Computational analyses of mechanically induced collagen fiber remodeling in the aortic heart valve. *Journal of Biomechanical Engineering*, 125(4):549–557.

Duisters, R. F., Tijsen, A. J., Schroen, B., Leenders, J. J., Lentink, V., van der Made, I., Herias, V., van Leeuwen, R. E., Schellings, M. W., Barenbrug, P., Maessen, J. G., Heymans, S., Pinto, Y. M., Creemers, E. E. (2009). miR-133 and miR-30 regulate connective tissue growth factor: implications for a role of microRNAs in myocardial matrix remodeling. *Circulation Research*, 104(2):170–178.

Dvinge, H., Git, A., Gräf, S., Salmon-Divon, M., Curtis, C., Sottoriva, A., Zhao, Y., Hirst, M., Armisen, J., Miska, E. A., Chin, S. F., Provenzano, E., Turashvili, G., Green, A., Ellis, I., Aparicio, S., Caldas, C. (2013). The shaping and functional consequences of the microRNA landscape in breast cancer. *Nature*, 497(7449):378–382.

Ehrlich, J. R., Cha, T. J., Zhang, L., Chartier, D., Villeneuve, L., Hébert, T. E., Nattel, S. (2004). Characterization of a hyperpolarization-activated time-dependent potassium current in canine cardiomyocytes from pulmonary vein myocardial sleeves and left atrium. T*he Journal of Physiology*, 557(Pt 2):583–597.

Ehrlich, J. R., Hohnloser, S. H., Nattel, S. (2006). Role of angiotensin system and effects of its inhibition in atrial fibrillation: clinical and experimental evidence. *European Heart Journal*, 27(5):512–518.

Ellinor, P. T., Yoerger, D. M., Ruskin, J. N., & MacRae, C. A. (2005). Familial aggregation in lone atrial fibrillation. *Human Genetics*, 118(2):179–184.

Ellinor, P. T., Lunetta, K. L., Glazer, N. L., Pfeufer, A., Alonso, A., Chung, M. K., … Kääb, S. (2010). Common variants in KCNN3 are associated with lone atrial fibrillation. *Nature Genetics*, 42(3):240-244.

Ellinor, P. T., Lunetta, K. L., Albert, C. M., Glazer, N. L., Ritchie, M. D., Smith, A. V, … Kääb, S. (2012). Meta-analysis identifies six new susceptibility loci for atrial fibrillation. *Nature Genetics*, 44(6):670-675.

Factor, S. M., Robinson, T. F. (1988). Comparative connective tissue structure-function relationships in biologic pumps. *Laboratory Investigation; a journal of technical methods and pathology*, 58(2):150–156.

Fox, C. S., Parise, H., D'Agostino, R. B., Lloyd-Jones, D. M., Vasan, R. S., Wang, T. J., … Benjamin, E. J. (2004). Parental atrial fibrillation as a risk factor for atrial fibrillation in offspring. *JAMA: The Journal of the American Medical Association*, 291(23):2851–2855.

Franco, D., Chinchilla, A., & Aránega, A. E. (2012). Transgenic insights linking Pitx2 and atrial arrhythmias. *Frontiers in Physiology*, 3:206.

Friedman, R. C., Farh, K. K., Burge, C. B., Bartel, D. P. (2009). Most mammalian mRNAs are conserved targets of microRNAs. *Genome Research*, 19(1):92–105.

Frustaci, A., Chimenti, C., Bellocci, F., Morgante, E., Russo, M. A., Maseri, A. (1997). Histological substrate of atrial biopsies in patients with lone atrial fibrillation. *Circulation*, 96(4):1180–1184.

Fuster, V., Rydén, L. E., Cannom, D. S., Crijns, H. J., Curtis, A. B., Ellenbogen, K. A., Halperin, J. L., Le Heuzey, J. Y., Kay, G. N., Lowe, J. E., Olsson, S. B., Prystowsky, E. N., Tamargo, J. L., Wann, S., Smith, S. C. Jr., Jacobs, A. K., Adams, C. D., Anderson, J. L., Antman, E. M., Halperin, J. L., Hunt, S. A., Nishimura, R., Ornato, J. P., Page, R. L., Riegel, B., Priori, S. G., Blanc, J. J.,…. Zamorano, J. L. College of Cardiology/American Heart Association Task Force on Practice Guide lines; European Society of Cardiology Committee for Practice Guidelines; European Heart Rhythm Association; Heart Rhythm Society (2006). ACC/AHA/ESC 2006 Guidelines for the Management of Patients with Atrial Fibrillation: a report of the American College of Cardiology/American Heart Association Task Force on Practice Guidelines and the European Society of Cardiology Committee for Practice. *Circulation*, 114(7):e257–354.

Gaborit, N., Steenman, M., Lamirault, G., Le Meur, N., Le Bouter, S., Lande, G., Léger, J., Charpentier, F., Christ, T., Dobrev, D., Escande, D., Nattel, S., Demolombe, S. (2005). Human atrial ion channel and transporter subunit gene-expression remodeling associated with valvular heart disease and atrial fibrillation. *Circulation*, 112(4):471–481.

Gan, Z., Rumsey, J., Hazen, B. C., Lai, L., Leone, T. C., Vega, R. B., Xie, H., Conley, K. E., Auwerx, J., Smith, S. R., Olson, E. N., Kralli, A., Kelly, D. P. (2013). Nuclear receptor/microRNA circuitry links muscle fiber type to energy metabolism. *The Journal of Clinical Investigation*, 123(6):2564–2575.

Girmatsion, Z., Biliczki, P., Bonauer, A., Wimmer-Greinecker, G., Scherer, M., Moritz, A., Bukowska, A., Goette, A., Nattel, S., Hohnloser, S. H., Ehrlich, J. R. (2009). Changes in microRNA-1 expression and IK1 up-regulation in human atrial fibrillation. *Heart Rhythm: the official journal of the Heart Rhythm Society*, 6(12): 1802–1809.

Go, A. S., Hylek, E. M., Phillips, K. A., Chang, Y., Henault, L. E., Selby, J. V., Singer, D. E. (2001). Prevalence of diagnosed atrial fibrillation in adults: national implications for rhythm management and stroke prevention: the AnTicoagulation and Risk Factors in Atrial Fibrillation (ATRIA) Study. *JAMA*, 285(18):2370-2375.

Goette, A., Arndt, M., Röcken, C., Staack, T., Bechtloff, R., Reinhold, D., Huth, C., Ansorge, S., Klein, H. U., Lendeckel, U. (2002). Calpains and cytokines in fibrillating human atria. *American Journal of Physiology. Heart and Circulatory Physiology*, 283(1):H264–H272.

Gollob, M. H., Green, M. S., Tang, A. S., Gollob, T., Karibe, A., Ali Hassan, A. S., … Hassan, A. S. (2001). Identification of a gene responsible for familial Wolff-Parkinson-White syndrome. *The New England Journal of Medicine*, 344(24): 1823–1831.

Gollob, M. H., Jones, D. L., Krahn, A. D., Danis, L., Gong, X.-Q., Shao, Q., … Bai, D. (2006). Somatic mutations in the connexin 40 gene (GJA5) in atrial fibrillation. *The New England Journal of Medicine*, 354(25):2677-2688.

Gomez, D. E., Alonso, D. F., Yoshiji, H., Thorgeirsson, U. P. (1997). Tissue inhibitors of metalloproteinases: structure, regulation and biological functions. *European Journal of Cell Biology*, 74(2):111–122.

Gramley, F., Lorenzen, J., Knackstedt, C., Rana, O. R., Saygili, E., Frechen, D., Stanzel, S., Pezzella, F., Koellensperger, E., Weiss, C., Münzel, T., Schauerte, P. (2009). Age-related atrial fibrosis. *Age (Dordrecht, Netherlands)*, 31(1):27–38.

Grammer, J. B., Böhm, J., Dufour, A., Benz, M., Lange, R., Bauernschmitt, R. (2005). Atrial fibrosis in heart surgery patients. Decreased collagen III/I ratio in postoperative atrial fibrillation. *Basic Research in Cardiology*, 100(3):288–294.

Gregory, R. I., Chendrimada, T. P., Cooch, N., Shiekhattar, R. (2005). Human RISC couples microRNA biogenesis and posttranscriptional gene silencing. *Cell*, 123(4): 631–640.

Greiser, M., Halaszovich, C. R., Frechen, D., Boknik, P., Ravens, U., Dobrev, D., Lückhoff, A., Schotten, U. (2007). Pharmacological evidence for altered src kinase regulation of I Ca,L in patients with chronic atrial fibrillation. *Naunyn-Schmiedeberg's Archives of Pharmacology*, 375(6):383–392.

Grundvold, I., Bodegard, J., Nilsson, P. M., Svennblad, B., Johansson, G., Östgren, C. J., Sundström, J. (2015). Body weight and risk of atrial fibrillation in 7,169 patients with newly diagnosed type 2 diabetes; an observational study. *Cardiovascular Diabetology*, 14:5.

Gudbjartsson, D. F., Arnar, D. O., Helgadottir, A., Gretarsdottir, S., Holm, H., Sigurdsson, A., … Stefansson, K. (2007). Variants conferring risk of atrial fibrillation on chromosome 4q25. *Nature*, 448(7151):353–357.

Harada, M., Luo, X., Qi, X. Y., Tadevosyan, A., Maguy, A., Ordog, B., Ledoux J., Kato, T., Naud, P., Voigt, N., Shi, Y., Kamiya, K., Murohara, T., Kodama, I., Tardif, J. C., Schotten, U., Van Wagoner, D. R., Dobrev, D., Nattel S. (2012). Transient receptor potential canonical-3 channel-dependent fibroblast regulation in atrial fibrillation. *Circulation*, 126(17):2051–2064.

Hodgson-Zingman, D. M., Karst, M. L., Zingman, L. V, Heublein, D. M., Darbar, D., Herron, K. J., … Olson, T. M. (2008). Atrial natriuretic peptide frameshift mutation in familial atrial fibrillation. *The New England Journal of Medicine*, 359(2):158–65.

Hoit, B. D., Takeishi, Y., Cox, M. J., Gabel, M., Kirkpatrick, D., Walsh, R. A., Tyagi, S. C. (2002). Remodeling of the left atrium in pacing-induced atrial cardiomyopathy. *Molecular and Cellular Biochemistry*, 238(1-2):145-150.

Hong, K., Bjerregaard, P., Gussak, I., & Brugada, R. (2005). Short QT syndrome and atrial fibrillation caused by mutation in KCNH2. *Journal of Cardiovascular Electrophysiology*, 16(4):394-396.

Huang, R. T., Xue, S., Xu, Y. J., Zhou, M., & Yang, Y. Q. (2013). A novel NKX2.5 loss-of-function mutation responsible for familial atrial fibrillation. *International Journal of Molecular Medicine*, 31(5):1119-1126.

Hunyady, L., Catt, K. J. (2006). Pleiotropic AT1 receptor signaling pathways mediating physiological and pathogenic actions of angiotensin II. *Molecular Endocrinology (Baltimore, Md.)*, 20(5):953–970.

Ihida-Stansbury, K., McKean, D. M., Gebb, S. A., Martin, J. F., Stevens, T., Nemenoff, R., … Jones, P. L. (2004). Paired-related homeobox gene Prx1 is required for pulmonary vascular development. *Circulation Research*, 94(11):1507-1514.

Iwasaki, Y. K., Nishida, K., Kato, T., Nattel, S. (2011). Atrial fibrillation pathophysiology: implications for management. *Circulation*, 124(20):2264–2274.

Iwasaki, Y., Kato, T., Xiong, F., Shi, Y. F., Naud, P., Maguy, A., Mizuno, K., Tardif, J. C., Comtois, P., Nattel, S. (2014). Atrial Fibrillation Promotion With Long-Term Repetitive Obstructive Sleep Apnea in a Rat Model. *Journal of the American College of Cardiology*, 64(19):2013–2023.

Ju, H., Dixon, I. M. (1996). Extracellular matrix and cardiovascular diseases. *The Canadian Journal of Cardiology*, 12(12):1259–1267.

Kagan, H. M., Trackman, P. C. (1991). Properties and function of lysyl oxidase. *American Journal of Respiratory Cell and Molecular Biology*, 5(3):206–210.

Kakkar, R., Lee, R. T. (2010). Intramyocardial fibroblast myocyte communication. *Circulation Research*, 106(1):47–57.

Kannel, W. B., Wolf, P. A., Benjamin, E. J., Levy, D. (1998). Prevalence, incidence, prognosis, and predisposing conditions for atrial fibrillation: population-based estimates. *The American Journal of Cardiology*, 82(8A):2N–9N.

Katz, A. M. (2002). Proliferative signaling and disease progression in heart failure. *Circulation journal: official journal of the Japanese Circulation Society*, 66(3): 225–231.

Kawara, T., Derksen, R., de Groot, J. R., Coronel, R., Tasseron, S., Linnenbank, A. C., Hauer , R. N., Kirkels, H., Janse, M. J., de Bakker, J. M. (2001). Activation delay after premature stimulation in chronically diseased human myocardium relates to the architecture of interstitial fibrosis. *Circulation*, 104(25):3069–3075.

Kazemian, P., Gollob, M. H., Pantano, A., & Oudit, G. Y. (2011). A Novel Mutation in the RYR2 Gene Leading to Catecholaminergic Polymorphic Ventricular Tachycardia and Paroxysmal Atrial Fibrillation: Dose-Dependent Arrhythmia-Event Suppression by β-Blocker Therapy. *Canadian Journal of Cardiology*, 27(6):870.

Kim, N. H., Ahn, Y., Oh, S. K., Cho, J. K., Park, H. W., Kim, Y. S., Hong, M. H., Nam, K. I., Park, W. J., Jeong, M. H., Ahn, B. H., Choi, J. B., Kook, H., Park, J. C., Jeong, J. W., Kang, J. C. (2005). Altered patterns of gene expression in response to chronic atrial fibrillation, *International Heart Journal*, 46(3):383-395.

Kim, V. N., Han, J., Siomi, M. C. (2009). Biogenesis of small RNAs in animals. *Nature Reviews. Molecular Cell Biology*, 10(2):126–139.

Kirchhof, P., Kahr, P. C., Kaese, S., Piccini, I., Vokshi, I., Scheld, H. H., … Brown, N.

A. (2011). PITX2c is expressed in the adult left atrium, and reducing Pitx2c expression promotes atrial fibrillation inducibility and complex changes in gene expression. *Circulation: Cardiovascular Genetics*, 4(2):123-133.

Kneller, J., Sun, H., Leblanc, N., Nattel, S. (2002). Remodeling of Ca^{2+}-handling by atrial tachycardia: Evidence for a role in loss of rate-adaptation. *Cardiovascular Research*, 54(2):416–426.

Kneller, J., Zou, R., Vigmond, E. J., Wang, Z., Leon, L. J., Nattel, S. (2002). Cholinergic atrial fibrillation in a computer model of a two-dimensional sheet of canine atrial cells with realistic ionic properties. *Circulation Research*, 90(9):E73–E87.

Kumagai, K., Nakashima, H., Urata, H., Gondo, N., Arakawa, K., Saku, K. (2003). Effects of angiotensin II type 1 receptor antagonist on electrical and structural remodeling in atrial fibrillation. *Journal of the American College of Cardiology*, 41(12):2197–2204.

Lagos-Quintana, M., Rauhut, R., Yalcin, A., Meyer, J., Lendeckel, W., & Tuschl, T. (2002). Identification of tissue-specific MicroRNAs from mouse. *Current Biology*, 12(9):735–739.

Latronico, M. V., Condorelli, G. (2008). On the road to the definition of the cardiac miRNome in human disease states. *Journal of Molecular and Cellular Cardiology*, 45(2):162–164.

Laurent, G. J. (1987). Dynamic state of collagen: pathways of collagen degradation in vivo and their possible role in regulation of collagen mass. *The American Journal of Physiology*, 252(1 Pt 1):C1–C9.

Li, D., Fareh, S., Leung, T. K., Nattel, S. (1999). Promotion of atrial fibrillation by heart failure in dogs: atrial remodeling of a different sort. *Circulation*, 100(1):87–95.

Li, D., Shinagawa, K., Pang, L., Leung, T. K., Cardin, S., Wang, Z., Nattel, S. (2001). Effects of Angiotensin-Converting Enzyme Inhibition on the Development of the Atrial Fibrillation Substrate in Dogs With Ventricular Tachypacing-Induced Congestive Heart Failure. *Circulation*, 104(21), 2608–2614.

Li, H., Li, S., Yu, B., Liu, S. (2012). Expression of miR-133 and miR-30 in chronic atrial fibrillation in canines. *Molecular Medicine Reports*, 5(6):1457–1460.

Li, R. G., Wang, Q., Xu, Y. J., Zhang, M., Qu, X. K., Liu, X., … Yang, Y. Q. (2013). Mutations of the SCN4B-encoded sodium channel β4 subunit in familial atrial fibrillation. *International Journal of Molecular Medicine*, 32(1):144-150.

Li, Y. Y., McTiernan, C. F., Feldman, A. M. (2000). Interplay of matrix metalloproteinases, tissue inhibitors of metalloproteinases and their regulators in cardiac matrix remodeling. *Cardiovascular Research*, 46(2):214–224.

Liang, Y., Ridzon, D., Wong, L., Chen, C. (2007). Characterization of microRNA expression profiles in normal human tissues. *BMC Genomics*, 8:166.

Ling, T. Y., Wang, X. L., Chai, Q., Lau, T. W., Koestler, C. M., Park, S. J., Daly, R. C., Greason, K. L., Jen, J., Wu, L. Q., Shen, W. F., Shen, W. K., Cha, Y. M., Lee, H. C. (2013). Regulation of the SK3 channel by microRNA-499 - Potential role in atrial fibrillation. *Heart Rhythm*, 10(7):1001–1009.

Liu, X., Wang, F., Knight, A. C., Zhao, J., & Xiao, J. (2012). Common variants for atrial fibrillation: Results from genome-wide association studies. *Human Genetics*, 131(1):33-39.

Lloyd-Jones, D. M., Wang, T. J., Leip, E. P., Larson, M. G., Levy, D., Vasan, R. S., … Benjamin, E. J. (2004). Lifetime risk for development of atrial fibrillation: The framingham heart study. *Circulation*, 110(9):1042–1046.

Lu, Y., Zhang, Y., Wang, N., Pan, Z., Gao, X., Zhang, F., Zhang, Y., Shan, H., Luo, X., Bai, Y., Sun, L., Song, W., Xu, C., Wang, Z., Yang, B. (2010). MicroRNA-328 Contributes to Adverse Electrical Remodeling in Atrial Fibrillation/Clinical Perspective. Circulation, 122(23):2378–2387.

Lund, E., Güttinger, S., Calado, A., Dahlberg, J. E., Kutay, U. (2004). Nuclear export of microRNA precursors. *Science (New York, N.Y.)*, 303(5654):95–98.

Luo, X., Zhang, H., Xiao, J., Wang, Z. (2010). Regulation of human cardiac ion channel genes by microRNAs: theoretical perspective and pathophysiological implications. *Cellular Physiology and Biochemistry*, 25(6):571–586.

Luo, X., Pan, Z., Shan, H., Xiao, J., Sun, X., Wang, N., Lin, H., Xiao, L., Maguy, A., Qi, X. Y., Li, Y., Gao, X., Dong, D., Zhang, Y., Bai, Y., Ai, J., Sun, L., Lu, H., Luo, X. Y., Wang, Z., Lu, Y., Yang, B., Nattel S. (2013). MicroRNA-26 governs profibrillatory inward-rectifier potassium current changes in atrial fibrillation. *The Journal of Clinical Investigation*, 123(5):1939–1951.

Luo, X., Yang, B., Nattel, S. (2015). MicroRNAs and atrial fibrillation: mechanisms and translational potential. *Nature Reviews Cardiology*, 12(2):80-90.

Macri, V., Mahida, S. N., Zhang, M. L., Sinner, M. F., Dolmatova, E. V., Tucker, N. R., … Ellinor, P. T. (2014). A novel trafficking-defective HCN4 mutation is associated with early-onset atrial fibrillation. *Heart Rhythm*, 11, 1055–1062.

Makiyama, T., Akao, M., Shizuta, S., Doi, T., Nishiyama, K., Oka, Y., … Horie, M. (2008). A Novel SCN5A Gain-of-Function Mutation M1875T Associated With Familial Atrial Fibrillation. *Journal of the American College of Cardiology*, 52(16):1326-1334.

Manolio, T. A., Collins, F. S., Cox, N. J., Goldstein, D. B., Hindorff, L. A., Hunter, D. J., … Visscher, P. M. (2009). Finding the missing heritability of complex diseases. *Nature*, 461(7265):747–753.

Martin, R. I. R., Babaei, M. S., Choy, M.-K., Owens, W. A., Chico, T. J. A., Keenan, D., … Keavney, B. D. (2015). Genetic variants associated with risk of atrial fibrillation regulate expression of PITX2, CAV1, MYOZ1, C9orf3 and FANCC. *Journal of Molecular and Cellular Cardiology*, 85:207-214.

Matassini, M. V., Brambatti, M., Guerra, F., Scappini, L., Capucci A. (2015). Sleep-disordered breathing and atrial fibrillation: review of the evidence. *Cardiology in Review*, 23(2):79–86.

Maesen, B., Nijs, J., Maessen, J., Allessie, M., Schotten, U. (2012). Post-operative atrial fibrillation: a maze of mechanisms. *Europace*, 14(2):159–174.

Mahida, S., Lubitz, S. A., Rienstra, M., Milan, D. J., Ellinor, P. T. (2011). Monogenic atrial fibrillation as pathophysiological paradigms. *Cardiovascular Research*, 89(4):692-700

Mahida, S., Ellinor, P. T. (2012). New Advances in the Genetic Basis of Atrial Fibrillation. *Journal of Cardiovascular Electrophysiology*, 23(12):1400–1406.

Mahnkopf, C., Badger, T. J., Burgon, N. S., Daccarett, M., Haslam, T. S., Badger, C. T., McGann, C. J., Akoum, N., Kholmovski, E., Macleod, R. S., Marrouche, N. F. (2010). Evaluation of the left atrial substrate in patients with lone atrial fibrillation using delayed-enhanced MRI: Implications for disease progression and response to catheter ablation. *Heart Rhythm*, 7(10):1475–1481.

Manabe, I., Shindo, T., Nagai, R. (2002). Gene expression in fibroblasts and fibrosis involvement in cardiac hypertrophy. *Circulation Research*, 91(12):1103-1113.

Medugorac, I., Jacob, R. (1983). Characterisation of left ventricular collagen in the rat. *Cardiovascular Research*, 17(1):15–21.

Meszaros, J. G., Gonzalez, A. M., Endo-Mochizuki, Y., Villegas, S., Villarreal, F., Brunton, L. L. (2000). Identification of G protein-coupled signaling pathways in cardiac fibroblasts: cross talk between G(q) and G(s). *American Journal of Physiology. Cell Physiology*, 278(1):C154–C162.

Mommersteeg, M. T. M., Brown, N. A., Prall, O. W. J., De Gier-De Vries, C., Harvey, R. P., Moorman, A. F. M., & Christoffels, V. M. (2007). Pitx2c and Nkx2-5 are required for the formation and identity of the pulmonary myocardium. *Circulation Research*, 101(9):902-909.

Mommersteeg, M. T. M., Hoogaars, W. M. H., Prall, O. W. J., De Gier-De Vries, C., Wiese, C., Clout, D. E. W., … Christoffels, V. M. (2007). Molecular pathway for the localized formation of the sinoatrial node. *Circulation Research*, 100(3):354-362.

Montgomery, R. L., Hullinger, T. G., Semus, H. M., Dickinson, B. A., Seto, A. G., Lynch, J. M., … Van Rooij, E. (2011). Therapeutic inhibition of miR-208a improves cardiac function and survival during heart failure. *Circulation*, 124(14):1537-1547.

Nattel, S. (2002). New ideas about atrial fibrillation 50 years on. *Nature*, 415(6868):219– 226.

Nattel, S., Maguy, A., Le Bouter, S., Yeh, Y. H. (2007). Arrhythmogenic ion-channel remodeling in the heart: heart failure, myocardial infarction, and atrial fibrillation. *Physiological Reviews*, 87(2):425–456.

Nattel, S., Burstein, B., Dobrev, D. (2008). Atrial remodeling and atrial fibrillation: mechanisms and implications. *Circulation. Arrhythmia and Electrophysiology*, 1(1):62–73.

Nattel, S., Andrade, J., Macle, L., Rivard, L., Dyrda, K., Mondesert, B., Khairy, P. (2014). New Directions in Cardiac Arrhythmia Management: Present Challenges and Future Solutions. *The Canadian Journal of Cardiology*, 30(12S), S420–S430.

Nattel, S., Harada, M. (2014). Atrial remodeling and atrial fibrillation: Recent advances and translational perspectives. *Journal of the American College of Cardiology*, 63(22):2335–2345.

Ohtani, K., Yutani, C., Nagata, S., Koretsune, Y., Hori, M., Kamada, T. (1995). High prevalence of atrial fibrosis in patients with dilated cardiomyopathy. *Journal of the American College of Cardiology*, 25(5):1162–1169.

Olesen, M. S., Nielsen, M. W., Haunsø, S., Svendsen, J. H. (2014). Atrial fibrillation: the role of common and rare genetic variants. *European Journal of Human Genetic: EJHG*, 22(3):297–306.

Orenes-Piñero, E., Montoro-García, S., Patel, J. V., Valdés, M., Marín, F., Lip, G. Y. (2013). Role of microRNAs in cardiac remodelling: New insights and future perspectives. *International Journal of Cardiology*, 167(5):1651–1659.

Pandit, S. V, Berenfeld, O., Anumonwo, J. M., Zaritski, R. M., Kneller, J., Nattel, S., Jalife, J. (2005). Ionic determinants of functional reentry in a 2-D model of human atrial cells during simulated chronic atrial fibrillation. *Biophysical Journal*, 88(6):3806–3821.

Porter, K. E., Turner, N. A. (2009). Cardiac fibroblasts: at the heart of myocardial remodeling. *Pharmacology & Therapeutics*, 123(2):255-278.

Posch, M. G., Boldt, L. H., Polotzki, M., Richter, S., Rolf, S., Perrot, A., … Haverkamp, W. (2010). Mutations in the cardiac transcription factor GATA4 in patients with lone atrial fibrillation. *European Journal of Medical Genetics*, 53(4):201-203.

Prinz, C., Hering, D., Bitter, T., Horstkotte, D., Faber, L. (2011). Left atrial size and left ventricular hypertrophy correlate with myocardial fibrosis in patients with hypertrophic cardiomyopathy. *Acta Cardiologica*, 66(2):153–157.

Prockop, D. J., Kivirikko, K. I. (1995). Collagens: molecular biology, diseases, and potentials for therapy. *Annual Review of Biochemistry*, 64:403–434.

Prystowsky, E. N. (2000). Management of atrial fibrillation: therapeutic options and clinical decisions. *The American Journal of Cardiology*, 85(10A):3D–11D.

Robinson, T. F., Cohen-Gould, L., Factor, S. M. (1983). Skeletal framework of mammalian heart muscle. Arrangement of inter- and pericellular connective tissue structures. *Laboratory Investigation; a journal of technical methods and pathology*, 49(4):482–498.

Robinson, T. F., Factor, S. M., Capasso, J. M., Wittenberg, B. A., Blumenfeld, O. O., Seifter, S. (1987). Morphology, composition, and function of struts between cardiac myocytes of rat and hamster. *Cell and Tissue Research*, 249(2):247–255.

Robinson, T. F., Geraci, M. A., Sonnenblick, E. H., Factor, S. M. (1988). Coiled perimysial fibers of papillary muscle in rat heart: morphology, distribution, and changes in configuration. *Circulation Research*, 63(3):577–592.

Rodefeld, M. D., Branham, B. H., Schuessler, R. B., Hand, D. E., Gamache, C. M., Platt, J. W., Labarbera, S. P., Cox, J. L., Boineau, J. P. (1997). Global electrophysiological mapping of the atrium: computerized three-dimensional mapping system. *Pacing and Clinical Electrophysiology: PACE*, 20(9 Pt 1):2227-2236.

Rosenkranz, S. (2004). TGF-β1 and angiotensin networking in cardiac remodeling. *Cardiovascular Research*, 63(3):423-432.

Ross, R. S., Borg, T. K. (2001). Integrins and the myocardium. *Circulation Research*, 88(11):1112–1119.

Rossow, C. F., Dilly, K. W., Santana, L. F. (2006). Differential calcineurin/NFATc3 activity contributes to the I_{to} transmural gradient in the mouse heart. *Circulation* Research, 98(10):1306–1313.

Ruvkun, G., Ambros, V., Coulson, A., Waterston, R., Sulston, J., Horvitz, H. R. (1989). Molecular genetics of the Caenorhabditis elegans heterochronic gene lin-14. *Genetics*, 121(3):501–516.

Ruvkun, G., Giusto, J. (1989). The Caenorhabditis elegans heterochronic gene lin-14 encodes a nuclear protein that forms a temporal developmental switch. *Nature*, 338(6213):313-319.

Sakabe, M., Shiroshita-Takeshita, A., Maguy, A., Dumesnil, C., Nigam, A., Leung, T. K., Nattel, S. (2007). Omega-3 polyunsaturated fatty acids prevent atrial fibrillation associated with heart failure but not atrial tachycardia remodeling. *Circulation*, 116(19):2101–2109.

Schnabel, R. B., Yin, X., Gona, P., Larson, M. G., Beiser, A. S., McManus, D. D., … Levy, D. (2015). 50 year trends in atrial fibrillation prevalence, incidence, risk factors, and mortality in the Framingham Heart Study: A cohort study. *The Lancet*, 386(9989):154–162.

Schoonderwoerd, B. A., Smit, M. D., Pen, L., Van Gelder, I. C. (2008). New risk factors for atrial fibrillation: causes of "not-so-lone atrial fibrillation." *Europace*, 10(6):668-73.

Schotten, U., Haase, H., Frechen, D., Greiser, M., Stellbrink, C., Vazquez-Jimenez, J. F., Morano, I., Allessie, M. A., Hanrath, P. (2003). The L-type Ca2+-channel subunits α1C and β2 are not downregulated in atrial myocardium of patients with chronic atrial fibrillation. *Journal of Molecular and Cellular Cardiology*, 35(5): 437–443.

Schotten, U., Verheule, S., Kirchhof, P., Goette, A. (2011). Pathophysiological mechanisms of atrial fibrillation: a translational appraisal. *Physiological Reviews*, 91(1):265–325.

Shan, H., Zhang, Y., Lu, Y., Zhang, Y., Pan, Z., Cai, B., Wang, N., Li, X., Feng, T., Hong, Y., Yang, B. (2009). Downregulation of miR-133 and miR-590 contributes to nicotine-induced atrial remodelling in canines. *Cardiovascular Research*, 83(3):465–472.

Shiroshita-Takeshita, A., Brundel, B. J., Burstein, B., Leung, T. K., Mitamura, H., Ogawa, S., Nattel, S. (2007). Effects of simvastatin on the development of the atrial fibrillation substrate in dogs with congestive heart failure. *Cardiovascular Research*, 74(1):75–84.

Shyu, K. G., Lu, M. J., Wang, B. W., Sun, H. Y., Chang, H. (2006). Myostatin expression in ventricular myocardium in a rat model of volume-overload heart failure. *European Journal of Clinical Investigation*, 36(10):713–719.

Sinner, M. F., Ellinor, P. T., Meitinger, T., Benjamin, E. J., Kääb, S. (2011). Genome-wide association studies of atrial fibrillation: Past, present, and future. *Cardiovascular Research*, 89(4):701-709.

Sinner, M. F., Tucker, N. R., Lunetta, K. L., Ozaki, K., Smith, J. G., Trompet, S., … Ellinor, P. T. (2014). Integrating genetic, transcriptional, and functional analyses to identify 5 novel genes for atrial fibrillation. *Circulation*, 130(15):1225-1235.

Small, E. M., Frost, R. J., Olson, E. N. (2010). MicroRNAs add a new dimension to cardiovascular disease. *Circulation*, 121(8):1022–1032.

Song, S. J., Poliseno, L., Song, M. S., Ala, U., Webster, K., Ng, C., Beringer, G., Brikbak, N. J., Yuan, X., Cantley, L. C., Richardson, A. L., Pandolfi, P. P. (2013). MicroRNA-antagonism regulates breast cancer stemness and metastasis via TET-family-dependent chromatin remodeling. *Cell*, 154(2):311–324.

Spinale, F. G. (2007). Myocardial matrix remodeling and the matrix metalloproteinases: influence on cardiac form and function. *Physiological Reviews*, 87(4):1285–1342.

Spinale, F. G., Coker, M. L., Heung, L. J., Bond, B. R., Gunasinghe, H. R., Etoh, T., Goldberg, A. T., Zellner, J. L., Crumbley, A. J. (2000). A matrix metalloproteinase induction/activation system exists in the human left ventricular myocardium and is upregulated in heart failure. *Circulation*, 102(16):1944–1949.

Sun, Y., Zhang, J., Zhang, J. Q., Weber, K. T. (2001). Renin expression at sites of repair in the infarcted rat heart. *Journal of Molecular and Cellular Cardiology*, 33(5):995– 1003.

Sutton, M. G., Sharpe, N. (2000). Left ventricular remodeling after myocardial infarction: pathophysiology and therapy. *Circulation*, 101(25):2981–2988.

Tao, Y., Zhang, M., Li, L., Bai, Y., Zhou, Y., Moon, A. M., … Martin, J. F. (2014).

Pitx2, an atrial fibrillation predisposition gene, directly regulates ion transport and intercalated disc genes. *Circulation: Cardiovascular Genetics*, 7(1):23-32.

Tarone, G., Balligand, J. L., Bauersachs, J., Clerk, A., De Windt, L., Heymans, S., Hilfiker-Kleiner, D., Hirsch, E., Iaccarino, G., Knöll, R., Leite-Moreira, A. F., Lourenço, A. P., Mayr, M., Thum, T., Tocchetti C. G. (2014). Targeting myocardial remodelling to develop novel therapies for heart failure: A position paper from the Working Group on Myocardial Function of the European Society of Cardiology. *European Journal of Heart Failure*, 16(5):494-508.

Ter Keurs, H. E., Boyden, P. A. (2007). Calcium and arrhythmogenesis. *Physiological Reviews*, 87(2):457–506.

Terentyev, D., Belevych, A. E., Terentyeva, R., Martin, M. M., Malana, G. E., Kuhn, D. E., Abdellatif, M., Feldman, D. S., Elton, T. S., Györke, S. (2009). miR-1 overexpression enhances $Ca^{(2+)}$ release and promotes cardiac arrhythmogenesis by targeting PP2A regulatory subunit B56alpha and causing CaMKII-dependent hyperphosphorylation of RyR2. *Circulation Research*, 104(4):514–521.

Thampatty, B. P., Wang, J. H. C. (2007). Mechanobiology of fibroblasts. *Mechanosensitivity in Cells and Tissues* (Chapter 16, pp. 351–378, edited by Kamkin and Kiseleva, Springer Netherlands).

Thijssen, V. L., van der Velden, H. M., van Ankeren, E. P., Ausma, J., Allessie, M. A., Borgers, M., van Eys, G. J., Jongsma, H. J. (2002). Analysis of altered gene expression during sustained atrial fibrillation in the goat. *Cardiovascular Research*, 54(2):427-437.

Thomas, C. V, Coker, M. L., Zellner, J. L., Handy, J. R., Crumbley, A. J. 3rd., Spinale, F. G. (1998). Increased matrix metalloproteinase activity and selective upregulation in LV myocardium from patients with end-stage dilated cardiomyopathy. *Circulation*, 97(17):1708–1715.

Thum, T., Gross, C., Fiedler, J., Fischer, T., Kissler, S., Bussen, M., Galuppo, P., Just, S., Rottbauer, W., Frantz, S., Castoldi, M., Soutschek, J., Koteliansky, V., Rosenwald, A., Basson, M. A., Licht, J. D., Pena, J. T., Rouhanifard, S. H., Muckenthaler, M. U., Tuschl, T., Martin, G. R., Bauersachs, J., Engelhardt, S. (2008). MicroRNA-21 contributes to myocardial disease by stimulating MAP kinase signalling in fibroblasts. *Nature*, 456(7224):980–984.

Tucker, N. R., Ellinor, P. T. (2014). Emerging directions in the genetics of atrial fibrillation. *Circulation Research*, 114(9):1469–1482.

Van Rooij, E., Sutherland, L. B., Qi, X., Richardson, J. A, Hill, J., Olson, E. N. (2007). Control of stress-dependent cardiac growth and gene expression by a microRNA. *Science (New York, N.Y.)*, 316(5824):575–579.

Van Rooij, E., Quiat, D., Johnson, B. A., Sutherland, L. B., Qi, X., Richardson, J. A., Kelm, R. J. Jr., Olson, E. N. (2009). A Family of microRNAs Encoded by Myosin Genes Governs Myosin Expression and Muscle Performance. *Developmental Cell*, 17(5):662–673.

Van Rooij, E., Olson, E. N. (2012). MicroRNA therapeutics for cardiovascular disease: opportunities and obstacles. *Nature Reviews. Drug Discovery*, 11(11):860–872.

Verheule, S., Sato, T., Everett IV, T., Engle, S. K., Otten, D., Rubart-Von Der Lohe, M., Nakajima, H. O., Nakajima, H., Field, L. J., Olgin, J. E. (2004). Increased vulnerability to atrial fibrillation in transgenic mice with selective atrial fibrosis caused by overexpression of TGF-β1. *Circulation Research*, 94(11):1458–1465.

Voigt, N., Friedrich, A., Bock, M., Wettwer, E., Christ, T., Knaut, M., Strasser, R. H, Ravens, U., Dobrev, D. (2007). Differential phosphorylation-dependent regulation of constitutively active and muscarinic receptor-activated $I_{K,ACh}$ channels in patients with chronic atrial fibrillation. *Cardiovascular Research*, 74(3):426–437.

Voigt, N., Maguy, A., Yeh, Y. H., Qi, X., Ravens, U., Dobrev, D., Nattel, S. (2008). Changes in $I_{K,ACh}$ single-channel activity with atrial tachycardia remodelling in canine atrial cardiomyocytes. *Cardiovascular Research*, 77(1):35–43.

Wakili, R., Voigt, N., Kääb, S. Dobrev, D., Nattel, S. (2011). Recent advances in the molecular pathophysiology of atrial fibrillation. *The Journal of Clinical Investigation*, 121(8):2955–2968.

Wang, J., Klysik, E., Sood, S., Johnson, R. L., Wehrens, X. H. T., & Martin, J. F. (2010). Pitx2 prevents susceptibility to atrial arrhythmias by inhibiting left-sided pacemaker specification. *Proceedings of the National Academy of Sciences of the United States of America*, 107(21):9753-9758.

Wang, J., Sun, Y.-M., & Yang, Y.-Q. (2012). Mutation spectrum of the GATA4 gene in patients with idiopathic atrial fibrillation. *Molecular Biology Reports*, 39(8):8127-3815.

Wang, X. H., Huang, C. X., Wang, Q., Li, R. G., Xu, Y. J., Liu, X., … Yang, Y. Q. (2013). A novel GATA5 loss-of-function mutation underlies lone atrial fibrillation. *International Journal of Molecular Medicine*, 31(1):43-50.

Weber, K. T. (1989). Cardiac interstitium in health and disease: the fibrillar collagen network. *Journal of the American College of Cardiology*, 13(7):1637–1652.

Weber, K. T., Brilla, C. G. (1991). Pathological hypertrophy and cardiac interstitium. Fibrosis and renin-angiotensin-aldosterone system. *Circulation*, 83(6):1849–1865.

Weber, K. T., Sun, Y., Tyagi, S. C., Cleutjens, J. P. (1994). Collagen network of the myocardium: function, structural remodeling and regulatory mechanisms. *Journal of Molecular and Cellular Cardiology*, 26(3):279–292.

Weber, K. T., Sun, Y., Bhattacharya, S. K., Ahokas, R. A., Gerling, I. C. (2013). Myofibroblast-mediated mechanisms of pathological remodeling of the heart. *Nature Reviews. Cardiology*,10(1):15-26.

Weiss, A., Leinwand, L. A. (1996). The mammalian myosin heavy chain gene family. *Annual Review of Cell and Developmental Biology*, 12:417-439.

Wijffels, M. C., Kirchhof, C. J., Dorland, R., Allessie, M. A. (1995). Atrial fibrillation begets atrial fibrillation. A study in awake chronically instrumented goats. *Circulation*, 92(7):1954–1968.

Wu, T. J., Ong, J. J, Hwang, C., Lee, J. J, Fishbein, M. C, Czer, L., Trento, A., Blanche, C., Kass, R. M., Mandel, W. J., Karagueuzian, H. S, Chen, P. S. (1998). Characteristics of wave fronts during ventricular fibrillation in human hearts with dilated cardiomyopathy: role of increased fibrosis in the generation of reentry. *Journal of the American College of Cardiology*, 32(1):187-196.

Xia, M., Jin, Q., Bendahhou, S., He, Y., Larroque, M. M., Chen, Y., … Chen, Y. (2005). A Kir2.1 gain-of-function mutation underlies familial atrial fibrillation. *Biochemical and Biophysical Research Communications*, 332(4):1012-1019.

Xiao, H., Lei, H., Qin, S., Ma, K., Wang, X. (2010). TGF-β1 expression and atrial myocardium fibrosis increase in atrial fibrillation secondary to rheumatic heart disease. *Clinical Cardiology*, 33(3):149–156.

Xu, G. J., Gan, T. Y., Tang, B. P., Chen, Z. H., Ailiman, M., Zhou, X. H., Jiang, T., Song, J. G., Guo, X., Li, Y. D., Miao, H. J., Zhang, Y., Li, J. X. (2013). Changes in microRNAs expression are involved in age-related atrial structural remodeling and atrial fibrillation. *Chinese Medical Journal*, 126(8):1458–1463.

Yang, B., Lin, H., Xiao, J., Lu, Y., Luo, X., Li, B., Zhang, Y., Xu, C., Bai, Y., Wang, H., Chen, G., Wang, Z. (2007). The muscle-specific microRNA miR-1 regulates cardiac arrhythmogenic potential by targeting GJA1 and KCNJ2. *Nature Medicine*, 13(4):486–491.

Yang, Y., Xia, M., Jin, Q., Bendahhou, S., Shi, J., Chen, Y., … Chen, Y. (2004). Identification of a KCNE2 gain-of-function mutation in patients with familial atrial fibrillation. *American Journal of Human Genetics*, 75(5):899-905.

Yi, S., Liu, X., Zhong, J., & Zhang, Y. (2014). Role of caveolin-1 in atrial fibrillation as an anti-fibrotic signaling molecule in human atrial fibroblasts. *PloS One*, 9(1):e85144.

Yue, L., Feng, J., Li, G. R., Nattel, S. (1996). Transient outward and delayed rectifier currents in canine atrium: properties and role of isolation methods. *The American Journal of Physiology*, 270(6 Pt 2):H2157–2168.

Yue, L., Melnyk, P., Gaspo, R., Wang, Z., Nattel, S. (1999). Molecular mechanisms underlying ionic remodeling in a dog model of atrial fibrillation. *Circulation Research*, 84(7):776–784.

Yue, L., Xie, J., Nattel, S. (2011). Molecular determinants of cardiac fibroblast electrical function and therapeutic implications for atrial fibrillation. *Cardiovascular Research*, 89(4):744–753.

Zhang, C. (2008). MicroRNomics: a newly emerging approach for disease biology. *Physiological Genomics*, 33(2):139–147.

Zhang, X., Chen, S., Yoo, S., Chakrabarti, S., Zhang, T., Ke, T., … Wang, Q. K. (2008). Mutation in Nuclear Pore Component NUP155 Leads to Atrial Fibrillation

and Early Sudden Cardiac Death. *Cell*, 135(6):1017–1027.

Zhang, W., Zhong, M., Yang, G. R., Li, J. P., Guo, C., Wang, Z., Zhang, Y. (2008). Matrix metalloproteinase-9/tissue inhibitors of metalloproteinase-1 expression and atrial structural remodeling in a dog model of atrial fibrillation: inhibition with angiotensin-converting enzyme. *Cardiovascular Pathology: the official journal of the Society for Cardiovascular Pathology*, 17(6):399–409.

Zhu, H., Fan, G.-C. (2011). Extracellular/circulating microRNAs and their potential role in cardiovascular disease. *American Journal of Cardiovascular Disease*, 1(2): 138–149.

CHAPTER 2: STRUCTURAL CHARACTERIZATION

The impulse propagation in the heart depends on the excitability of individual cardiomyocytes, the impulse transmission between them and their 3-dimensional (3D) arrangement. These factors operate across a wide range of spatial scales, and normal function at each level ensures that electric activation spreads across the cardiac chambers in a stable rhythm, thus triggering efficient contraction (Smaill *et al.*, 2013). The normal myocardium consists of two major components, a cellular part and an acellular component, which is represented by the extracellular matrix (ECM). The cardiac ECM, that is mainly constituted by a network of fibrillar collagen fibers (Caulfield & Borg, 1979), represents the three-dimensional scaffold that defines the geometry and the muscular architecture of the cardiac chambers. The discontinuous arrangement of myocytes and extracellular connective tissue at the tissue scale can give rise to current source-to-sink mismatch, spatiotemporal distribution of refractoriness, and rate-sensitive electric instability, that contribute to the initiation and maintenance of reentrant cardiac arrhythmias (Smaill *et al.*, 2013). During disease progression collagen fibers undergo both qualitative and quantitative changes, that can interfere with the electrical impulse propagation, thus predisposing to arrhythmogenesis (Tarone *et al.*, 2014). Knowledge about the content and distribution of fibrosis may be of relevance in the context of AF, where the dynamic patterns of wavelet propagation can be supported by the 3D collagen structure.

To investigate the tissue properties that can be involved in the formation of a pro-arrhythmic substrate, a structural characterization of human atrial samples obtained from patients undergoing cardiac surgery who developed or not AF, has been performed. Particular attention was devoted to fibrosis content, quantified by using the well established histological staining method Picrosirius red (Junqueira *et al.*, 1979) in combination with a specific image analysis tool. It is well accomplished that interstitial fibrosis creates conduction delay causing the electrical impulse to propagate through alternative pathways, eventually impinging on tissue that has already recovered excitability, thus causing reactivation and a further increase in the number of re-entrant circuits (Allessie *et al.*, 2002; Nattel, 2002). More recently, experimental (Eckstein *et*

al., 2011, 2013; Schuessler *et al.*, 1993) and clinical (Allessie *et al.*, 2010; de Groot *et al.*, 2010) mapping studies have shown that the dynamic patterns of wavelet propagation can be further complicated by the three-dimensional structure of the atria and the presence of epi-endocardial dissociation, which can support 3D reentrant circuits and epicardial breakthrough. Despite some studies have described the histological substrate of atrial fibrillation in humans (Frustaci *et al.*, 1997; Nguyen *et al.*,2009), no information about the 3D collagen content within the human atrial wall has been provided. For these reasons, the 3D intramural profile of fibrotic content in the atrial wall was investigated here for the first time. Specifically, 5 microns serial tissue sections crossing the whole biopsy were collected, imaged and analyzed, in order to provide the complete intramural profile of fibrotic content throughout the atrial tissue, i.e., from the outer side (the epicardium) to the inner side (the endocardium) of the atrial wall. Clinical studies have suggested that in addition to its amount, also the pattern of fibrosis may play an important role in arrhythmogenicity (Kawara *et al.*, 2001). In this perspective, non-linear optical (NLO) microscopy techniques, such as two-photon excited fluorescence (TPEF) and second harmonic generation (SHG) microscopy, have been recently indicated as powerful tools for the imaging of thick specimens (Helmchen & Denk, 2005; Rubart, 2004). In particular, SHG microscopy thanks to its high sensitivity to collagen and intrinsic optical sectioning capability, has been used to reveal collagen organization in a variety of tissues, including human dermis, keloid and tumor microenvironment (Adur *et al.*,2014; Cicchi *et al.*, 2010, 2013). Nevertheless, the application to human cardiac tissues (Caorsi *et al.*, 2013; Martin *et al.*,2013), and in particular to the relation between atrial collagen and AF, remain sparse (Chiu *et al.*, 2010; Tsai *et al.*, 2010). In the second part of this chapter, a detailed analysis of 3D collagen network properties was performed by applying SHG microscopy to atrial tissue samples collected in cardiac surgery patients with or without AF. A quantitative assessment of collagen network properties, such as orientation and texture scale along tissue depth, was obtained by applying a spectral analysis framework on SHG images. The combination of the results derived from these different methodological approaches, aiming to define the quantity and the 3D spatial pattern of the collagen network throughout the atrial tissue, could provide new important information about the structural characterization of AF substrate.

2.1 Quantification of collagen content and intramural distribution in human atrial tissue samples by Picrosirius red staining

MATERIALS AND METHODS

Human tissue collection and processing

Tissue specimens from the right atrial appendage were collected from 15 individuals (all males) undergoing cardiac surgery. In particular, seven patients (range 61 ± 12 years) presented in normal sinus rhythms following intervention (SR group), while eight patients (range 74 ± 5 years) displayed AF (AF group). After excision cardiac biopsies were immediately fixed in 4% formalin buffered solution and stored at room temperature (RT). Subsequently, tissue specimens were dehydrated in graded alcohols, embedded in paraffin and cut in 5 μm serial sections (sections per sample ~ 100; stained sections ~ 50) by using a microtome (Leica Biosystems, Milan, Italy). Tissue sections were collected and stored at RT until staining procedures.

Picrosirius red staining

Tissue sections were placed in an oven at 60°C for one hour and subsequently in two stages of xylene (1X for 30 minutes, 1X for 5 minutes) for deparaffinization. After that they were hydrated to distilled water by graded alcohols (2X 100%, 1X 90%, 1X 70%, 5 minutes each). After a pre-treatment with 0,2 % solution of aqueous phosphomolybdic acid (Sigma-Aldrich, Milan, Italy) for 2 minutes, the selected tissue sections were stained with 0.1% solution of Sirius Red F3BA (Direct Red 80, CI 35780) (Sigma-Aldrich, Milan, Italy) in saturated aqueous solution of picric acid for one hour, at room temperature. Sections were subsequently rinsed in two stages of acidified water, 1 minute each, and 70% ethanol for 45 seconds. Sections were dehydrated in ascending concentrations of ethanol (1X 80%, 1X 90%, 2X 100%, 5 seconds each) and cleared in two stages of xylene for 5 seconds each. Slices were finally mounted with a drop of mounting medium and a glass cover slip.

Imaging and quantification of fibrosis

Picrosirius red stained sections were examined by light microscopy (DMIL microscope combined with DFC420 camera, Leica, Germany). Section images were acquired (Leica Application Suite, Leica, Germany) randomly within the entire tissue area at magnification 4X by using both bright field and polarized light (images per sample ~100; overall images ~1400). Captured images were subsequently analyzed using a custom made software, developed in Matlab R2013b (MathWorks Inc., Natick, Massachusetts, US), able to identify and quantify Picrosirius red signals. Specifically, in order to quantify collagen content in each sample, both bright field and polarized light images were used (Figure 1). All the images were corrected from the vignetting effect of the lenses (decrease in brightness at the periphery of the image) by dividing each image by a vignetting profile built from a white image acquired at the beginning of each microscopy imaging session.

The corrected bright field images were white-balanced via RGB histogram analysis, which also allowed to automatically segment the background region from the tissue region. Polarized light images were normalized assuming that picrosirius red signal was proportional to collagen density and tissue thickness. The normalized polarized light images were thresholded, separating regions with high-density collagen from poor density ones. Finally, the fraction of the tissue composed of collagen was computed as the ratio of the area of the collagen region over the total tissue area previously segmented. The 3D profile of collagen content was obtained in each patient by displaying the fraction of collagen in subsequent sample slices as a function of the slice depth, going from the epicardial to the endocardial walls. Fibrosis spatial profiles were fitted by an exponential decay curve:

$$y(x) = A1e^{-\frac{x}{t1}} + y0 \ ,$$

where *y(x)* is the fibrosis fraction at depth *x* and *A1*, *y0* and *t1* are positive constants. The parameter *y0* obtained from the fit was used as an estimate of fibrosis content in the deeper (endocardial) layers. Data fitting was performed in Origin Pro 8 (OriginLab Corporation, Northampton, Massachusetts).

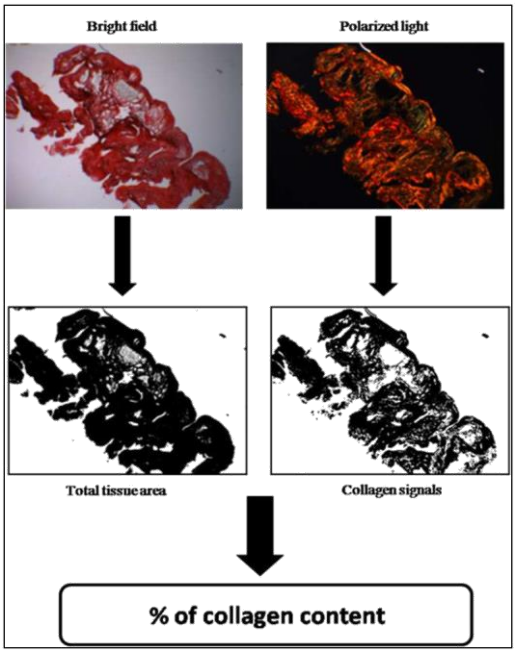

Figure 1: Main steps of the fibrosis quantification assessed by Picrosirius red staining in combination with an optimized image analysis software. Stained sections were examined both on bright field and polarized light microscopy. Subsequently, the images were processed by a custom made image analysis software, providing the collagen percentage for each section.

Statistical analysis

Data are expressed as mean ± standard deviation, or median (interquartile range, IQR), depending on data normality (Lilliefor test). Differences between steady state fibrosis values in the AF group versus SR group were assessed by Wilcoxon-Mann-Whitney test. A p value < 0.05 was considered statistically significant.

RESULTS

Intramural profile of fibrotic content in the whole population

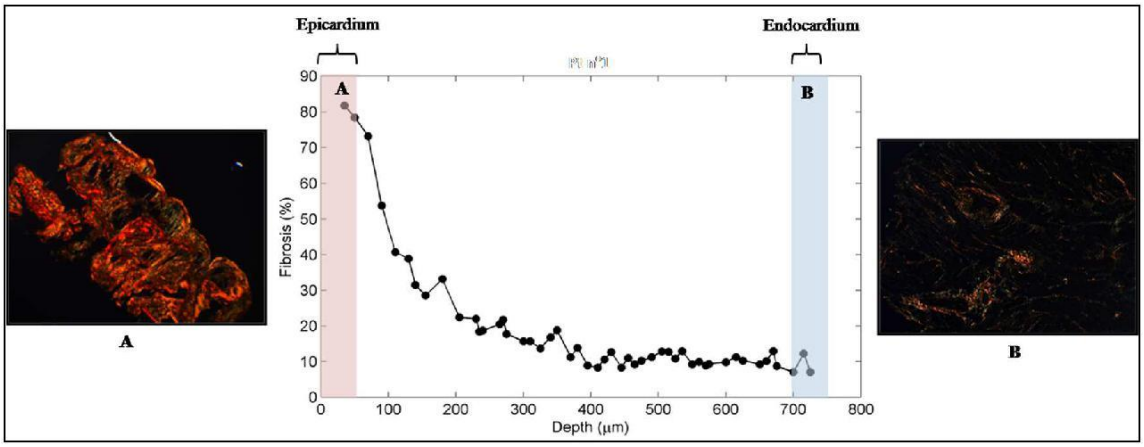

Figure 2: Intramural profile of fibrotic content. Graph and images referred to a representative patient in SR. Tissue sections evaluated N=50; total images analyzed N=100. A) 5 µm tissue section from the epicardium stained with Picrosirius red and visualized on polarized light; (B) 5 µm tissue section from the endocardium stained with Picrosirius red and visualized on polarized light.

It is well accomplished the an accumulation of collagen fibers across the atrial wall may support the propagation of multiple excitation wavelets, creating slow conduction areas, barriers to wave propagation and/or anchoring points for reentries. In this perspective, a better knowledge about the 3D collagen content throughout the atrial wall could be of importance in order to characterize possible mechanistic contributors to AF. Figure 2 displays a representative example of the intramural profile of fibrotic content, performed by applying Picrosirius red on serial tissue sections (5 µm thickness each) along the entire atrial wall. In particular, the central graph shown the percentage of collagen content from the outer side (the epicardium, left) to the inner myocardial region (the endocardium, right) throughout the atria. The trend of the intramural fibrotic content along tissue depth followed an exponential decay behaviour: a rapid decrease in collagen content was observed within the first 200 µm (from ~80 to 20%), which was followed by a further slight decrease (from ~ 20 to 10%) between 200-400 µm. Finally, at a depth of around 400-750 µm collagen content values displayed almost constant values of around ~10%, indicating the reaching of a steady state condition.

This trend of collagen content along tissue depth resulted evident in figure 2A and B, which show representative images taken in the epicardium and in the endocardium, respectively. In particular, in Figure 2A collagen occupied almost the entire tissue area

(~80%), as highlighted by a strong red signal. On the contrary, in figure 2B collagen percentage was relatively low (~10%) as indicated by a very fade signal.

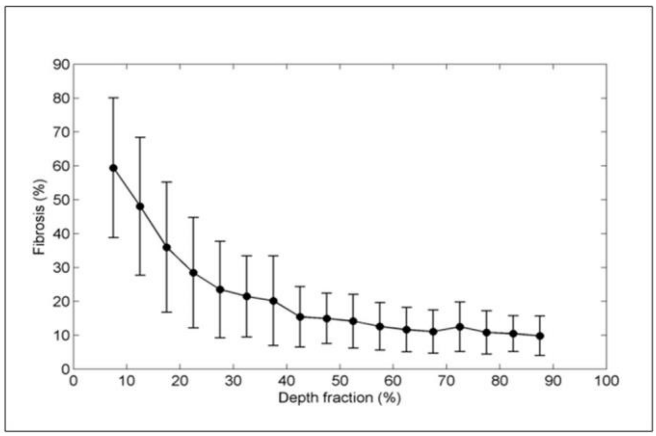

Figure 3: Average and variability of the intramural profile of fibrotic content in the overall population. The fibrotic trend of collagen content assessed in the overall population of patients resulted in a consistent average curve. To align different thickness of patients' samples depth is expressed in relative units (fraction, %). N=14 (8 AF, 7 SR).

The results concerning the intramural profile of fibrotic content assessed in the overall patient population are represented in Figure 3, which displays the average curve obtained by aligning and averaging different patients curves. Despite differencies in collagen content values, the decreasing trend of fibrotic content previously described was consistently observed in the overall population of patients, resulting in a decreasing average curve. In the overall population of patients, the collagen content rapidly decreased from 58.5 ± 20.2 % to 29.5 ± 15.2 % within ~ 20% of the total tissue depth. A further slight decrease to 19.4 ± 13.5 % was observed in the interval 20-40% of tissue depth. Finally, for depths larger than half of the tissue thickness, the average collagen content oscillated between 10-11%, with a group variability of 6%. The error bar of the fibrotic values at each depth fraction point indicated variability among different individuals.

Comparison of the intramural profile in AF and SR patients

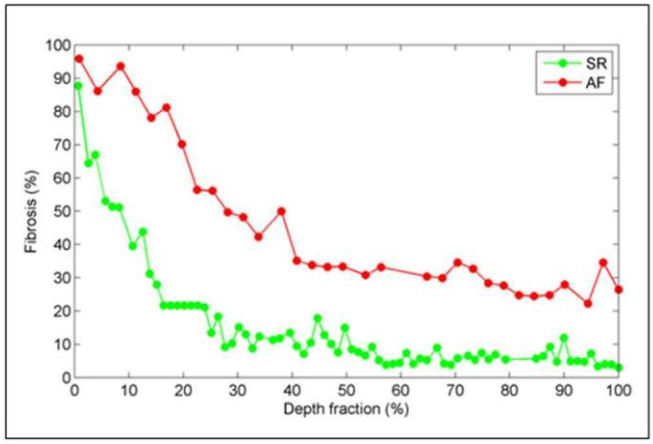

Figure 4: Comparisons of intramural profiles of fibrotic content in AF versus SR patients. Collagen content decreases from the epicardium to the endocardium in both AF and SR patients. Higher steady state values of fibrotic content are observable in AF. To align different thickness of patients' samples depth is expressed in relative units (%). Representative examples.

Following the analysis of the whole population, the intramural profiles of fibrotic content were evaluated in AF compared to SR patients (Figure 4). In accordance with previous results, the typical decreasing trend of collagen content along tissue depth was observed in both AF and SR individuals. However, marked differences were observed in the steady state values of fibrosis (within the 30-100% of depth fraction). Specifically, the AF patient showed higher fibrotic values (above 20%) compared to the control in SR (mean value ~10%), which suggested the penetration of collagen fibers in the deepest myocardial layers in presence of AF.

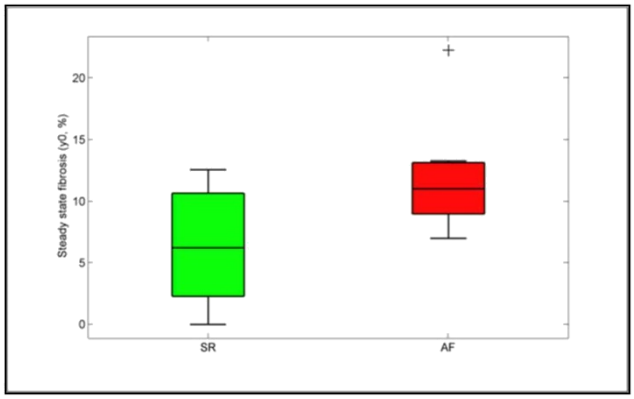

Figure 5: Steady-state fibrotic content in AF versus SR patients. The AF group showed higher steady state fibrotic values compared to SR group (p=0.08). N=15 (8 AF, 7 SR).

To test the existence of differences in the penetration of fibrosis in the endocardial layers between AF and SR patients, the steady state fibrotic content was evaluated in each patient by fitting of an exponential decay curve (fit adjusted $R2 = 0.92 \pm 0.06$) and the values were compared in the AF versus SR groups. The results are summarized in Figure 5 and confirmed the behaviour observed in the representative examples. Indeed, the AF group showed higher values of fibrotic content (median 10.3, IQR 7.9-13.0) compared to SR patients (median 6.2, IQR 2.3-10.6; p=0.08).

DISCUSSION

Atrial fibrosis is thought to be one of the most important factors in the formation of a substrate for AF (Nattel, 2004; Spach & Boineau, 1997). Atrial fibrosis has been observed in biopsies from patients with AF (Kostin *et al.,* 2002) and in patients with specific risk factors for AF, such as valvular disease (Anné *et al.,* 2005), rheumatic heart disease (Luo *et al.*,2007; Pham & Fenoglio, 1982), dilated and hypertrophic cardiomyopathy (Ohtani *et al.,* 1995) and advanced age (Lie & Hammond, 1988). In addition, the histological substrate of atrial fibrillation has been investigated in humans (Frustaci *et al.,* 1997; Nguyen *et al.,* 2009), but without providing information on its 3D arrangement. The increase in interstitial collagen influences both the mechanical and the electrical properties of the heart, increasing muscle stiffness and reducing coupling between adjacent muscle fiber bundles. Clinical studies have also suggested a role for fibrotic tissue in wave break formation (Wu *et al.,* 1998), conduction delays, conduction blocks, and "zig-zag" course of conduction (de Bakker *et al.,* 2006; Kawara *et al.,* 2001). In this perspective, a better knowledge about the fibrotic content within the atrial tissue wall may provide novel insights about the structural features of a pro-arrhythmic substrate.

In this section, a histological method for the assessment of fibrotic content in atrial tissue samples was introduced. Specifically, Picrosirius red staining (F3BA), which represents one of the most used and sensitive methods for the identification of fibrillar collagen (Junqueira *et al.,* 1979), was applied to atrial tissue sections in combination with a custom made software optimized for quantitative image analysis. Picrosirius red is a strong, linear, anionic dye, which comprises six sulfonate groups that can associate along cationic collagen fibers, enhancing their natural birefringence under polarized light (Junqueira *et al.,* 1979; Montes & Junqueira, 1991). It is well reported that Picrosirius red in association with morphometric image analysis, allows for qualitative and quantitative characterization of collagen network both in normal and pathological tissues (Lattouf *et al.,* 2014). Nonetheless, despite numerous studies have largely indicated its use for the assessment of collagen content in cardiac tissue (Dolber & Spach, 1987; Hadi *et al.,* 2011; Iles *et al.,* 2015; Whittaker *et al.*,1994), none of these studies provided information about the 3D fibrotic profile throughout the human atrial walls.

Here for the first time, an accurate method for the quantification of the intramural collagen in human tissue atrial samples was described. Specifically, 5 μm thickness

serial sections throughout the whole biopsy were collected, imaged, and subsequently analyzed by using a semi-automated software customized for quantitative analysis of histological images. Despite the time-consuming procedure, this approach offers many important advantages. Firstly, in contrast to other traditional techniques used for collagen quantification (Diez *et al.,* 1995; Medugorac, 1980), this method produces no complete tissue disruption. Secondly, Picrosirius red is an anionic dye so, in contrast to the application of fluorescent dyes, the reaction with collagen fibers is highly specific and quantitative, thus minimizing the risk to obtain uncertainties or false results. Thirdly, the application of a semi-automated software optimized for quantitative analysis of histological sections images, allowed for the quantitative and reliable analysis of hundreds of images in a relatively short time.

The quantitative analysis of the intramural profile of fibrotic content performed on atrial tissue samples in the overall population yielded a consistent average curve of collagen content distribution, throughout the myocardial wall. In particular, a strong decrease in the fibrotic content from the outer, the epicardium, to the inner region, the endocardium, was consistently observed in the overall population, with collagen content reaching a steady state in the deep endocardial layers. Despite this globally decreasing trend of collagen was observed in both AF and SR patients, marked differences were observed in the steady state values of collagen in the two groups. Indeed, collagen stabilized on higher values in the AF versus SR groups, indicating a deeper penetration of fibrosis in the myocardial tissue associated with the disease.

Collectively, these findings support the hypothesis that an accumulation of fibrotic tissue within the myocardial wall may represent an important mechanistic contributor in the pathophysiology of AF. Studies have indicated that structural changes in cardiac disorders often affect passive electrical properties, increasing non-uniformity and altering anisotropy. This disturbs normal electrical impulse propagation and is, consequently, a substrate for arrhythmia (Dhein *et al.,* 2014). In particular, the results of our study suggest that the presence of intramural changes in collagen content and the penetration of fibrosis in the deepest myocardial layers in AF patients may participate in the formation of a 3D structural substrate, which may favour the maintenance of the arrhythmia by supporting intramural reentrant pathways and increased epi-endocardial dissociation (Allessie *et al.,* 2010; de Groot *et al.,* 2010; Eckstein *et al.,* 2011, 2013; Schuessler *et al.,* 1993).

To conclude, the application of an accurate histological approach here described, have shown its capability to quantify and detect differences in the collagen content and distribution within the atrial tissue wall, in AF versus SR patients.

BIBLIOGRAPHY

Adur, J., Carvalho, H. F., Cesar, C. L., Casco, V. H. (2014). Nonlinear optical microscopy signal processing strategies in cancer. *Cancer Informatics*, 13:67–76.

Allessie, M. A., de Groot, N. M., Houben, R. P., Schotten, U., Boersma, E., Smeets, J. L., Crijns, H. J. (2010). Electropathological substrate of long-standing persistent atrial fibrillation in patients with structural heart disease longitudinal dissociation. *Circulation. Arrhythmia and Electrophysiology*, 3:606–615.

Allessie, M., Ausma, J., Schotten, U. (2002). Electrical, contractile and structural remodeling during atrial fibrillation. *Cardiovascular Research*, 54(2):230–246.

Anné, W., Willems, R., Roskams, T., Sergeant, P., Herijgers, P., Holemans, P., Ector, H., Heidbüchel, H. (2005). Matrix metalloproteinases and atrial remodeling in patients with mitral valve disease and atrial fibrillation. *Cardiovascular Research*, 67(4):655–666.

Caorsi, V., Toepfer, C., Sikkel, M. B., Lyon, A. R., MacLeod, K., Ferenczi, M. A. (2013). Non-linear optical microscopy sheds light on cardiovascular disease. *PLoS One*, 8(2):e56136.

Caulfield, J. B., Borg, T. K. (1979). The collagen network of the heart. *Laboratory Investigation; a journal of technical methods and pathology*, 40(3):364–372.

Chiu, Y. W., Lo, M. T., Tsai, M. R., Chang, Y. C., Hsu, R. B., Yu, H. Y., Sun, C. K., Ho, Y. L. (2010). Applying harmonic optical microscopy for spatial alignment of atrial collagen fibers. *PLoS One*, 5(11):e13917.

Cicchi, R., Kapsokalyvas, D., De Giorgi, V., Maio, V., Van Wiechen, A., Massi, D., Lotti, T., Pavone, F. S. (2010). Scoring of collagen organization in healthy and diseased human dermis by multiphoton microscopy. *Journal of Biophotonics*, 3(1-2):34–43.

Cicchi, R., Vogler, N., Kapsokalyvas, D., Dietzek, B., Popp, J., Pavone, F. S. (2013). From molecular structure to tissue architecture: Collagen organization probed by SHG microscopy. *Journal of Biophotonics*, 6(2):129–142.

de Bakker, J. M., van Rijen, H. M. (2006). Continuous and discontinuous propagation in heart muscle. *Journal of Cardiovascular Electrophysiology*, 17(5):567-573.

de Groot, N. M., Houben, R. P., Smeets, J. L., Boersma, E., Schotten, U., Schalij, M. J., Crijns, H., Allessie, M. A. (2010). Electropathological substrate of longstanding persistent atrial fibrillation in patients with structural heart disease: Epicardial breakthrough. *Circulation*, 122(17):1674–1682.

Dhein, S., Seidel, T., Salameh, A., Jozwiak, J., Hagen, A., Kostelka, M., Hindricks, G., Mohr, F. W. (2014). Remodeling of cardiac passive electrical properties and susceptibility to ventricular and atrial arrhythmias. *Frontiers in Physiology*, 5:424.

Diez, J., Laviades, C., Monreal, I., Gil, M. J., Panizo, A., Pardo, J. (1995). Toward the biochemical assessment of myocardial fibrosis in hypertensive patients. *The American Journal of Cardiology*, 76(13):14D–17D.

Dolber, P. C., Spach, M. S. (1987). Picrosirius red staining of cardiac muscle following phosphomolybdic acid treatment. *Stain Technology*, 62(1):23–26.

Eckstein, J., Maesen, B., Linz, D., Zeemering, S., van Hunnik, A., Verheule, S., Allessie, M., Schotten, U. (2011). Time course and mechanisms of endo-epicardial electrical dissociation during atrial fibrillation in the goat. *Cardiovascular Research*, 89(4):816–824.

Eckstein, J., Zeemering, S., Linz, D., Maesen, B., Verheule, S., van Hunnik, A., Crijns, H., Allessie, M. A., Schotten, U. (2013). Transmural conduction is the predominant mechanism of breakthrough during atrial fibrillation: Evidence from simultaneous endo-epicardial high-density activation mapping. *Circulation. Arrhythmia and Electrophysiology*, 6(2):334–341.

Frustaci, A., Chimente, C., Bellocci, F., Morgante, E., Russo, M. A., Maseri, A. (1997). Histological substrate of atrial biopsies in patients with lone atrial fibrillation. *Circulation*, 96(4):1180–1184.

Hadi, A. M., Mouchaers, K. T., Schalij, I., Grunberg, K., Meijer, G. A., Vonk-Noordegraaf, A., van der Laarse, W. J., Beliën, J. A. (2011). Rapid quantification of myocardial fibrosis: a new macro-based automated analysis. *Cellular Oncology (Dordrecht)*, 34(4):343–354.

Helmchen, F., Denk, W. (2005). Deep tissue two-photon microscopy. *Nature Methods*, 2(12):932–940.

Iles, L. M., Ellims, A. H., Llewellyn, H., Hare, J. L., Kaye, D. M., McLean, C. A., Taylor, A. J. (2015). Histological validation of cardiac magnetic resonance analysis of regional and diffuse interstitial myocardial fibrosis. *European Heart Journal Cardiovascular Imaging*, 16(1):14–22.

Junqueira, L. C., Bignolas, G., Brentani, R. R. (1979). Picrosirius staining plus polarization microscopy, a specific method for collagen detection in tissue sections. *The Histochemical Journal*, 11(4):447–455.

Kawara, T., Derksen, R., de Groot, J. R., Coronel, R., Tasseron, S., Linnenbank, A. C., Hauer , R. N., Kirkels, H., Janse, M. J., de Bakker, J. M. (2001). Activation delay after premature stimulation in chronically diseased human myocardium relates to the architecture of interstitial fibrosis. *Circulation*, 104(25):3069–3075.

Kostin, S., Klein, G., Szalay, Z., Hein, S., Bauer, E. P., Schaper, J. (2002). Structural correlate of atrial fibrillation in human patients. *Cardiovascular Research*, 54(2):361–379.

Lattouf, R., Younes, R., Lutomski, D., Naaman, N., Godeau, G., Senni, K., Changotade, S. (2014). Picrosirius red staining: a useful tool to appraise collagen networks in

normal and pathological tissues. *The Journal of Histochemistry and Cytochemistry: official journal of the Histochemistry Society*, 62(10):751–758.

Lie, J. T., Hammond, P. I. (1988). Pathology of the senescent heart: anatomic observations on 237 autopsy studies of patients 90 to 105 years old. *Mayo Clinic Proceedings*, 63(6):552–564.

Luo, M. H., Li, Y. S., Yang, K. P. (2007). Fibrosis of collagen I and remodeling of connexin 43 in atrial myocardium of patients with atrial fibrillation. *Cardiology*, 107(4):248–253.

Martin, T. P., Norris, G., McConnell, G., Currie, S. (2013). A novel approach for assessing cardiac fibrosis using label-free second harmonic generation. *The International Journal of Cardiovascular Imaging*, 29(8):1733–1740.

Medugorac, I. (1980). Collagen content in different areas of normal and hypertrophied rat myocardium. *Cardiovascular Research*, 14(9):551–554.

Montes, G. S., Junqueira, L. C. (1991). The use of the Picrosirius-polarization method for the study of the biopathology of collagen. *Memórias Do Instituto Oswaldo Cruz*, 86 Suppl 3:1–11.

Nattel, S. (2004). Defining "culprit mechanisms" in arrhythmogenic cardiac remodeling. *Circulation Research*, 94(11):1403–1405.

Nattel, S. (2002). New ideas about atrial fibrillation 50 years on. *Nature*, 415(6868):219– 226.

Nguyen, B. L., Fishbein, M. C., Chen, L. S., Chen, P. S., Masroor, S. (2009). Histopathological substrate for chronic atrial fibrillation in humans. *Heart Rhythm: the official journal of the Heart Rhythm Society*, 6(4):454–460.

Ohtani, K., Yutani, C., Nagata, S., Koretsune, Y., Hori, M., Kamada, T. (1995). High prevalence of atrial fibrosis in patients with dilated cardiomyopathy. *Journal of the American College of Cardiology*, 25(5):1162–1169.

Pham, T. D., Fenoglio, J. J. Jr. (1982). Right atrial ultrastructural in chronic rheumatic heart disease. *International Journal of Cardiology*, 1(3-4):289–304.

Rubart, M. (2004). Two-photon microscopy of cells and tissue. *Circulation Research*, 95(12):1154–1166.

Schuessler, R. B., Kawamoto, T., Hand, D. E., Mitsuno, M., Bromberg, B. I., Cox, J. L., Boineau, J. P. (1993). Simultaneous epicardial and endocardial activation sequence mapping in the isolated canine right atrium. *Circulation*, 88(1):250–263.

Smaill, B. H., Zhao, J., Trew, M. L. (2013). Three-dimensional impulse propagation in myocardium: arrhythmogenic mechanisms at the tissue level. *Circulation Research*, 112(5):834–848.

Spach, M. S., Boineau, J. P. (1997). Microfibrosis produces electrical load variations due to loss of side- to-side cell connections: a major mechanism of structural heart disease arrhythmias. P*acing and Clinical Electrophysiology: PACE*, 20(2 Pt 2):397– 413.

Tarone, G., Balligand, J. L., Bauersachs, J., Clerk, A., De Windt, L., Heymans, S., Hilfiker-Kleiner, D., Hirsch, E., Iaccarino, G., Knöll, R., Leite-Moreira, A. F., Lourenço, A. P., Mayr, M., Thum, T., Tocchetti, C. G. (2014). Targeting myocardial remodelling to develop novel therapies for heart failure: a position paper from the Working Group on Myocardial Function of the European Society of Cardiology. *European Journal of Heart Failure*, 16(5):494-508.

Tsai, M. R., Chiu, Y. W., Lo, M. T., Sun, C. K. (2010). Second-harmonic generation imaging of collagen fibers in myocardium for atrial fibrillation diagnosis. *Journal of Biomedical Optics*, 15(2):026002.

Whittaker, P., Kloner, R. A., Boughner, D. R., Pickering, J. G. (1994). Quantitative assessment of myocardial collagen with picrosirius red staining and circularly polarized light. *Basic Research in Cardiology*, 89(5):397–410.

Wu, T. J., Ong, J. J, Hwang, C., Lee, J. J, Fishbein, M. C, Czer, L., Trento, A., Blanche, C., Kass, R. M., Mandel, W. J., Karagueuzian, H. S, Chen, P. S. (1998). Characteristics of wave fronts during ventricular fibrillation in human hearts with dilated cardiomyopathy: role of increased fibrosis in the generation of reentry. *Journal of the American College of Cardiology*, 32(1):187-196.

Part of this chapter is included in the paper: *"A Spectral Approach for the Quantitative Description of Cardiac Collagen Network from Nonlinear Optical Imaging"*, by Masè M, Cristoforetti A, **Avogaro L**, Tessarolo F, Piccoli F, Caola I, Pederzolli C, Graffigna A, Ravelli F. published in Conf Proc IEEE Eng Med Biol Soc. 2015, 6257-60.

2.2 Quantification of collagen fiber orientation and scale dimension in human atrial tissue samples by Non-linear Optical Imaging

MATERIALS AND METHODs

Human tissue section collection and preparation

Right atrial appendage samples were collected from 12 individuals (all males) undergoing cardiac surgery. In particular, seven patients (range 71±9 years) presented in normal sinus rhythm following intervention (SR group), while five patients (range 76±4 years) displayed AF (AF group). After excision cardiac biopsies were immediately fixed in 4% formalin buffered solution and stored at room temperature (RT). Prior to the microscope examination, a portion of each appendage (about 10 mm^2) was separate with a scalpel, washed twice in phosphate buffered solution (PBS) and mounted onto a custom-made holder, the epicardium facing upward. In order to minimize morphological surface variability and preserve sample hydration, a cover slip was gently pressed against the epicardial surface by springs.

Nonlinear Optical Imaging

Samples were imaged in a two-photon microscope system (Ultima IV, Prairie Technologies, Middleton, WI, USA), combining an upright microscope (BX-61W, Olympus, Tokyo, Japan) with a Ti:saffire fs-pulsed laser (Mai Tai Deep See HP, Spectra-Physics, Santa Clara, USA) (Figure 6). The system included a pre-chirp module for wide-range dispersion compensation. The laser was tuned to 1040 nm for SHG imaging. A pockels cell controlled the laser beam power, which was adjusted within 10 and 20 mW at the sample surface. Galvo-mirrors were used to scan the samples. The excitation light was strongly focused onto the sample by a water immersion objective (60X, NA 0.9, Olympus) and two fields per patient were acquired The SHG signal was collected in an epigeometry, separated from the backscattered excitation light by a dichroic beamsplitter (cutoff at 660 nm), and splitted by a PMT dichroic mirror (575

nm) into two beams. The first component (channel A) was filtered by a 70 nm bandpass filter centred a 525 nm (Chroma Technology, Rockingham, VT, USA), before being detected by photomultiplier tubes (Hamamatus Photonics, Hamamatus City, Japan). The second component (channel B) was filtered by a bandpass of 607/45nm before detection. SHG signal was detected in the channel A. Broadband luminescence of elastin was revealed in channel B.

SHG images were acquired with 512X512 pixel digital resolution, 174 µm field of view dimension, using a pixel dwell time of 40 µs. 3D stacks were obtained by optical sectioning of the tissue at 1 µm interval from the epicardial surface down to a maximal depth of 50 µm.

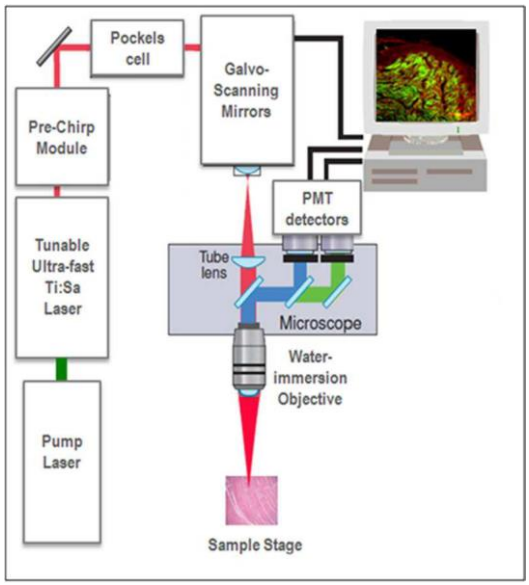

Figure 6: Two-photon microscopy set-up. Two-photon microscope system (Ultima IV, Prairie Technologies, Middleton, WI, USA), was set-up by combining an upright microscope (BX-61W, Olympus, Tokyo, Japan) with a Ti:saffire fs-pulsed laser (Mai Tai Deep See HP, Spectra-Physics, Santa Clara, USA).

Image processing and spectral analysis

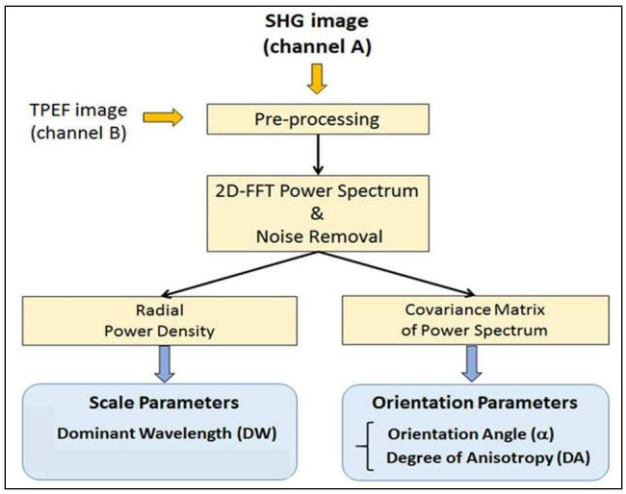

Figure 7: Flowchart of the spectral analysis framework applied to SHG images to extract quantitative indexes (cyan boxes) of the scale and orientation properties of the collagen network.

In order to obtain information concerning the 3D properties of the collagen network, such as fiber orientation (angle and anisotropy indexes) and scale dimension (dominant wavelength index) within the atrial tissue wall, a spectral analysis framework (sketched in Figure 7) was applied to the SHG images.

Image processing and spectral analysis were performed by a custom made program developed in Matlab R2013b. The analysis was applied to 738 images (450 SR and 288 AF) to extract multiple frequency-domain features of the collagen network structure. The main steps of the analysis are summarized in Figure 7 and comprised: 1) image pre-processing to enhance the collagen signal; 2) Fast Fourier Transform (FFT) and noise removal; 3) calculation of the radial power density and extraction of the texture scale index; 4) computation and diagonalization of the power spectrum covariance matrix and extraction of the fiber orientation indexes.

Image pre-processing was aimed to enhance the collagen signal and reduce the elastin component, and consisted in the subtraction of the signal in channel B from the signal in channel A. The FFT was calculated on squared ROIs (length L = 174 µm and size N = 512 pixels) of the pre-processed image $I(x,y)$, applying a 2D Tukey window $w_T(x,y)$ (α = 0.5, separable form) to reduce spectral leakage at high frequency. A smooth occlusion mask, $w_O(x,y)$, was applied to exclude non-tissue parts and tissue borders from FFT computation. The 2D-FFT, expressed as a function of the spectroscopic wave numbers v_x and v_y, was thus given by:

$$F(v_x, v_y) = \sum_{\substack{x=0\_(N-1)L \\ y=0\_(N-1)L}} w_T(x,y) w_O(x,y) I(x,y) e^{-\frac{2\pi i}{N}(v_x x + v_y y)}$$

The 2D power spectrum $PS(v_x, v_y) = |F(v_x, v_y)|^2$ was corrected from both periodic and white noise components. Periodic noise was removed by applying a despeckle filter in the mid-high frequency region (v_x, $v_y > 10/L$) of the *PS*. White noise was estimated by a fitting procedure and subtracted from the *PS*.

In order to extract quantitative measures of the scale properties of the collagen texture, the radial power density (RPD) was computed as a function of radial wave numbers $v_i = i/L$, $i=0,1,\ldots N/2$, by integrating the power spectrum $\widetilde{PS}$ = PS-W with respect to the polar angle. The integral was estimated as a discrete summation weighted by the ring windows rw_i:

$$RPD(v_i) = \sum_{\substack{v_x=-N/2L \ldots N/2L \\ v_y=-N/2L \ldots N/2L}} rw_i(v_x, v_y) \widetilde{PS}(v_x, v_y)$$

Where rw_i takes non-zero values only in a 2/L thick zone proximal to v_i, according to a raised cosine function of the radial wavenumber $v = \sqrt{v_x^2 + v_y^2}$:

$$rw_i(v_x, v_y) = \begin{cases} \frac{1}{2}\left(1 + \cos(\pi L(v - v_i))\right) & \mathbf{v_{i-1} \le v \le v_{i+1}} \\ \mathbf{0} \quad \mathbf{v < v_{i-1} \ or \ v > v_{i+1}} \end{cases}$$

The scale properties of the collagen network were quantified in terms of the dominant wavelength (DW), which was defined based on the percentiles of the RPD distribution.

The dominant wavelength (DW) was related to the average dimension of the collagen texture and was defined as:

$$\mathbf{DW} = \frac{\mathbf{1}}{\mathbf{v_{50}}}$$

where v_{50} is the 50th percentile of the RPD, restricted to the 0.01-1 ∝m-1 range.

Two additional indexes, related to the presence of fiber orientation in the collagen network, were obtained computing the covariance matrix of $\widetilde{PS}$ in the [v_{25} - v_{75}] range.

The covariance matrix was diagonalized to obtain the eigenvalues, e_{max} and e_{min}, and the corresponding orthogonal eigenvectors, $\boldsymbol{v_{min}}$ and $\boldsymbol{v_{max}}$.

The dominant orientation of the fibers was indicated by the orientation angle α, defined by the direction of v_{min} in the range 0-180°.
The degree of anisotropy (*DA*) of the fibers was defined by the two eigenvalues, as:

$$DA = 1 - \sqrt{\frac{e_{min}}{e_{max}}}$$

The index ranges between 0 and 1, with 0 indicating the absence of a preferential direction (equal eigenvalues in the two orthogonal directions), and values close to 1 indicating maximal anisotropy (e_{max} dominating over e_{min}).

Statistical analysis

Data are expressed as mean and standard deviation or median and interquartile range (IQR), as pertinent. The variability of the average direction of the fibers (α) along tissue depth in each patient was assessed in terms of standard deviation using circular statistics. Statistical differences between index distributions in SR versus AF patient images were assessed by Wilcoxon-Mann-Whitney test, given the non-normality of the overall distributions (Lilliefor test). A p-value < 0.05 was considered statistically significant.

RESULTS

Properties of collagen network in AF compared to SR patients

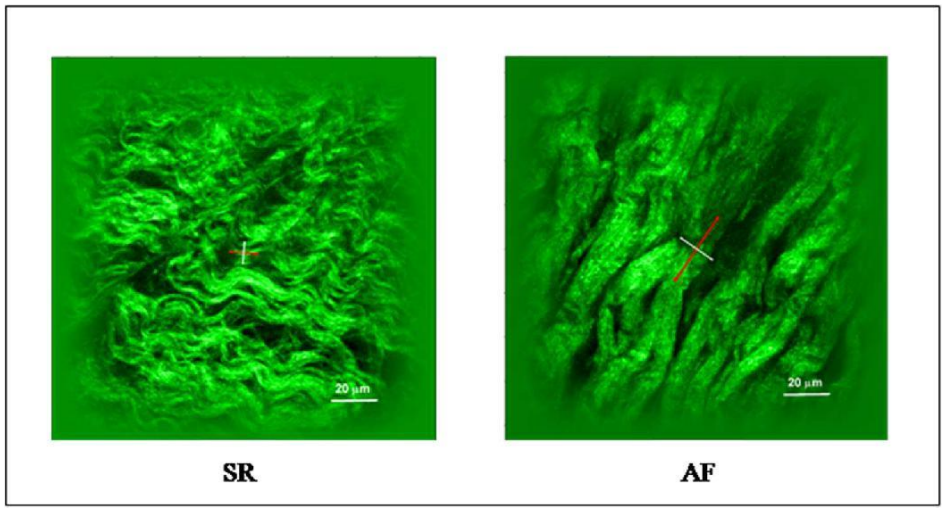

Figure 8: Optically sectioned ex-vivo atrial tissue samples from a patient with SR (left panel) and a patient with AF (right panel), imaged by SHG microscopy. The White line indicates the Dominant Wavelength, DW; the direction of the Red line indicates the dominant orientation of the fibers, while its length is proportional to the degree of anisotropy, DA. Representative images.

Representative examples of SHG microscopy applied to atrial tissue samples collected from SR and AF patients are shown in Figure 8. In the patient with SR (left panel) collagen shows a fine architecture characterized by thin fibrils with changing angles and directions. Conversely, in the AF patient (right panel) collagen tended to pack-up in larger bundles of defined directions. The different properties of the collagen network observed in the two samples were quantified by the spectral analysis indexes. As concerns the texture scale, the presence of thin fibers in the SR patient resulted in a smaller dominant wavelength (DW=10 µm, as indicated by the white line), while fibers packing-up in the AF patient led to a higher DW value (DW=17.8 µm). As concerns fiber orientation, the structure of thin fibers with varying orientation in the SR patient, resulted in a lower degree of anisotropy (DA=0.28, as indicated by the red line) with respect to the AF case (DA=0.50), where thick oriented bundles of collagen were present.

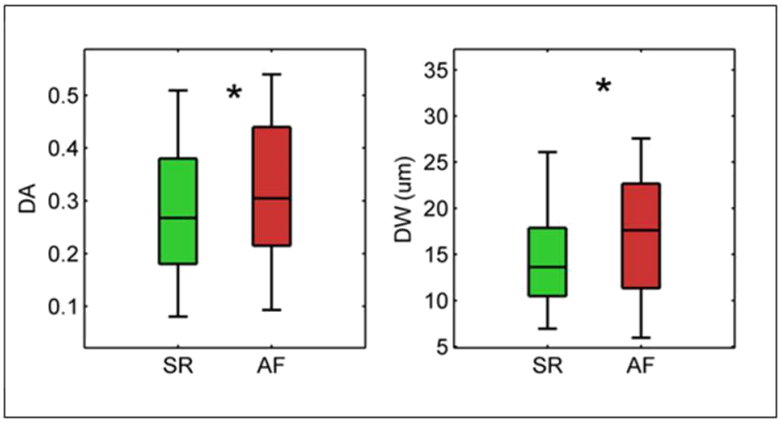

Figure 9: Fiber anisotropy (DA) and scale dimension (DW) in the overall patient population. Degree of anisotropy and dominant wavelength values resulted increased in AF compared to SR group. N=12 (5 AF, 7 SR). *, p<0.001 AF versus SR images.

The results of the analysis of the whole image database, summarized in Figure 9, confirmed the results of the representative examples, evidencing significant differences in the anisotropy and scale properties of the collagen network in the SR versus AF patients. In particular, anisotropy values (Figure 9, left panel) resulted higher in AF (median 0.30, IQR 0.21-0.44) with respect to the SR group (median 0.27, IQR 0.18-0.38; p<0.001: SR versus AF images). In addition, also dominant wavelength (Figure 9, right panel) values resulted significantly increased (median 17.6 µm, IQR 11.3-22.7 µm) in AF compared to SR patients (median 13.6 µm, IQR 10.5-17.9 µm ; p<0.001:SR versus AF images). Nonetheless, high variability was found in the overall results for both groups, suggesting possible differences in the properties of collagen throughout the tissue.

Depth profile in the sub-epicardial layers in AF compared to SR patients

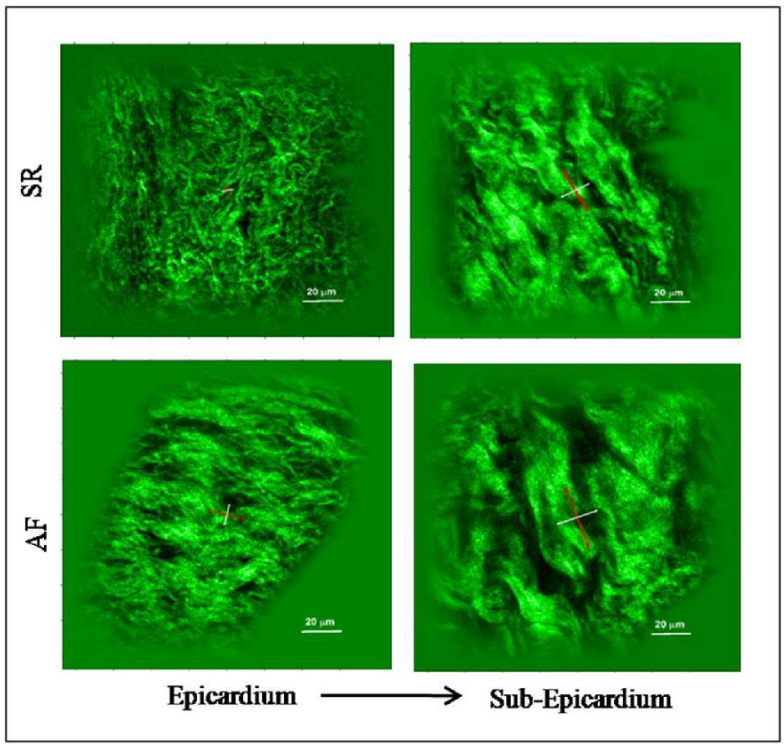

Figure 10: Optically sectioned ex-vivo atrial tissue samples from a patient with SR (upper images) and a patient with AF (lower images) imaged by SHG microscopy, taken from the epicardium (left) and the sub-epicardium (right). Representative images.

After the global evaluation of collagen properties in AF compared to SR groups, a detailed depth analysis of the 3D collagen network throughout the atrial tissue was performed. Figure 10 shows representative SHG images of atrial samples collected from SR and AF patients, at different tissue depth. Image analysis of the outer epicardium layers (depth of 0-20 µm, Figure 10, left side) and the sub-epicardium (depth of 20-35 µm, Figure 10, right side), revealed changes in collagen network properties across tissue wall. Specifically, in both SR and AF representative patients, collagen scale increased passing from the epicardial to the subepicardial layers, as well the main orientation of the fibers changed along tissue depth, suggesting fiber rotation.

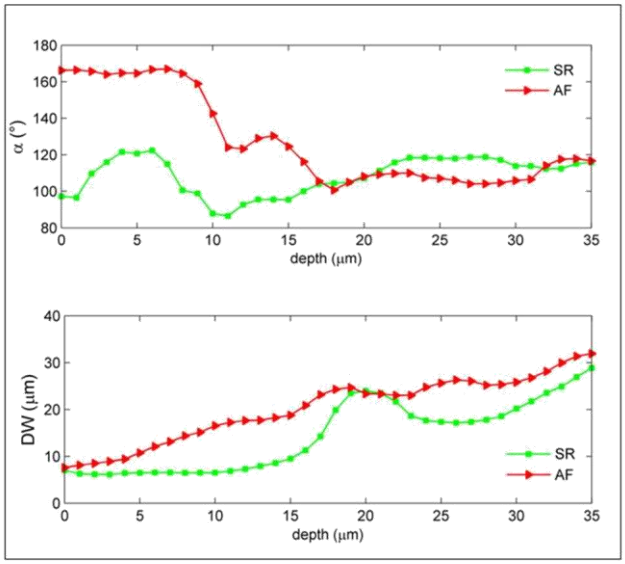

Figure 11: Collagen fibers angles (*α*)(upper panel) and scale dimension (DW)(lower panel) along tissue depth in SR (green) and AF (red) patients. Representative examples.

These qualitative considerations were quantitatively confirmed by applying spectral analysis to subsequent optical sections throughout the atrial tissue. The results of the in-depth analysis in two representative AF and SR patients are displayed in Figure 11, which shows the change in the average orientation angle of the fibers (*α*, upper panel) and dominant scale of the collagen texture (*DW*, lower panel) as a function of tissue depth. The variation in α values indicates the rotation of collagen fibers rotate along tissue depth in both AF and SR patients. Nonetheless, while in the SR patient (in green) α showed small oscillations (ranging between 86-122°, standard deviation 10.3°), larger oscillations were observed in the AF patient (ranging between 101-167°, standard deviation 24.9°), especially within the first 10 μm of depth. As concern scale dimension, dominant wavelength values changed along tissue depth in both cases (from 10 to 30 μm), although larger scale values were observed in the presence of AF (20.2 ± 7.0 μm), compared to SR (14.4 ± 7.5 μm).

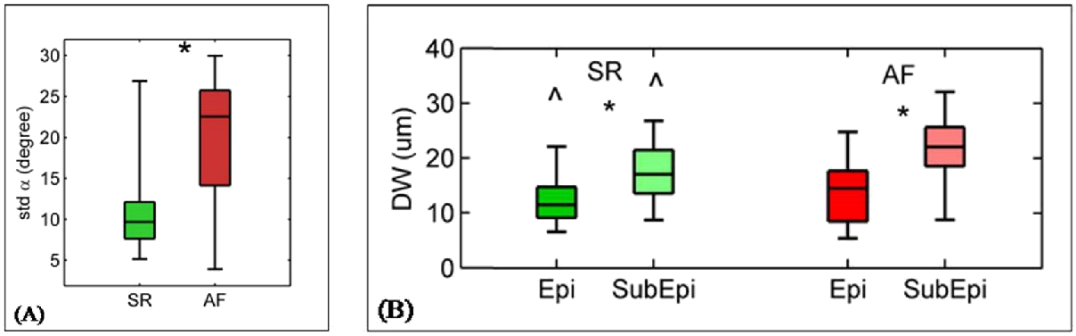

Figure 12: Variability of collagen orientation (α)(A) and scale dimension (DW)(B) in SR (green) and AF (red) patient populations at a different depth. N=12 (5 AF, 7 SR); A) *, p<0.05: SR versus AF patients; B) *, p<0.001: Epi VS Sub-Epi tissues; ^, p<0.05: SR versus AF images.

The results of the analysis of the whole image database, displayed in Figure 12, corroborated the results in the representative patients. In terms of orientation changes (panel A), the AF group showed larger changes (std) of the fiber direction angle throughout the tissue (median 22.5°, IQR 14.1°-25.7°) compared to the SR group (median 9.7° , IQR 7.6°-12.1°; (p<0,05: SR versus AF patients). As concerns collagen scale (panel B), DW values changed between the epicardium (Epi) and the subepicardium (SubEpi), assuming larger values in the epicardial layer in both groups (Epi: 11.5 [9.1-14.7] μm ; SubEpi: 17.1 [13.6-21.5] μm in SR; Epi: 14.5 [8.5-17.7] μm; SubEpi 22.0 [18.5-25.6] μm in AF). Nonetheless, in both subareas, larger DW values were observed in AF as compared to SR patients (p<0.05, AF versus SR images). Differently from scale and average orientation, the degree of anisotropy show no consistent changes as a function of depth in the overall population.

DISCUSSION

Experimental and clinical studies have identified in structural remodeling the so-called "second factor" in the formation of the AF substrate, and an important contributor for arrhythmogenesis (Allessie, 2002; Kottkamp, 2013). Inactive collagenous septa between cardiomyocytes may indeed support the propagation of multiple excitation wavelets in AF, creating slow conduction areas, barriers to wave propagation and/or anchoring points for reentries. For these reasons, an accurate investigation of the structural properties of the atrial collagen network is necessary for a mechanistic understanding of AF.

During the last decades, new optical microscopy techniques have been developed that use non-linear light-matter interactions to generate signal contrast (Denk *et al.,* 1990; Helmchen & Denk, 2002; Mertz, 2004; Campagnola *et al.,* 2003; Zipfel *et al.,* 2003). Nonlinear optical microscopy (NLO) techniques, which comprise two-photon excited fluorescence (TPEF) and second harmonic generation (SHG) microscopy, possess special features that make them less sensitive to scattering and thus suitable for high-resolution imaging of thick tissue specimens. In particular, SHG microscopy can provide morphological and functional images of anisotropic biological structures with high hyperpolarizability, such as collagen. Importantly, SHG microscopy represents a nondestructive imaging tool that allows a clear and selective visualization of collagen fibers, without sample staining or pretreatments (Cicchi *et al.,* 2013).

In this section, a novel approach for the characterization of collagen network properties in atrial tissue samples based on NLO microscopy was described. In particular, by applying second harmonic generation (SHG) microscopy in combination with a spectral analysis framework, a multiparametric description of the properties of collagen network in atrial tissue samples was provided.

The analysis of SHG images of atrial tissue samples collected from SR and AF patients revealed that in SR patients collagen network showed a fine architecture characterized by thin fibrils, with changing angles and directions. On the contrary, in AF patients collagen tended to pack-up in larger bundles of defined directions. These differences were quantified by spectral analysis indexes, which revealed that collagen in AF patients displays significantly higher fiber anisotropy and larger scale dimension with respect to SR patients. This evidence suggests the remodeling of the atrial connective tissue in presence of the arrhythmia, with fibers packing up in larger oriented bundles. The optical sectioning capability of NLO microscopy was used to provide a detailed

analysis of the 3D collagen features in the epicardial and subepicardial layers (35 μm depth). The analysis of the images throughout the outer myocardial layers revealed that collagen network properties changed from the epicardium to the sub-epicardium, in both AF and SR patients. The results of the whole image database indicated that collagen fibers rotated from the epicardium to the sub-epicardial layers in both AF and SR groups, assuming larger orientation changes in AF patients. Similarly, collagen scale increased from the epicardium to the sub-epicardium, with higher values in AF group. Taken together, these findings evidence a spatial rearrangement and thickening of the 3D collagen network in AF patients, suggesting a possible role in the development of the arrhythmia. Accordingly, some studies (Chiu *et al.,* 2010; Tsai *et al.,* 2010) have also found larger entropy values of collagen fiber angles in AF versus SR patients, although indexes were computed by a different approach.

The multiparametric description of collagen network revealed that fibers orientation (described by angle and anisotropy indexes) and scale dimension (described by dominant wavelength values), resulted increased in AF tissues, suggesting possible remodeling processes. In this perspective, a growing body of evidence have indicated that an increased and disorganized pattern of 3D collagen network across the myocardium may impair the electrical impulse propagation, predisposing to the formation of epicardial breakthrough as well as 3D reentrant circuits, thus resulting in AF.

The methodology here proposed have also shown its capability to detect and quantify differences in the morphology and organization of the collagen network in the atrial tissue of AF versus SR patients. These results may provide new information about the structural features that characterized a pro-arrhythmic substrate, useful to a better understanding of the mechanisms that underlie AF.

BIBLIOGRAPHY

Allessie, M., Ausma, J., Schoetten, U. (2002). Electrical, contractile and structural remodeling during atrial fibrillation. *Cardiovascular Research*, 54(2):230–246.

Campagnola, P. J., Loew, L. M. (2003). Second-harmonic imaging microscopy for visualizing biomolecular arrays in cells, tissues and organisms. *Nature Biotechnology*, 21(11):1356–1360.

Chiu, Y. W., Lo, M. T., Tsai, M. R., Chang, Y. C., Hsu, R. B., Yu, H. Y., Sun, C. K., Ho, Y. L. (2010). Applying harmonic optical microscopy for spatial alignment of atrial collagen fibers. *PLoS One*, 5(11):e13917.

Cicchi, R., Vogler, N., Kapsokalyvas, D., Dietzek, B., Popp, J., Pavone, F. S. (2013). From molecular structure to tissue architecture: collagen organization probed by SHG microscopy. *Journal of Biophotonics*, 6(2):129–142.

Denk, W., Strickler, J. H., Webb, W. W. (1990). 2-Photon Laser Scanning Fluorescence Microscopy. *Science*, 248(4951):73–76.

Helmchen, F., Denk, W. (2002). New developments in multiphoton microscopy. *Current Opinion in Neurobiology*, 12(5):593–601.

Kottkamp, H. (2013). Human atrial fibrillation substrate: towards a specific fibrotic atrial cardiomyopathy. *European Heart Journal*, 34(35):2731–2738.

Mertz, J. (2004). Nonlinear microscopy: new techniques and applications. *Current Opinion in Neurobiology*, 14(5):610-616.

Tsai, M. R., Chiu, Y. W., Lo, M. T., Sun, C. K. (2010). Second-harmonic generation imaging of collagen fibers in myocardium for atrial fibrillation diagnosis. *Journal of Biomedical Optics*, 15(2):026002.

Zipfel, W. R., Williams, R. M., Webb, W. W. (2003). Nonlinear magic: multiphoton microscopy in the biosciences. *Nature Biotechnology*, 21(11):1369–1377.

CHAPTER 3: MOLECULAR CHARACTERIZATION

Over the last decades, different mechanisms have been proposed to explain the development and progression of AF. Genetic mutations, functional impairment, expression deregulation of ion channels, transporters, intracellular Ca^{2+}-handling and other relevant proteins, can contribute to creating a structural and metabolic substrate which may result in electrical disturbances, predisposing to AF (Wang *et al.,* 2011). In this perspective, recent studies have indicated that an altered regulation of gene expression may play a pivotal role in the mechanisms of atrial remodeling that underlie AF. Nonetheless, the frequent mismatch between mRNA and protein levels of gene expression has encouraged many researchers to investigate the regulatory mechanisms at post-transcriptional level. In particular, it has been recently demonstrated that microRNAs, which are a class of endogenous short RNA sequences that negatively regulate gene expression, are involved in the control of AF, thus providing novel insights into the molecular basis of the pathogenesis of AF (Luo *et al.,* 2015; Santulli *et al.,* 2014; Wang *et al.,* 2011). A growing body of evidence has indicated that miRNAs are differently expressed in the failing myocardium, and may play an important role in cardiac disease progression by targeting genes that govern diverse function in cardiac remodeling, including myocardial fibrosis (Topkara & Mann, 2011).

Various methodologies have been applied in order to characterize qualitatively and quantitatively the expression patterns of miRNAs, associated with pathological versus normal conditions (Moreno-Moya *et al.,* 2014). Nonetheless, qPCR remains the gold standard method for detection of specific sets of miRNAs (Chen *et al.,* 2005; Schmittgen *et al.,* 2008; Yan *et al.,* 2013). To accurately determine the levels of analyzed miRNAs, their expression data are usually normalized relatively to endogenous and/or exogenous reference genes. Nevertheless, no general agreement between different normalization strategies has been found, to date. In addition, there is a lack of information regarding reliable housekeeping genes for miRNAs analysis in cardiac tissue, in particular for the study of AF.

In this chapter, the expression patterns of some miRNAs known to target genes involved in different mechanisms that underlie AF were investigated. Specifically, human atrial tissue samples collected during cardiac surgery from patients with and without AF were processed for high-quality RNA extraction and subsequent qPCR analysis. A panel of miRNAs (miR-1, miR-133a/b, miR-30c, miR-29a/b, miR-208a/b,

miR-328, miR-499, miR-590 and miR-21) was selected after an accurate review of the literature.

The goal of the study was to test the existence of different miRNAs expression patterns between AF patients and individuals in normal sinus rhythm, with particular attention to miRNAs involved in fibrotic remodeling. The accomplishment of this goal required the performance of preliminary analyses in order to 1. devise a specific protocol for high-quality RNA extraction from cardiac tissue, and 2. identify a proper endogenous reference gene for normalization of miRNA expression levels. The issue of RNA extraction is addressed in Appendix (p.122), where four different protocols were tested on tissue samples from a "model" pig heart and compared in terms of RNA yield and quality. The issue of data normalization is addressed in the first part of this chapter. This presents a detailed analysis of the performance of five commonly used endogenous reference transcripts (5S, U6, SNORD48, SNORD44, miR-16) by using different well-established analysis tools, such as NormFinder (Andersen *et al.*, 2004), GeNorm (Vandesompele *et al.*, 2002), BestKeeper (Pfaffl *et al.*, 2004) and ΔCt method (Silver *et al.*, 2006). The best reference gene obtained from this preliminary analysis was applied for the normalization of miRNAs expression levels in the patients' population, which is presented in the second part of this chapter. The analysis of miRNAs expression profiles in patients with and without AF is complemented with a correlation analysis of miRNAs levels and previously obtained histological data (see Chapter 2.1), in order to identify a possible relationship between miRNAs and fibrosis.

3.1 Determination of the most suitable reference gene for miRNAs' data normalization

MATERIALS AND METHODS

Patient samples

Tissue samples from the right atrial appendage were collected from 20 patients (all males) undergoing cardiovascular surgery. In particular, eleven patients (range 67 ± 12 years) displayed normal sinus rhythm following the intervention (SR group), while nine patients (range 76 ± 4 years) displayed AF (AF group).

Human tissue processing and RNA isolation

Small biopsies (~25-100 mg) of the right atrial appendage were collected immediately after the cardiac intervention, flash frozen on pre-chilled liquid isopentane and stored at -80°C until RNA isolation. Samples were treated according to an optimized protocol, specifically designed to obtain high quality and high yield RNA extraction (see Appendix, p.124). Briefly, frozen tissues samples were placed in a sterile 15 ml polypropylene tube containing 1,5 ml of pre-cooled Qiazol reagent (Qiagen, Milan, Italy) and subsequently homogenize with a polytron (Omni-TH International, Kennesaw, USA) on ice, at the half of the speed.

The total RNA (including miRNAs) was extracted using the miRNeasy mini kit (Qiagen, Milan, Italy) according to the manufacturer's protocol. RNA concentration and purity were assessed spectrophotometrically by Nanodrop ND-1000 (Thermo Scientific, Wilmington, DE, USA). RNA integrity was evaluated for each sample using Agilent 2100 Bioanalyzer (Agilent Technologies, Santa Clara, CA, USA). RNA aliquots were stored at -80°C until use.

Selection of candidate reference genes

Candidate reference genes were selected based on a literature survey (Table 1). In particular, the transcripts considered have been used as normalizers in different miRNAs' cardiac tissue studies.

Reference Gene	RNA type	References
5S	Ribosomal RNA	Zhang et al., 2012
miR-16	microRNA	Nishi et al., 2013 Roy et al., 2009
SNORD44	Small nucleolar RNA	Ferreira et al., 2014
SNORD48	Small nucleolar RNA	Sauer et al., 2014
U6	Small nuclear RNA	Satoh et al., 2010 Cooley et al., 2012 Adam et al., 2012 Villar et al., 2013 García et al., 2013 Song et al., 2014 Liu et al., 2014 Dong et al., 2014

Table 1: Summary of the literature-based selection of the candidate reference genes.

Reverse transcription qPCR (RT-qPCR)

The total RNA isolated from each tissue sample was reverse-transcribed using miRCURY LNA™ Universal cDNA Synthesis kit II (Exiqon, Vedbaek, Denmark) according to the manufacturer's protocol. qRT-PCR assays based on SYBR Green I were performed using miRCURY LNA™ PCR primers set (Exiqon, Vedbaek, Denmark) on the following selected RNAs: 5S, U6, SNORD48, SNORD44B, hsa-miR-16-5p. qPCR reactions were performed using ExiLENT SYBR® Green master mix (Exiqon, Vedbaek, Denmark) in a CFX384 Real-Time PCR Detection System (Bio-Rad Laboratories, Milan, Italy). The 10 µl PCR reaction contained 4 µl of the diluted cDNA template, 5 µl of SYBR® Green master mix and 1 µl of PCR primer mix. The reaction protocol was as follows: 95°C for 10 minutes, followed by 40 amplification cycles of 95°C for 10 seconds and 60°C for 1 minute. Each patient sample was assessed in technical triplicates. The threshold cycle (Ct) was defined as the fractional cycle number at which fluorescence exceeded the given threshold.

Data analysis and software-based selection of endogenous reference genes

Data analysis was performed by a custom made software, developed in Matlab R2013b (MathWorks Inc., Natick, Massachusetts, US), which allowed preprocessing of raw data and evaluation of reference gene performance according to different algorithms. For each patient sample and reference gene Ct values were estimated as average of the technical triplicates Cts, after removal of the outliers (Ct values that differed more than 1 from the Ct median). Ct values or relative expression values (i.e. $2^{-(Ct-min(Ct))}$), where min (Ct) indicates the minimum of the Ct value of the reference gene over the population), were used as inputs for subsequent analysis.

In order to consider different aspects in the evaluation of reference gene performance, gene expression stability was evaluated according to four reliable, widely-used algorithms, such as GeNorm (Vandesompele *et al.,* 2002), BestKeeper (Pfaffl *et al.,* 2004), ΔCt method (Silver *et al.,* 2006), NormFinder (Andersen *et al.,* 2004), which are briefly described in the following.

GeNorm (Vandesompele *et al.,* 2002), the first algorithm introduced to evaluate the stability of reference genes, is based on the assumption that the expression ratio of two reference genes should be constant across samples. Consistently, a "gene stability measure" (*M*-value) is defined as the average pairwise variation of a particular reference gene with all other tested candidate reference gene. Based on *M*-values, a repeated process of stepwise exclusion of the worst scoring reference genes is performed till the best pair of reference genes is identified.

BestKeeper (Pfaffl *et al.,* 2004) uses as input raw *Ct* data and assumes that proper reference genes should display low variability and a similar expression pattern. Thus, gene ranking is performed by computing the complete descriptive statistics of the reference genes to evaluate their variability and executing pair-wise correlation analysis of the genes *Cts* to evaluate pattern similarities.

The ΔCt method (Silver *et al.,* 2006) is based on assumptions similar to GeNorm, but "pairs of reference genes" are quantitatively compared based on the variability (standard deviation) of the differences of their *Cts* (*ΔCt*) over the samples. The stability of each gene is thus quantified, as the average of the standard deviations obtained by the pair-wise comparisons with all other reference genes.

NormFinder (Andersen *et al.*, 2004) is based on a solid mathematical model of gene expression and statistical framework, which allows to estimate not only the overall expression variation of the candidate genes but also the variations between sample subgroups of the same set (e.g., AF versus SR samples). Thus, differently from the other methods, the algorithm allows to test candidate genes directly on the disease of interest. A stability value ρ is obtained for each candidate gene, which combines intra- and inter-group variations, and provides a direct measure of the systematic error introduced when using the gene for normalization.

The results of the four analysis were combined to evaluate the global performance of the reference genes. The overall ranking of the genes was obtained as the geometric mean of the rankings given by each of the analyses.

RESULTS

Quantity and integrity

Quantity of total RNA varied between different tissue samples. RIN number were comprised between 5.2 and 8.6. (Table 2).

Sample	Concentration (ng/µl)	RIN number
Patient 1	512,32	7,2
Patient 2	1.302	7,5
Patient 3	331,1	7
Patient 4	517,2	5,2
Patient 5	246,2	5,3
Patient 6	104,4	6,9
Patient 7	117,3	6,5
Patient 8	130,4	8,5
Patient 9	117,3	8,2
Patient 10	55	8,3
Patient 11	79	8,2
Patient 12	109,6	7,7
Patient 14	131,3	8,2
Patient 16	79,8	8,6
Patient 17	124,7	8,6
Patient 18	267,8	8
Patient 19	76,1	8,4
Patient 20	69,8	8
Patient 22	85,8	8,4
Patient 23	91,4	8,4
Patient 24	108,9	7,7
Patient 25	139,9	7,1
Patient 26	156,2	8

Table 2: Total RNA quantity and integrity for each tissue sample examined.

Expression stability of the candidate reference genes-determination of the most suitable reference genes

The distributions of the *Ct* values of the five reference genes over the whole sample set are shown in Figure 1, while the descriptive statistics of the distributions given by BestKeeper are reported in Table 3. Candidate genes displayed different average values and variability levels. 5S RNA showed the highest expression level (lowest average *Ct*

value of 18.9), which is consistent with its role of an essential component of the ribosomes of all living organisms. The lowest expression level was observed for SNORD44B, which displayed an average *Ct* value of 26.7. As concerns the variability over the whole data set, SNORD48 and miR-16 displayed the lowest standard deviations, 0.66 and 0.69, respectively. 5S and U6 showed the highest variability (1.21 and 1.76, respectively), both beyond the limit of acceptance (<1) for consistent normalizers, while SNORD44B displayed a variability at the limit of acceptance (~1). The ranking of reference genes based on *Ct* variability (Figure 2) assessed SNORD48 as the best and U6 as the worst reference genes.

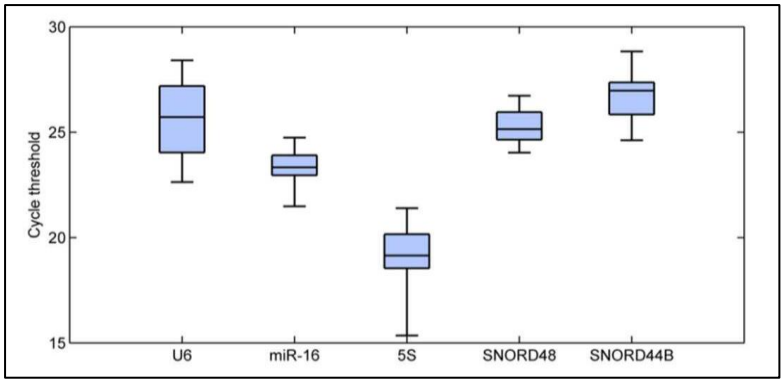

Figure 1: qPCR cycle threshold (Ct) values for the five candidate reference genes obtained from human atrial tissue samples. Data are median (solid line), interquartile (box) and 5th and 95th ranges (whiskers). Patient population N=20 (11 SR, 9 AF).

Candidate Genes	U6	miR-16	5S	SNORD48	SNORD44B	BK (N=5)	BK (N=3)
NS	20	20	20	20	20	20	20
geo Mean [Ct]	25.51	23.35	18.86	25.29	26.72	23.77	25.08
ar Mean [Ct]	25.58	23.37	18.94	25.30	26.75	23.79	25.09
Min [Ct]	22.49	20.75	15.17	23.88	24.34	21.82	23.86
Max [Ct]	28.46	24.91	21.49	26.78	28.90	25.22	26.78
Std [± Ct]	1.67	0.69	1.21	0.66	1.01	0.68	0.57
CV [% Ct]	6.54	2.94	6.38	2.62	3.78	2.86	2.28

Table 3. Descriptive statistics of the five candidate reference genes, based on their Ct values, as provided by BestKeeper. NS = number of samples; geo = geometric; ar = arithmetic; Std = standard deviation; CV = coefficient of variance; BK = BestKeeper index, calculated over all genes (N=5) and with the exception of the two genes with the highest variability (N=3).

The analysis of the correlation provided by BestKeeper is reported in Table 4. SNORD48, SNORD44B and 5S displayed significant correlation when compared to one another and to BestKeeper (BK) index (N=5), while U6 correlated just with 5S and BK index (N=5, calculated over all reference genes). Interestingly, miR-16 did not correlate with any other gene nor with BK index (N=5). A significant correlation for miR16 was observed only with BK index (N=3), which was calculated excluding the two reference genes with variability above tolerance.

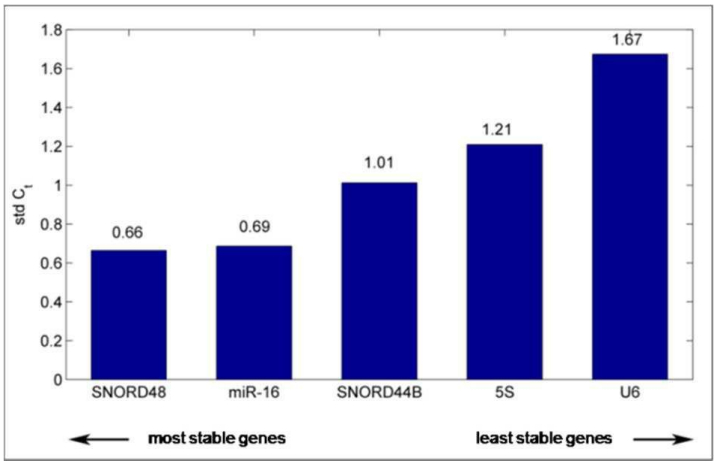

Figure 2: BestKeeper ranking for reference gene stability, based on *Ct* variability (standard deviation, std). SNORD48 showed the lowest variability (highest stability) across the analyzed samples. Patient population N=20 (11 SR, 9 AF).

Versus	**U6**	**miR-16**	**5S**	**SNORD48**	**SNORD44**
miR-16	-0.239	-	-	-	-
p-value	0.312				
5S	0.613	-0.123	-	-	-
p-value	0.004	0.603			
SNORD48	0.145	-0.033	0.536	-	-
p-value	0.543	0.890	0.015		
SNORD44	0.187	-0.045	0.657	0.911	-
p-value	0.429	0.851	0.002	0.001	
BK (N=5) versus	**U6**	**miR-16**	**5S**	**SNORD48**	**SNORD44**
Coeff. of corr. (r)	0.681	0.054	0.922	0.687	0.762
p-value	0.001	0.821	0.001	0.001	0.001
BK (N=3) versus	**U6**	**miR-16**	**5S**	**SNORD48**	**SNORD44**
Coeff. of corr. (r)	-	0.450	-	0.849	0.859
p-value	-	0.046	-	0.001	0.001

Table 4. Repeated pair-wise correlation analysis of candidate reference genes. Genes are pairwise correlated one with another and with the BestKeeper (BK) index, calculated on all genes (N=5) and with the exception of the two genes with the highest variability (N=3). For each comparison, the Pearson coefficient of correlation (r) and its significance (p-value) are reported.

The analysis of gene stability performed by GeNorm is reported in Figure 3, which shows the procedure of step-wise exclusion of the candidate genes with the highest *M*-value (poorest stability). The analysis indicated U6 as the worst reference gene (its exclusion resulted in a decrease of the *M*-value from 1.64 to 1.39), while miR16 and 5S followed with intermediate stability values (1.39 and 1.12, respectively). The stepwise procedure terminated identifying SNORD48 and SNORD44 as the most stable pair of candidate genes with an *M*-value of 0.62.

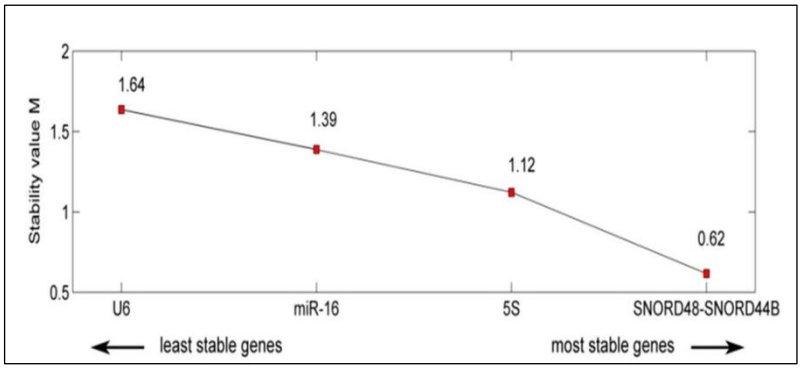

Figure 3: Expression stability plot for reference gene selection by GeNorm analysis. GeNorm proceeds by calculation of the gene stability measure (*M*-value) per gene from the least (left) to the most stable (right). SNORD48 and SNORD44B showed the highest expression stability across the 20 analyzed samples. Patient population N=20 (11 SR, 9 AF).

Similar results were obtained by application of the ΔCt method, as displayed in Figure 4. U6 resulted the least stable gene, with the highest average standard deviation of ΔCt for pairwise comparisons (2.01), followed by miR16 (1.83). Intermediate values of the average std were observed for 5 S (1.61). The most stable genes were SNORD48 (1.33) and SNORD44B (1.41), first and second of the ΔCt ranking, respectively.

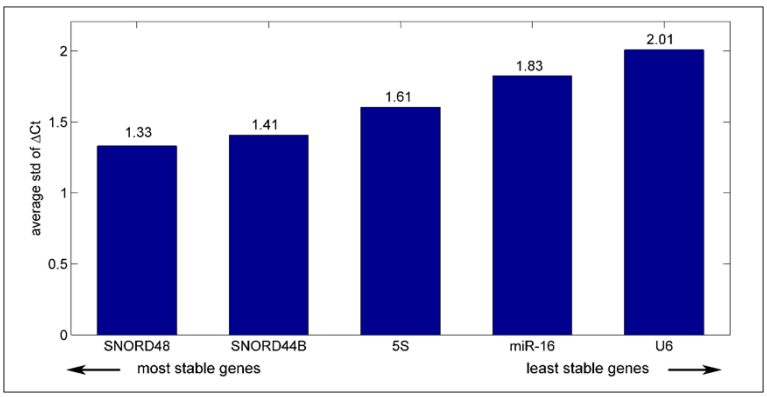

Figure 4: ΔCt analysis for reference gene selection. Comparison of the average values of the variabilities of ΔCt values calculated for each candidate gene with the remaining genes. SNORD48 displays the lowest variability and thus the highest stability across the analyzed samples.
Patient population N=20 (11 SR, 9 AF).

The results of the variability analysis performed by NormFinder are displayed in Figure 5. The top panel (A) shows the overall evaluation in terms of stability index ρ, while the lower panel (B) evidences the contributions of inter-group (box) and intra-group (whiskers) variations to the stability index. The worst overall performance was again shown by U6 (ρ=0.63), which displayed large values of both inter-group (-0.45) and intra-group variabilities (1.14). Despite their small inter-group variabilities (-0.13 and 0.08), 5 S and miR16 displayed very high intra-group variabilities (0.58 and 1.19), which severely affected their overall performance (ρ=0.40 and 0.46). SNORD44 displayed intermediate values of intra-group (0.23) and inter-group variability (0.25), ranking second with a ρ=0.39. SNORD48 showed the highest overall stability (ρ=0.32), with intermediate inter-group variations (0.25), but the smallest intra-group variability (0.05).

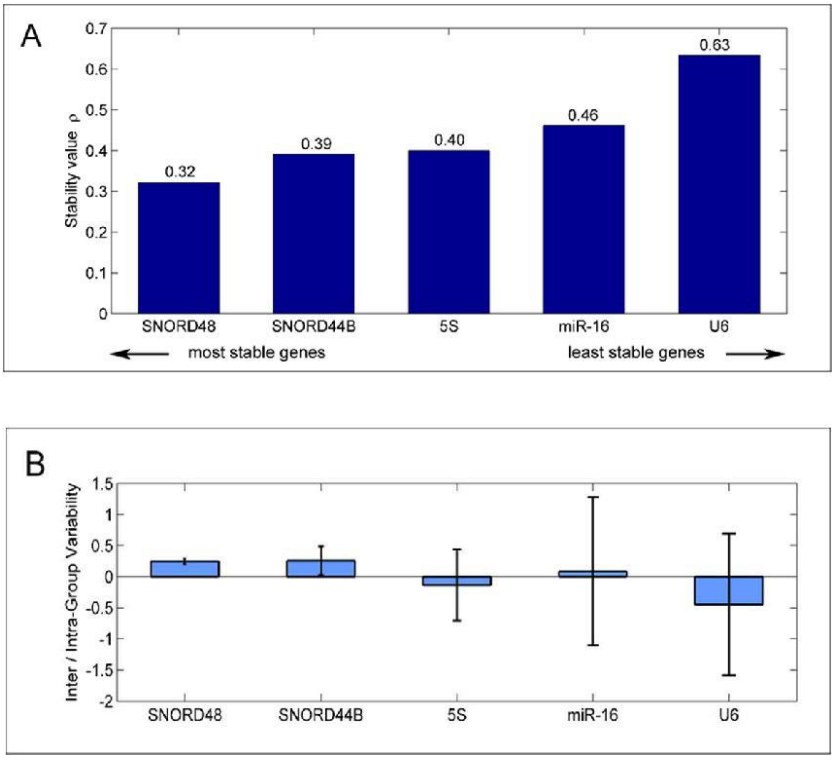

Figure 5: Expression stability plot for reference gene selection by NormFinder analysis. A) Overall stability index (ρ) of each candidate gene. **B)** Intergroup (color box) and intra-group (error bars) contributions to overall stability of each reference gene. SNORD48 displayed the highest stability across the analyzed samples. Patient population N=20.

Rank	Gene	Comprehensive	BestKeeper	GeNorm	Delta Ct	NormFinder
1	SNORD48	1	0.66	0.62	1.33	0.32
2	SNORD44B	1.9	1.01	0.62	1.41	0.39
3	5S	3.2	1.21	1.12	1.61	0.40
4	miR16	3.4	0.69	1.39	1.83	0.46
5	U6	5	1.67	1.64	2.01	0.63

Table 5. Stability of candidate reference genes according to the four evaluation algorithms. Gene are ordered based on their overall performance, where the comprehensive ranking was obtained as the geometric mean of the rankings obtained by the four techniques.

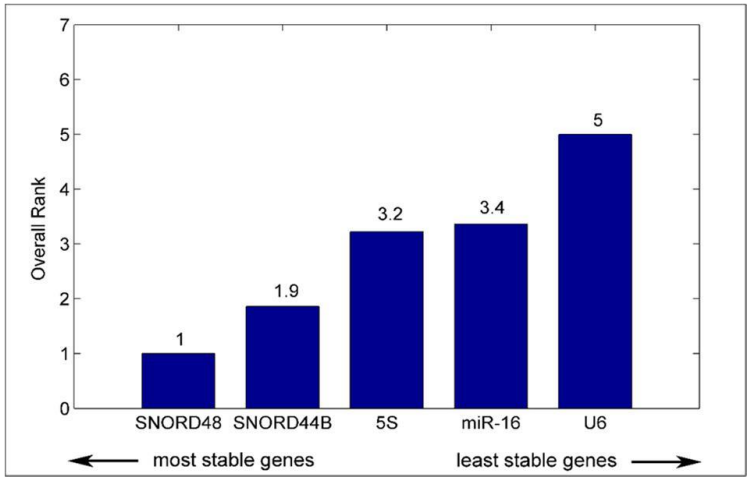

Figure 6: Overall ranking of the five candidate reference genes. The overall positioning is calculated as the geometric mean of the rankings obtained by BestKeeper, GeNorm, ΔCt and NormFinder analysis. SNORD48 displayed the best overall ranking and U6 the worst.

A summary of the performance of the reference genes according to the four different algorithms is provided in Table 5, while the global evaluation of gene stability is shown in Figure 6. The comprehensive ranking (geometric mean of the four rankings) of the reference genes assessed SNORD48 as the most stable gene (it performed best according to all algorithms), followed by SNORD44, 5S, and miR-16. U6 was the least stable gene, displaying the worst overall ranking (it performed worst according to all algorithms).

DISCUSSION

Despite numerous studies have indicated several methods to measure miRNAs expression levels, qPCR remain the gold standard technique for detection of certain sets of miRNAs. qPCR is a very specific, sensitive and relatively inexpensive assay, which allows for the detection of very small quantities of miRNAs in different samples. Nevertheless, an accurate normalization of non-biological variances has to be applied in order to provide reliable and significant results (Bustin *et al.,* 2002; Pfaffl *et al.,* 2001, 2002). Non-biological variances refer to variations in PCR efficiency, amount of starting material by sample-to-sample variation, RNA integrity, RT efficiency and cDNA sample loading (Karge *et al.,* 1998; Mannhalter *et al.,* 2000). In order to compensate for these internal non-biological differences, the use of appropriate endogenous reference genes, that have to be selected based on their empirically proven appropriateness in defined experimental conditions, is essential. In this context, it is well accomplished that good reference genes should have low SDs of expression levels across samples, as well as similar expression patterns when compared. Control genes, which are often referred to as "housekeeping genes", are frequently used to normalize miRNAs expression levels between different samples. Although several genes and standardization methods have been applied, to date no general consensus about an optimal normalization strategy has been achieved. In this section, a reliable and empirically derived reference framework for normalization of qPCR data in human atrial tissue samples was introduced. Specifically, five candidate transcripts as 5S rRNA, U6, SNORD48, SNORD44, and miR-16 were selected based on a literature survey, and their performances were quantitatively evaluated by applying multiple proven analysis tools, such as BestKeeper, GeNorm, NormFinder and the DeltaCt (ΔCt) methods. This multi-technique evaluation of reference genes allowed us to take into account different aspects, which contribute to the concept of gene stability. Indeed, as observed in this study, although genes may perform better in terms of overall variability, they may display poor similarity of expression or inter/intra-group variability. Therefore, all these features need to be properly evaluated and scored for a solid and reliable choice of the normalizer. The results obtained by the analysis of the qPCR cycle threshold (Ct) values/relative expression of the five candidates according to the different techniques, showed that the normalizers displayed different expression

levels and variability properties in the patient population considered. In particular, in contrast with its frequent use as normalizer, U6 showed the highest variability across the entire population compared to the other transcripts, and the highest intergroup variability, suggesting its unsuitability as reference gene in this context. Despite its low overall variability and inter-group variability, miR-16 displayed a high intra-group variations and expression patterns dissimilar from the other reference genes (e.g., poor correlation and high variability of *ΔCt*), which greatly affected its overall performance.

5S RNA displayed the highest expression levels compared to the other candidates. Indeed, it is an integral component of the large ribosomal subunit in all organisms (Gray *et al.*,1999). 5S showed large variability in the expression levels within the entire population, although it showed good correlation with three of the other reference genes, suggesting a similar pattern of expression. SNORD44B displayed the lowest expression levels compared to the other candidates, and intermediate performance in terms of variability and similarity of expression with the other genes. Lastly, SNORD48 showed the lowest overall variability of expression and intra-group variations, high similarity with other gene expression and intermediate inter-group variability. All these features contributed to its best scores according to all algorithms. The overall positioning calculated as the geometric mean of the rankings obtained by BestKeeper, ΔCt, GeNorm and NormFinder indicated for SNORD48 the overall best ranking while for U6 the worst. The scoring of the best and worst reference gene was corroborated by the complete agreement of the four technique for their positioning.

Collectively, the results here proposed were in line with the literature. In this context, several works have reported U6 as an unsuitable reference gene for miRNAs studies. In a recent study performed by Xiang et al. in serum samples from patients with different tumors, they found large fluctuations in RNU6 expression and a relatively stable expression of miR-16 (Xiang *et al.,* 2014). A study performed by Lamba and collaborators in hepatic tissues indicated that both RNU6 and RNU6B were not suitable as endogenous controls for the normalization of miRNAs' data (Lamba *et al.,* 2014). In addition, by the analysis of the levels of RNU6B in serum samples of healthy volunteers, intensive care unit patients and patients with liver fibrosis, Benz et al. found that RNU6B displayed a high variability between the cohorts, suggesting a disease-specific dysregulation (Benz *et al.,* 2013). Wotschofsky et al. also found that RNU6B was not a suitable normalizer in miRNAs' expression studies on renal cell carcinoma. In addition, they also validated other candidates including RNU48, which resulted the

most stably expressed (Wotschofsky *et al.*, 2011). In another study, performed by Torres and collaborators in tissue samples of endometrioid endometrial carcinoma they identified RNU48 among the most stably expressed snRNAs both in malignant and normal tissues (Torres *et al.*, 2013). In contrast, Brattelid and coworkers, after the evaluation of several normalization candidates, found RNU6B among the most optimal candidates in isolated ex vivo rat hearts (Brattelid *et al.*, 2011).

To conclude, the choice of an endogenous reference gene is a critical step to avoid misinterpreted data and to identify real changes in miRNAs' expression levels. Different reference genes, such as small nuclear/nucleolar RNAs, have been commonly used in miRNAs' expression studies. Despite these small RNAs share similar properties and great abundance, their expression levels can change under different experimental conditions and may be affected by specific diseases. For these reasons, an accurate methodology to test the suitability of these genes for the set of samples under analysis should always be validated. This preliminary study identified SNORD48 as the best single reference gene. Nevertheless, reference gene combinations can be considered in future studies as a way to further improve normalization performance (Vandesompele *et al.*, 2002), where allowed by experimental conditions.

BIBLIOGRAPHY

Adam ,O., Löhfelm, B., Thum, T., Gupta, S. K., Puhl, S. L., Schäfers, H. J, Böhm M, Laufs U. (2012). Role of miR-21 in the pathogenesis of atrial fibrosis. *Basic Research in Cardiology*, 107(5):278.

Andersen, C. L., Jensen, J. L., Ørntoft, T. F. (2004). Normalization of real-time quantitative reverse transcription-PCR data: a model-based variance estimation approach to identify genes suited for normalization, applied to bladder and colon cancer data sets. *Cancer Research*, 64(15):5245–5250.

Benz, F., Roderburg, C., Vargas Cardenas, D., Vucur, M., Gautheron, J., Koch, A., Zimmermann, H., Janssen, J., Nieuwenhuijsen, L., Luedde, M., Frey, N., Tacke, F., Trautwein, C., Luedde, T. (2013). U6 is unsuitable for normalization of serum miRNA levels in patients with sepsis or liver fibrosis. *Experimental & Molecular Medicine*, 45:e42.

Brattelid, T., Aarnes, E. K., Helgeland, E., Guvaåg, S., Eichele, H., Jonassen, A. K. (2011). Normalization strategy is critical for the outcome of miRNA expression analysis in the heart. *Physiological Genomics*, 43(10):604-610.

Bustin, S. A. (2002). Quantification of mRNA using real-time reverse transcription PCR (RT-PCR): trends and problems. *Journal of Molecular Endocrinology*, 29(1):23-39.

Chen, C., Ridzon, D. A., Broomer, A. J., Zhou, Z., Lee, D. H., Nguyen, J. T., Barbisin, M., Xu, N. L., Mahuvakar, V. R., Andersen, M. R., Lao, K. Q., Livak, K. J., Guegler, K. J. (2005). Real-time quantification of microRNAs by stem-loop RT-PCR. *Nucleic Acids Research*, 33(20):e179.

Cooley. N., Cowley, M. J., Lin, R. C., Marasco, S., Wong, C., Kaye, D. M., Dart, A. M., Woodcock, E. A. (2012). Influence of atrial fibrillation on microRNA expression profiles in left and right atria from patients with valvular heart disease. *Physiological Genomics*, 44(3):211-219.

Dong, S., Ma, W., Hao, B., Hu, F., Yan, L., Yan, X., Wang, Y., Chen, Z., Wang, Z. (2014). microRNA-21 promotes cardiac fibrosis and development of heart failure with preserved left ventricular ejection fraction by up-regulating Bcl-2. *International Journal of Clinical and Experimental Pathology*, 7(2):565-574.

Ferreira, L. R., Frade, A. F., Santos, R. H., Teixeira, P. C., Baron, M. A., Navarro, I. C., Benvenuti, L. A., Fiorelli, A. I., Bocchi, E. A., Stolf, N. A., Chevillard, C., Kalil, J., Cunha-Neto, E. (2014). MicroRNAs miR-1, miR-133a, miR-133b, miR-208a and miR-208b are dysregulated in Chronic Chagas disease cardiomyopathy. *International Journal of Cardiology*, 173(5):409-417.

García, R., Villar, A. V., Cobo, M., Llano, M., Martín-Durán, R., Hurlé, M. A., Nistal, J. F. (2013). Circulating levels of miR-133a predict the regression potential of left ventricular hypertrophy after valve replacement surgery in patients with aortic stenosis. J*ournal of the American Heart Association*, 2(4):e000211.

Gray, M. W., Burger, G., Lang B. F. (1999). Mitochondrial Evolution. *Science*, 283(5407):1476-1481.

Karge, W. H. 3rd., Schaefer, E. J., Ordovas, J. M. (1998). Quantification of mRNA by polymerase chain reaction (PCR) using an internal standard and a nonradioactive detection method. *Methods in Molecular Biology (Clifton, N.J.)*, 110:43–61.

Lamba, V., Ghodke-Puranik, Y., Guan, W., Lamba, J. K. (2014). Identification of suitable reference genes for hepatic microRNA quantitation. *BMC Research Notes*, 7:129.

Liu H, Qin H, Chen GX, Liang MY, Rong J, Yao JP, Wu ZK. (2014). Comparative expression profiles of microRNA in left and right atrial appendages from patients with reumatic mitral valve disease exhibiting sinus rhythm or atrial fibrillation. *Journal of Translational Medicine*, 12:90.

Luo, X., Yang, B., Nattel, S. (2015). MicroRNAs and atrial fibrillation: mechanisms and translational potential. *Nature Reviews. Cardiology*, 12(2):80–90.

Mannhalter, C., Koizar, D., Mitterbauer, G. (2000). Evaluation of RNA isolation methods and reference genes for RT-PCR analyses of rare target RNA. *Clinical Chemistry and Laboratory Medicine*, 38(2):171–177.

Moreno-Moya, J. M., Vilella, F., Simon, C. (2014). MicroRNA: key gene expression regulators. *Fertility and Sterility*, 101(6):1516–1523.

Nishi, H., Sakaguchi, T., Miyagawa, S., Yoshikawa, Y., Fukushima, S., Saito, S., Ueno, T., Kuratani, T., Sawa, Y. (2013). Impact of microRNA expression in human atrial tissue in patients with atrial fibrillation undergoing cardiac surgery. *PloS One*, 8(9):e73397.

Pfaffl, M. W. (2001). A new mathematical model for relative quantification in real-time RT-PCR. *Nucleic Acids Research*, 29(9):e45.

Pfaffl, M. W., Horgan, G. W., Dempfle, L. (2002). Relative expression software tool (REST) for group-wise comparison and statistical analysis of relative expression results in real-time PCR. *Nucleic Acids Research*, 30(9):e36.

Pfaffl, M. W., Tichopad, A., Prgomet, C., Neuvians, T. P. (2004). Determination of stable housekeeping genes, differentially regulated target genes and sample integrity: BestKeeper--Excel-based tool using pair-wise correlations. *Biotechnology Letters*, 26(6):509–515.

Roy, S., Khanna, S., Hussain, S. R., Biswas, S., Azad, A., Rink, C., Gnyawali, S., Shilo, S., Nuovo, G. J., Sen, C. K. (2009). MicroRNA expression in response to murine myocardial infarction: miR-21 regulates fibroblast metalloprotease-2 via phosphatase and tensin homologue. *Cardiovascular Research*, 82(1):21-29.

Satoh, M., Minami, Y., Takahashi, Y., Tabuchi, T., Nakamura, M. (2010). Expression of microRNA-208 is associated with adverse clinical outcomes in human dilated cardiomyopathy. *Journal of Cardiac Failure*, 16(5):404-410.

Santulli, G., Iaccarino, G., De Luca, N., Trimarco, B., Condorelli, G. (2014). Atrial fibrillation and microRNAs. *Frontiers in Physiology*, 5:15.

Sauer, E., Babion, I., Madea, B., Courts, C. (2014). An evidence based strategy for normalization of quantitative PCR data from miRNA expression analysis in forensic organ tissue identification. *Forensic Science International. Genetics*, 13:217-23.

Schmittgen, T. D., Lee, E. J., Jiang, J., Sarkar, A., Yang, L., Elton, T. S., Chen, C. (2008). Real-time PCR quantification of precursor and mature microRNA. *Methods (San Diego, California)*, 44(1):31–38.

Silver, N., Best, S., Jiang, J., Thein, S. L. (2006). Selection of housekeeping genes for gene expression studies in human reticulocytes using real-time PCR. *BMC Molecular Biology*, 7:33.

Song, C. L., Liu, B., Diao, H. Y., Shi, Y. F., Li, Y. X., Zhang, J. C., Lu, Y., Wang, G., Liu, J., Yu, Y. P., Guo, Z. Y., Wang, J. P., Zhao, Z., Liu, J. G., Liu, Y. H., Liu, Z. X., Cai, D., Li, Q. (2014). The protective effect of microRNA-320 on left ventricular remodeling after myocardial ischemia-reperfusion injury in the rat model. *International Journal of Molecular Sciences*, 15(10):17442-17456.

Topkara, V. K., Mann, D. L. (2011). Role of microRNAs in cardiac remodeling and heart failure. *Cardiovascular Drugs and Therapy/sponsored by the International Society of Cardiovascular Pharmacotherapy*, 25(2):171–182.

Torres, A., Torres, K., Wdowiak, P., Paszkowski, T., Maciejewski, R. (2013). Selection and validation of endogenous controls for microRNA expression studies in endometrioid endometrial cancer tissues. *Gynecologic Oncology*, 130(3):588–594.

Vandesompele, J., De Preter, K., Pattyn, F., Poppe, B., Van Roy, N., De Paepe, A., Speleman, F. (2002). Accurate normalization of real-time quantitative RT-PCR data by geometric averaging of multiple internal control genes. *Genome Biology*, *3*(7):RESEARCH0034.

Villar, A. V., García, R., Merino, D., Llano, M., Cobo, M., Montalvo, C., Martín-Durán, R., Hurlé, M. A., Nistal, J. F. (2013). Myocardial circulating levels of microRNA-21 reflect left ventricular fibrosis in aortic stenosis patients. *International Journal of Cardiology*, 167(6):2875-2881.

Wang, Z., Lu, Y., Yang, B. (2011). MicroRNAs and atrial fibrillation: new fundamentals. *Cardiovascular Research*, 89(4):710–721.

Wotschofsky, Z., Meyer, H. A., Jung, M., Fendler, A., Wagner, I., Stephan, C., Busch, J., Erbersdobler, A., Disch, A. C., Mollenkopf, H. J., Jung, K. (2011). Reference genes for the relative quantification of microRNAs in renal cell carcinomas and their metastases. *Analytical Biochemistry*, 417(2):233–241.

Xiang, M., Zeng, Y., Yang, R., Xu, H., Chen, Z., Zhong, J., Xie, H., Xu, Y., Zeng, X. (2014). U6 is not a suitable endogenous control for the quantification of circulating microRNAs. *Biochemical and Biophysical Research Communications*, 454(1):210– 214.

Yan, J., Zhang, N., Qi, C., Liu, X., Shangguan, D. (2013). One-step real time RT-PCR for detection of microRNAs. *Talanta*, 110:190-5.

Zhang Y, Wang X, Xu X, Wang J, Liu X, Chen Y. (2012). Distinct microRNA expression signatures in human right atrial and ventricular myocardium. *Molecular and Cellular Biochemistry*, 371(1-2):23-29.

3.2 MiRNAs expression profiles in AF compared to SR patients

MATERIALS AND METHODS

Patient samples

Tissue samples from the right atrial appendage were collected from 23 patients (all males) undergoing cardiac surgery. In particular, fourteen patients (range 67 ± 11 years) displayed normal sinus rhythm following the intervention (SR group), while nine patients (range 76 ± 4 years) displayed AF (AF group).

Human tissue processing and RNA isolation

The procedure is described in chapter 3.1. (p. 89).

Selection of AF-related miRNAs

miRNA	Change	Target/Effect	Reference
miR-1	↓	↑Kir2.1 -> ↑ I_{K1}	Girmatsion et al, *Heart Rhythm*, 2009
	↑	↓ Cx43 -> Slowed conduction	Wang et al, *J Mol Med*, 2008
miR-133	↑	↓ I_{Kr} I_{Ks}	Wang et al, *Cardiovasc Res*, 2010
miR-328	↑	↓ L-type Ca^{2+} channels	Lu et al, *Circulation*, 2010 Zhang et al, *Sci China Life Sci*, 2011
miR-21	↑	↑ Fibrosis, dysregulation of collagen-1 and 3	Cardin et al, *CircEP*, 2012
		↑ Connective tissue growth factor (CTGF) ↑ collagen content	Adam et al, *Basic Res Cardiol*, 2012
miR-30 and miR-133	↓	↑ Fibrosis and Inflammation	Li et al, *Mol Med Report*, 2012
		↑ Connective tissue growth factor (CTGF)	Duisters et al, *CircRes*, 2009
miR-29 (family)	↓	↑ Fibrotic response	Van Rooij et al, *PNAS*, 2008
miR-133 and miR-590	↓	↑ Transforming growth factor (TGF) and collagen	Shan et al, *Cardiovasc Res*, 2009
miR-208	↓	THRAP1 -> Hypertrophy and fibrosis	Van Rooij et al, *Science*, 2007 Callis et al, *J Clin Invest* 2009
miR-499	↑	↓ SK3 -> shortening of atrial potential duration (ADP)	Ling et al, *Heart Rhythm* 2013

Table 1: miRNAs involved in AF mechanisms.

As indicated in Table 1, AF-related miRNAs were selected based on a literature survey. In particular, some miRNAs have been demonstrated to be involved mainly in ionic remodeling (miR-1, miR-133, miR-328 and miR-499), while others in structural remodeling (miR-21, miR-30, miR-29, miR-208 and miR-590).

Reverse transcription qPCR (RT-qPCR)

The total RNA isolated from each tissue sample was reverse-transcribed using miRCURY LNA™ Universal cDNA Synthesis kit II (Exiqon, Vedbaek, Denmark) according to the manufacturer's protocol.

RT-qPCR assays based on SYBR Green I were performed using miRCURY LNA™ PCR primers set (Exiqon, Vedbaek, Denmark) on the following selected miRNAs: hsa-miR-1, hsa-miR-133a, hsa-miR-133b, hsa-miR-21, hsa-miR-29a, hsa-miR-29b, hsa-miR-30c, hsa-miR-328, hsa-miR-590, hsa-miR-499a, hsa-miR-208a, hsa-miR-208b (see Appendix, p.123). qPCR reactions were performed using ExiLENT SYBR® Green master mix (Exiqon, Vedbaek, Denmark) in a CFX384 Real-Time PCR Detection System (Bio-Rad Laboratories, Milan, Italy). The 10 µl PCR reaction contained 4µl of the diluted cDNA template, 5 µl of SYBR® Green master mix and 1 µl of PCR primer mix. The reaction protocol was as follows: 95°C for 10 minutes, followed by 40 amplification cycles of 95°C for 10 seconds and 60°C for 1 minute.

All RT-qPCR reactions, including the no-template controls, were performed in technical triplicates on a 384-well reaction plate (Bio-Rad Laboratories, Milan, Italy). The threshold cycle (*Ct*) was defined as the fractional cycle number at which fluorescence exceeded the given threshold.

Histological correlates

In a subgroup of twelve patients, 6 patients in SR (range 62 ± 12 years) and 6 patients in AF (range 76 ± 4 years), histological correlates were available for comparison with miRNA expression. As described in chapter 2.1, the 3D fibrosis profile was obtained in each patient by a section-by-section semiautomatic, quantitative analysis of 5 µm atrial tissue slices, stained by Picrosirius red. Patients' curves were fitted to extract the steady state value of fibrosis (y0) in the endocardial layers. This parameter was compared with miRNA expression to identify a potential correlation between miRNA and fibrosis.

Data analysis and statistical analysis

For each patient and miR, the *Ct* value was estimated as the average of the technical triplicate *Cts*, after removal of the outliers (*Ct* values that differed more than 1 from the *Ct* median). Expression levels were quantified in terms of relative normalized units, using SNORD48 as reference gene (RG, see paragraph 3.1).

Expression levels were quantified in terms of normalized units, using SNORD48 as reference gene (RG, see paragraph 3.1). Specifically, the normalized expression (NE) of a specific miR in a patient was given by:

$$NE(miR) = \frac{2^{-(CtmiR)}}{2^{-(CtRG)}}$$

where Ct_{miR} is the *Ct* value of the miR in the patient and Ct_{RG} is the *Ct* of the reference gene in the patient. In the equation, the maximal efficiency of the reaction ($E = 2$) was assumed.

Expression data in the AF and SR groups are expressed as median and interquartile range (IQR), due to the non-normality of most of the distributions (Lilliefor test). Accordingly, differences between miRNA expressions in SR versus AF groups were assessed Wilcoxon-Mann-Whitney test, if not differently indicated. Correlations between variables were tested by Pearson's correlation or Spearman's rank correlation analysis, as pertinent. Statistical significance was defined by a p-value < 0.05.

RESULTS

MiRNAs expression profiles in the overall population of patients

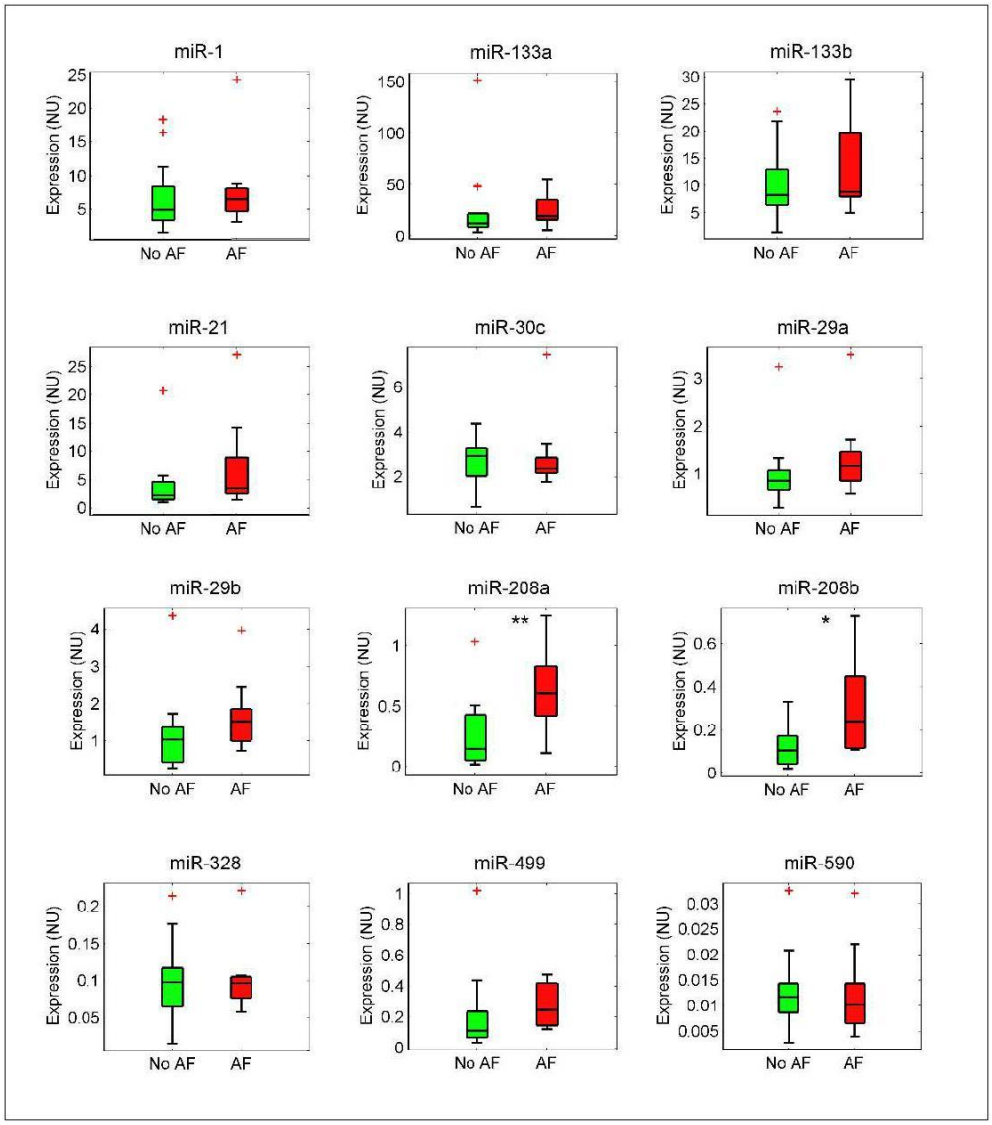

Figure 1: Comparison of miRNAs expression profiles in AF versus SR patient groups. Two miRNAs (208a and 208b) display statistically significant differences between the two populations, while one (miR-499) is close to significance (p=0.07). Data are expressed as normalized expressions (normalization using SNORD48 as normalizer). N=23 (14 SR, 9 AF). **, p<0.01; * p<0.05 In the box and whisker plot, the dark black line indicates the median, the box the interquartile range, and the whiskers the 1.5*IQR interval. Red crosses indicate outlier values.

miRNA	SR group	AF group	p-value
miR-1	4.91 [3.34-8.45]	6.46 [4.66-8.05]	NS (0.43)
miR-133a	12.83 [9.07-22.10]	19.52 [16.11-35.17]	NS (0.27)
miR-133b	8.29 [6.40-13.03]	8.82 [7.95-19.65]	NS (0.26)#
miR-21	2.26 [1.52-4.73]	3.46 [2.53-8.94]	NS (0.24)
miR-29a	0.85 [0.64-1.08]	1.16 [0.86-1.46]	NS (0.20)
miR-29b	1.03 [0.43-1.37]	1.52 [1.00-1.86]	NS (0.09)
miR-30c	2.93 [2.04-3.26]	2.37 [2.17-2.84]	NS (0.68)
miR-328	0.098 [0.06-0.12]	0.097 [0.08-0.10]	NS (0.92)
miR-590	0.012 [0.009-0.014]	0.010 [0.007-0.014]	NS (0.59)
miR-499a	0.11 [0.07-0.23]	0.25 [0.15-0.42]	NS (0.07)
miR-208a	**0.15 [0.05-0.43]**	**0.60 [0.42-0.83]**	**0.0099**$^{\#}$
miR-208b	**0.10 [0.04-0.17]**	**0.24 [0.12-0.45]**	**0.02**$^{\#}$

Table 2: Comparison of miRNAs expression profiles in AF versus SR patient groups. Data are median [IQR]. Data comparison is performed by Wilcoxon-Mann-Whitney test or Student's t-test (marked by #). NS, not significant.

The results concerning the expression levels of the 12 selected miRNAs are shown in Figure 1 and summarized in Table 2. MiRNAs were differently expressed between AF and SR patients. In particular miR-1, miR-133a, miR-133b, miR-21, mir-29a, miR-29b, miR-208a, miR-208b and miR-499 resulted up-regulated in AF compared to SR group. On the contrary, miR-30c and miR-590 resulted down-regulated in AF patients compared to SR. Only two miRNAs, miR-208a and miR-208b, showed statistical differences between the two groups ($p<0.01$ and $p<0.05$ for miR-208a and miR-208b, respectively), while only miR-499 resulted close to a significance ($p=0.07$).

Correlation between steady state fibrosis and miRNAs expression

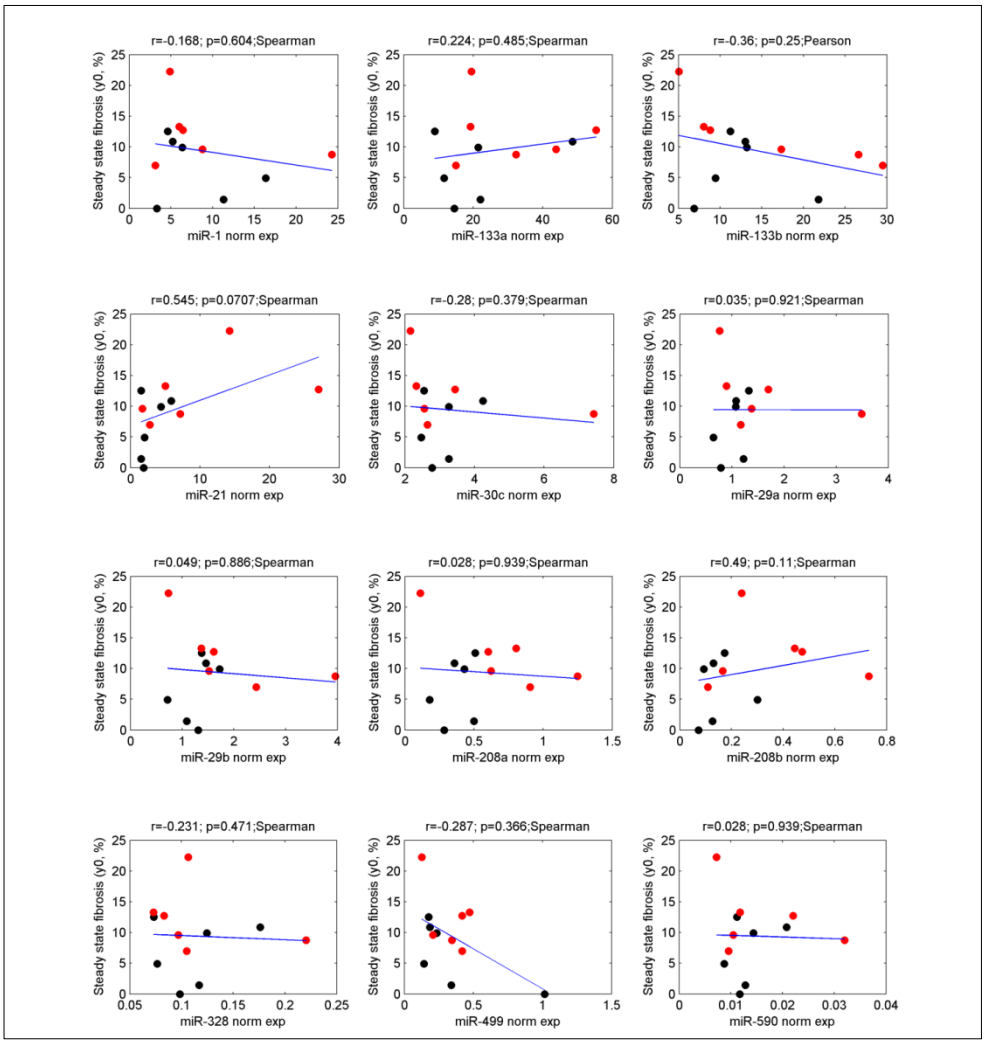

Figure 2: Correlation between steady state fibrosis and miRNAs expression levels. miR-21 and miR-208b are the closest to a significant correlation with fibrosis (positive correlation). Red dots indicated AF while black dots SR patients. N=12 (6 AF, 6 SR).

In order to investigate possible relationships between miRNAs expression levels and the fibrotic content (described in chapter 2.1), correlation measurements were performed on a sub-group of patients (Figure 2). Mir-1, miR-133a, miR-133b, miR-30c, miR-29a, miR-29b, miR-208a, miR-328, miR-499, and miR-590 showed no a significant correlation with steady state fibrosis. On the contrary, miR-21 (r=0.545; p=0.0707) and miR-208b (r=0.49; p=0.11) were the closest to a significant correlation with fibrosis.

DISCUSSION

In this section, the expression patterns of some miRNAs known to regulate diverse genes involved in different mechanisms of AF, such as electrical and structural remodeling, were investigated. The aim of the study was to find possible differences in miRNAs expression signature between AF patients versus individuals in SR. Human atrial tissue samples were collected during cardiac surgery from patients with and without AF, processed for RNA extraction, and submitted to qPCR analysis. A panel of miRNAs, including miR-1, miR-133a/b, miR-30c, miR-29a/b, miR-208a/b, miR-328, miR-499, miR-590 and miR-21, was selected based on a literature survey. Our findings revealed that the expression levels of some miRNAs were different in AF compared to SR patients. In particular, miR-1, miR-133a, miR-133b, miR-21, mir-29a, miR-29b, miR-208a, miR-208b and miR-499, resulted up-regulated in AF compared to SR group. Conversely, miR-30c, miR-328 and miR-590 resulted down-regulated in AF compared to SR patients. However, among these miRNAs, more marked differences in expressions between the two populations were observed for miR-208a and miR-208b, followed by miR-499. miR-208 is a highly conserved miRNA family, which includes two members, miR-208a and miR-208b, that share similar nucleotide sequences. miR-208a and miR-208b (accompanied with miR-499), are defined as "Myomirs" because they control muscle myosin content, myofiber identity, and muscle performance (van Rooij et al., 2009). Myosin (MHC), the major contractile protein of the cardiac muscle, is present in two isoforms: α-MHC (fast myosin) and β-MHC (slow myosin), which are encoded by Mhy6 and Mhy7 genes, respectively (Weiss & Leinwand, 1996). In the adult heart the Mhy6 gene co-expresses miR-208a, while Mhy7 and Mhy7b (the latter a more ancient myosin gene) co-express miR-208b and miR-499, respectively. miR-208b and miR-499 are functionally redundant, playing an important role in the specification of muscle fiber identity by activating slow and repressing fast myofiber gene programs (van Rooij et al., 2009). The deletion of miR-208a results in a decrease of β-MHC expression in the adult heart, thus providing evidence that miR-208a is involved both in the regulation of the expression of slow myosin genes, as well as in their intronic miRNAs (Callis *et al.,* 2009; Van Rooij *et al.,* 2009). Previous studies (Van Roij *et al.,* 2007) have also suggested the involvement of miR-208 in cardiomyocyte hypertrophy and fibrosis in response to stress and hypothyroidism. Nonetheless, transgenic overexpression of miR-208a in the heart has been demonstrated sufficient to induce hypertrophic growth in mice, resulting in a pronounced repression of the thyroid

hormone–associated protein 1 (THRAP1) and myostatin, two negative regulators of muscle growth and hypertrophy (Callis *et al.,* 2009). Montgomery and collaborators performed a study where they evaluated a therapeutic approach based on the manipulation of miR-208a levels (Montgomery *et al.,* 2011). In particular, hypertension-induced heart failure mice were injected subcutaneously with antimir-208a. The resultant miR-208 inhibition prevented pathological myosin switch and cardiac remodelling, thus improving overall cardiac function and survival. Other studies revealed that antagomir-208a could reduce the stretch-induced expression of endoglin and collagen type I in cultured cells (Shyu *et al.,* 2013). Interestingly, clinical studies showed that myocardial miR-208a resulted upregulated in patients with heart failure compared to the controls (Matkovich *et al.,* 2012). Taken together, these results suggest the potential use of miR-208a as a therapeutic target for the modulation of cardiac function and remodelling during the progression of heart disease.

A microarray analysis of miRNAs expression performed by Nishi and coworkers showed that 98 miRNAs were differently expressed in right atrial samples from AF patients compared to the SR group. Nevertheless, the subsequent validation by qRT-PCR assays revealed that only miR-21 and miR-208b were upregulated in the AF group compared to individuals in SR (Nishi *et al.,* 2013). In another microarray-based study on atrial samples from patients with valvular heart disease and AF versus patients with valvular heart disease alone, miR-21 resulted up-regulated, while miR-133a, miR-133b and miR-30c were down-regulated (Cooley *et al.,* 2012). On the contrary, Lu et al. observed a significant up-regulation of miR-328 and a down-regulation of miR-499 in the right atrium of AF patients compared to SR individuals (Lu *et al.,* 2010).

To investigate possible relationships between miRNAs expression levels and the fibrotic content correlation analysis was performed. Our analysis revealed that the sole miR-21 and miR-208b were close to a significant correlation with fibrotic content.

A similar study revealed a positive correlation between the expression of miR-21 and the percentage of fibrosis, while no significant correlation was observed for miR-208b expression (Nishi *et al.,* 2013). These discrepancies in the results may arise from different experimental settings and/or diverse methods for data normalization (as discussed in chapter 3.1). MiR-21 is universally expressed in mammal organs such as the spleen, the small intestine, the colon and the heart (Lagos-Quintana *et al.,* 2002). Despite many functional studies have attributed to miR-21 an oncogenic activity, its role in cardiovascular biology and disease has just recently received attention (Zhang,

2008). MiR-21 is mostly expressed in cardiac fibroblasts, where it targets and represses the translation of SPRY1, a negative regulator of the extracellular signal-regulated kinase ERK pathway (Thum *et al.,* 2008). ERK activation promotes fibrosis, so its derepression via miR-21 results pro-fibrotic. Experimental studies on animal models have shown that cardiac dysfunction enhanced susceptibility to AF and miR-21 up-regulation (Cardin *et al.,* 2012). In addition, other studies demonstrated that miR-21 knockdown suppressed atrial fibrosis, preventing AF development in rats with myocardial infarction (Cardin *et al.,* 2012). It has also been observed that AF patients may have increased levels of miR-21 as a result of the activation of the p21-Rac1/CTGF/lysyl oxidase pathway (Adam *et al.,* 2012).

In conclusion, the present study has revealed differences in miRNAs expression levels in AF versus SR patients and the existence of a relationship between the expression of some miRNAs and the fibrotic content. These findings could be of importance to characterize the pro-arrhythmic substrate of AF, thus representing a starting point for a better understanding of the molecular mechanisms causing AF. In future studies, major attention should be devoted to the study of miR-208a/b and miR-21, which showed more marked differences in the expression levels between SR and AF groups and higher correlation levels with fibrotic content. Several studies have also demonstrated that some miRNAs, including miR-208 and miR-21, are detectable not only intracellularly but also in body fluids such as blood, saliva and urine (Zhu & Fan, 2011). In this perspective, it could be interesting to perform a comparison between the expression levels of miRNAs enriched in myocardial tissue compared to their expression in the intravenous blood. These evaluations could be useful in order to explore the possible use of miRNAs as predictive biomarkers of fibrotic remodelling.

It is well known that the function of a miRNA is defined by the genes it targets and its effects on their expression. Nonetheless, a given miRNA can be predicted to target several hundred genes and different mRNAs have been predicted to be binding sites for 1 or multiple miRNAs. In this perspective, target determination by bioinformatic approaches followed by *in-vitro* validation techniques will be helpful to investigate the functions of selected miRNAs, such as miR208a/b and miR-21, in cardiac remodeling processes. In addition, studies aiming to establish miRNA cell type specificity could be also performed by applying *in-situ* techniques (e.g. *in-situ* hybridization or *in-situ* PCR). Indeed, these methodologies represent a powerful tool to identify and localize a precise

miRNAs directly at the tissue site, thus adding also a "molecular-histological" perspective to the characterization of atrial tissue.

LIMITATIONS OF THE STUDY

Although the present study has provided important information in the characterization of the structural and molecular pro-arrhythmic substrate of AF, some limitations need to be pointed out. First, the study population available for the analysis was limited, so further studies in an extended population are necessary to confirm and strengthen the significance of the overall results. In addition, due to sample availability, different but partially overlapping subgroups of patients were analyzed by the diverse analysis techniques. Second, due to the surgical procedure, only a small biopsy from the right atrial appendage was examined, while other parts of the atria, including the left atrium, could not be analyzed. Nevertheless, the present evaluation may be considered in line with the majority of the studies in the field. Third, human atrial samples were obtained from routine cardiac surgery interventions, thus, no “normal tissues” samples were available as control. Additional studies are needed to clarify this issue. Fourth, the present work was performed with native human tissues, so molecular insights for the cause of miRNA dysregulation were not provided. In addition, the exact targets and pathways by which alterations in miRNAs cause AF remain elusive. In this perspective, additional information about the biological significance of the changes observed in miRNAs expression levels in AF patients could be achieved with the development of novel experimental models, in which the levels of one or more miRNAs could be precisely manipulated and their effects on different cell components evaluated.

GENERAL DISCUSSION AND CONCLUSIONS

This work introduced a novel multi-technique approach for the study of the substrate of AF. The study was developed according to two main lines of investigation, structural and molecular, to better characterize the features of a potential pro-arrhythmic substrate at different scales. New protocols and data analysis tools were implemented and developed to define the 3D fibrotic profile and its spatial pattern, as well as to extract high-quality RNA and to quantify miRNAs expression in the human myocardium. The collagen content and its spatial properties were investigated by applying both histological and advanced microscopy techniques to human atrial tissue samples, collected during cardiac surgery in patients who developed or not AF. Despite some studies have described the histological substrate of atrial fibrillation in humans, no information about the 3D collagen content within the human atrial wall has been provided. Nonetheless, it is well known that the electrical impulse propagates in a 3D atrial substrate and interstitial fibrosis may create conduction blocks at different levels, leading the formation of complex 3D reentrant circuits (Nattel, 2002; Allessie *et al.*, 2002). In the present work an accurate method for the quantification of the intramural distribution of collagen in human atrial tissue samples was introduced for the first time. 5 μm thickness serial sections throughout the whole biopsy were collected, stained with Picrosirius red, imaged and analyzed by using a semi-automated software customized for quantitative analysis of histological images. The quantitative analysis of the intramural profile of the fibrotic content performed on atrial tissue samples in the overall population, yielded a consistent average curve of collagen content distribution throughout the myocardial wall, with a decrease in the fibrotic content from the epicardial to the endocardial wall. The AF group showed higher fibrotic values at the steady-state (i.e., in the mid-endocardium), compared to the SR group. Collectively, these findings support the hypothesis that an accumulation of fibrosis within the myocardial wall may represent an important structural contributor in the pathophysiology of AF. In addition to a quantitative analysis, it is also important to assess the features of fibrosis to understand how changes in its properties may interfere with the electrical impulse propagation. For these reasons collagen properties, such as fibers orientation and scale dimension, were evaluated by applying non-linear optical microscopy (NLO) techniques and in particular second harmonic generation (SHG). These advanced microscopy techniques posses special features that make them less

sensitive to scattering, and thus suitable for high-resolution imaging of thick tissue specimens. In particular, SHG microscopy can provide morphological and functional images of anisotropic biological structures with high hyperpolarizability, such as collagen. Importantly, SHG microscopy represents a nondestructive imaging tool that allows a clear and selective visualization of collagen fibers, without sample staining or pre-processing. In this work a novel approach for the characterization of collagen network properties in atrial tissue samples based on NLO microscopy, was introduced. In particular, by applying SHG microscopy in combination with a spectral analysis framework, a multiparametric description of the properties of the collagen network in atrial tissue samples was provided. The analysis revealed that in SR patients the collagen network showed a fine architecture characterized by thin fibrils with changing angles and directions, while in AF patients fibers tended to pack-up in larger bundles of defined directions. Overall, AF patients displayed collagen fibers with significantly higher anisotropy and larger scale dimension. Fibers orientation and scale dimension changed along tissue depth in both SR and AF patients, assuming larger values in AF tissues. These results highlight a spatial rearrangement and thickening of the 3D collagen network in AF patients, which may play a role in the development of the arrhythmia.

Evidence from numerous studies indicates that also an altered regulation of gene expression may play an important role in the mechanisms of atrial remodeling which underlie AF. Nonetheless, the frequent mismatch between mRNAs and protein levels of gene expression has promoted the investigation of the regulatory mechanisms at post-transcriptional level. In this context, miRNAs have been demonstrated to negatively regulate the gene expression of their targets by affecting mRNA stability or translation, resulting in repression of target genes. Changes in miRNA expression profiles, associated with both electrical and structural modifications, have been identified in numerous AF studies, suggesting the use of miRNAs as potential biomarkers and also as possible therapeutic targets for the treatment of AF. In the present work, we evaluated the expression pattern of some miRNAs known to target different genes involved in the mechanisms that underlie AF, in particular in fibrosis/collagen formation. A panel of miRNAs was selected based on the literature and analyzed by RT-qPCR in atrial samples from AF patients and SR individuals. In addition, to accurately determine the levels of analyzed miRNAs, a preliminary study aiming to establish the best endogenous reference genes for data normalization was performed. To

date no general agreement between different normalization strategies in miRNAs expression analysis has been found, resulting in conflicting data across different studies. Researchers usually select their endogenous reference genes for miRNAs expression according to the literature. Normalizers are usually small nuclear/nucleolar RNAs, which display similar properties and are abundantly expressed. Nevertheless, despite these transcripts show constant expression in single assays, their expression levels can change under different experimental as well as "physiopathological" conditions. Therefore, proposed normalizers should be first established across a subset of samples, and the combination of multiple reference genes may be more appropriate than a single universal normalizer (Shen *et al.*, 2015).

Multiple miRNAs have been indicated as potential participants in the modulation of fibrotic remodeling during AF. In this study differences in the expression levels of a subset of AF-related miRNAs, have been observed in AF compared to SR patients. In particular, miR-208a and miR-208b displayed more marked differences in expression differences between AF and SR patients. These miRNAs have been recently indicated as important players in the progression of cardiovascular disorders, such as fibrosis and arrhythmia (Huang *et al.*, 2015). Experimental studies have shown that miR-208 family is essential to maintain normal myocardial conduction, and it may be a therapeutic target in myocardial hypertrophy, fibrosis, and heart failure as well as a potential biomarker for acute myocardial infarction (Huang *et al.*, 2015).

Correlation analysis between miRNAs expression and histologically-assessed fibrotic content (described in chapter 3.2) revealed that miR-208b and miR-21 displayed a correlation with fibrosis close to statistical significance. Accordingly, miR-21 upregulation has been indicated to promote fibroblast survival and growth factor secretion, as well as to increase the extent of interstitial fibrosis (Thum *et al.*, 2008). Interestingly, a similar study performed by Nishi and collaborators indicated a positive relationship between the percentage of fibrosis and miR-21, but no significant correlations with miR-208b (Nishi *et al.*, 2013).

Future perspectives

Although the present study has provided important information in the characterization of the structural and molecular pro-arrhythmic substrate of AF, further studies in an extended population are necessary to confirm and strengthen the significance of the overall results.

In the future, additional investigations should be performed to characterize collagen subtypes, such as collagen type I and type III, which are predominant in the cardiac tissue and essential for the structural and functional integrity of the myocardium. Indeed, it has been shown that altered expression ratios of collagen types may impact the elasticity and stiffness of the heart (Doering *et al.*, 1988), thus enhancing susceptibility to reentrant arrhythmias (Weber *et al.*, 1992). Interestingly, a study performed by Grammer and collaborators showed that Col III/I ratio was significantly reduced in patients who developed AF after cardiac surgery compared to patient in SR, while mRNA expression levels remained unvaried (Grammer *et al.*, 2005). This suggests that atrial collagen composition is an important factor for the outcome of heart surgery patients with respect to the occurrence of AF. For these reasons, further investigations about collagen subtypes both at the mRNA and protein level, could provide new information for a deeper characterization of a fibrotic pro-arrhythmic substrate. On the other hand, concerning the molecular biology part, future experiments should be aimed at clarifying the roles of miR-208a/b and miR-21 in AF cardiac remodeling, first by analyzing putative target genes (e.g. THRAP1, myosin and SPRY1). In this perspective, bioinformatic approaches followed by *in-vitro* validation techniques and functional assays, may be helpful to investigate the possible functions of these miRNAs in cardiac remodeling.

Numerous studies have indicated the possible use miRNAs as potential biomarkers in diverse pathological conditions, such as cardiovascular disease. In this perspective, a comparison between the expression levels of miRNAs enriched in the myocardial tissue compared to their intravenous expression, maybe of great interest. Additionally, investigations aiming to establish miRNAs cell type specificity could be performed by applying *in-situ* techniques. Indeed, these methodologies represent a powerful tool to identify and precisely localize miRNAs at the tissue site, thus adding value and a new "molecular-histological" perspective to the characterization of the atrial tissue.

To conclude, this work introduced a multiscale approach for the study of the fibrotic substrate of AF. However, the clarification of the relationships between the extent and distribution of fibrosis, miRNAs expression and the risk of AF requires further investigation. To address these issues, a thorough understanding of the ways in which structural, molecular and also cellular remodeling alter 3D impulse propagation could be helpful for a better understanding of the mechanisms underlying AF, as well as beneficial for improving the clinical management of the arrhythmia.

BIBLIOGRAPHY

Adam, O., Löhfelm, B., Thum, T., Gupta, S. K., Puhl, S. L., Schäfers, H. J., Böhm, M., Laufs, U. (2012). Role of miR-21 in the pathogenesis of atrial fibrosis. *Basic Research in Cardiology*, 107(5):278.

Allessie, M., Ausma, J., Schotten, U. (2002). Electrical, contractile and structural remodeling during atrial fibrillation. *Cardiovascular Research*, 54(2):230-246.

Callis, T. E., Pandya, K., Seok, H. Y., Tang, R. H., Tatsuguchi, M., Huang, Z. P., Chen, J. F., Deng, Z., Gunn, B., Shumate, J., Willis, M. S., Selzman, C. H., Wang, D. Z. (2009). MicroRNA-208a is a regulator of cardiac hypertrophy and conduction in mice. *The Journal of Clinical Investigation*, 119(9):2772-2786.

Cardin, S., Guasch, E., Luo, X., Naud, P., Quang, K. Le, Shi, Y. F., Tardif, J. C., Comtois, P., Nattel, S. (2012). Role for MicroRNA-21 in atrial profibrillatory fibrotic remodeling associated with experimental postinfarction heart failure. *Circulation. Arrhythmia and Electrophysiology*, 5(5):1027–1035.

Cooley, N., Cowley, M. J., Lin, R. C., Marasco, S., Wong, C., Kaye, D. M., Dart, A. M., Woodcock, E. A. (2012). Influence of atrial fibrillation on microRNA expression profiles in left and right atria from patients with valvular heart disease. *Physiological Genomics*, 44(3):211–219.

Doering CW, Jalil JE, Janicki JS, Pick R, Aghili S, Abrahams C, Weber KT. (1988). Collagen network remodelling and diastolic stiffness of the rat left ventricle with pressure overload hypertrophy.*Cardiovascular Reseach*, 22(10):686-695.

Duisters, R. F., Tijsen, A. J., Schroen, B., Leenders, J. J., Lentink, V., van der Made, I., Herias, V., van Leeuwen, R. E., Schellings, M. W., Barenbrug, P., Maessen, J. G., Heymans, S., Pinto, Y. M., Creemers, E. E. (2009). MiR-133 and miR-30 regulate connective tissue growth factor: implications for a role of microRNAs in myocardial matrix remodeling. *Circulation Research*, 104(2):170-178.

Ellinor, P. T., Lunetta, K. L., Glazer, N. L., Pfeufer, A., Alonso, A., Chung, M. K., Sinner, M. F., de Bakker, P. I., Mueller, M., Lubitz, S. A., Fox, E., Darbar, D., Smith, N. L., Smith, J. D., Schnabel, R. B., Soliman, E. Z., Rice, K. M., Van Wagoner, D. R., Beckmann, B. M, van Noord, C., Wang, K., Ehret, G. B., Rotter, J. I., Hazen, S. L., Steinbeck, G., Smith, A. V., Launer, L. J., Harris, T. B., Makino, S., Nelis, M., Milan, D. J, Perz, S., Esko, T., Köttgen, A., Moebus, S., Newton-Cheh, C., Li, M., Möhlenkamp, S., Wang, T. J., Kao, W. H., Vasan, R. S., Nöthen, M. M., MacRae, C. A., Stricker, B. H., Hofman, A., Uitterlinden, A. G., Levy, D., Boerwinkle, E., Metspalu, A., Topol, E. J., Chakravarti, A., Gudnason, V., Psaty, B. M., Roden, D. M., Meitinger, T., Wichmann, H. E., Witteman, J. C., Barnard, J., Arking, D. E., Benjamin, E. J., Heckbert, S. R., Kääb, S. (2010). Common variants in KCNN3 are associated with lone atrial fibrillation. *Nature Genetics*, 42(3):240–244.

Girmatsion, Z., Biliczki, P., Bonauer, A., Wimmer-Greinecker, G., Scherer, M., Moritz, A., Bukowska, A., Goette, A., Nattel, S., Hohnloser, S. H., Ehrlich, J. R. (2009). Changes in microRNA-1 expression and I_{k1} up-regulation in human atrial fibrillation. *Heart Rhythm*, 6(12):1802-1809.

Grammer, J. B**.,** Böhm J**,** Dufour, A**.,** Benz, M**.,** Lange, R**.,** Bauernschmitt, R. (2005). Atrial fibrosis in heart surgery patients decreased collagen III/I ratio in postoperative atrial fibrillation. *Basic Research in Cardiology*, 100(3):288-294.

Huang, Y., Li, J. (2015). MicroRNA208 family in cardiovscular diseases: therapeutic implication and potential biomarker. *Journal of Physiology and Biochemistry*, 71(3):479-486.

Li, H., Li, S., Yu, B., Liu, S. (2012). Expression of miR-133 and miR-30 in chronic atrial fibrillation in canines. *Molecular Medicine Reports*, 5(6):1457-1460.

Ling, T. Y., Wang, X. L., Chai, Q., Lau, T. W., Koestler, C. M., Park, S. J., Daly, R. C., Greason, K. L., Jen, J., Wu, L. Q., Shen, W. F., Shen, W. K., Cha, Y. M., Lee, H. C. (2013). Regulation of the SK3 channel by microRNA-499 - Potential role in atrial fibrillation. *Heart Rhythm*, 10(7):1001–1009.

Lu, Y., Zhang, Y., Wang, N., Pan, Z., Gao, X., Zhang, F., Zhang Y, Shan, H., Luo, X., Bai, Y., Sun, L., Song, W., Xu, C., Wang, Z., Yang, B. (2010). MicroRNA-328 Contributes to Adverse Electrical Remodeling in Atrial Fibrillation. *Circulation*, 122(23):2378–2387.

Matkovich, S. J., Hu, Y., Eschenbacher, W. H., Dorn, L. E., Dorn, G. W. (2012). Direct and indirect involvement of MicroRNA-499 in clinical and experimental cardiomyopathy. *Circulation Research*, 111(5):521–531.

Montgomery, R. L., Hullinger, T. G., Semus, H. M., Dickinson, B. A., Seto, A. G., Lynch, J. M., Stack, C., Latimer, P. A., Olson, E. N., Van Rooij, E. (2011). Therapeutic inhibition of miR-208a improves cardiac function and survival during heart failure. *Circulation*, 124(14):1537–1547.

Nattel, S. (2002). Atrial fibrillation 50 years on. *Nature*, 415(6868):219-226.

Nishi, H., Sakaguchi, T., Miyagawa, S., Yoshikawa, Y., Fukushima, S., Saito, S., Ueno, T., Kuratani, T., Sawa, Y. (2013). Impact of microRNA expression in human atrial tissue in patients with atrial fibrillation undergoing cardiac surgery. *PloS One*, 8(9):e73397.

Olesen, M. S., Jabbari, J., Holst, A. G., Nielsen, J. B., Steinbrüchel, D. A., Jespersen, T., Haunsø, S., Svendsen, J. H. (2011). Screening of KCNN3 in patients with early-onset lone atrial fibrillation. *Europace*, 13(7):963–967.

Shan, H., Zhang, Y., Lu, Y., Zhang, Y., Pan, Z., Cai, B., Wang, N., Li, X., Feng, T., Hong, Y., Yang, B. (2009). Downregulation of miR-133 and miR-

590 contributes to nicotine-induced atrial remodelling in canines. *Cardiovascular Research*, 83(3):465-472.

Shen, Y., Tian, F., Chen, Z., Li, R., Ge, Q., Lu, Z. (2015). Amplification-based method for microRNA detection. *Biosensors & Bioelectronics*, 71:322-331.

Shieh, J. T., Huang, Y., Gilmore, J., Srivastava, D. (2011). Elevated miR-499 levels blunt the cardiac stress response. *PLoS One*, 6(5):e19481.

Shyu, K. G., Lu, M. J., Wang, B. W., Sun, H. Y., Chang, H. (2006). Myostatin expression in ventricular myocardium in a rat model of volume-overload heart failure. E*uropean Journal of Clinical Investigation*, 36(10):713–719.

Shyu, K. G., Wang, B. W., Wu, G. J., Lin, C. M., Chang, H. (2013). Mechanical stretch via transforming growth factor-β1 activates microRNA208a to regulate endoglin expression in cultured rat cardiac myoblasts. *European Journal of Heart Failure*, 15(1):36–45.

Thum, T., Gross, C., Fiedler, J., Fischer, T., Kissler, S., Bussen, M., Galuppo, P., Just, S., Rottbauer, W., Frantz, S., Castoldi, M., Soutschek, J., Koteliansky, V., Rosenwald, A., Basson, M. A., Licht, J. D., Pena, J. T., Rouhanifard, S. H., Muckenthaler, M. U., Tuschl, T., Martin, G. R., Bauersachs, J., Engelhardt, S. (2008). MicroRNA-21 contributes to myocardial disease by stimulating MAP kinase signalling in fibroblasts. *Nature*, 456(7224):980–984.

Van Rooij, E., Sutherland, L. B., Qi, X., Richardson, J. A., Hill, J., Olson, E. N. (2007). Control of stress-dependent cardiac growth and gene expression by a microRNA. *Science*, 316(5824):575-579.

Van Rooij, E., Sutherland, L. B., Thatcher, J. E., DiMaio, J. M., Naseem, R. H., Marshall, W. S., Hill, J. A., Olson, E. N. (2008). Dysregulation of microRNAs after myocardial infarction reveals a role of miR-29 in cardiac fibrosis. *Proceedings of the National Academy of Sciences of the United States of America*, 105(35):13027-13032.

Wang, Z., Luo, X., Lu, Y., Yang, B. (2008). MiRNAs at the heart of the matter. *Journal of Molecular Medicine (Berlin, Germany)*, 86(7):771-783.

Wang, Z., Lu, Y., Yang, B. (2008). MicroRNAs and atrial fibrillation: new fundamentals. *Cardiovascular Research*, 89(4):710-21.

Weber, K. T., Brilla, C. G. (1992). Factors associated with reactive and reparative fibrosis of the myocardium. *Basic Research in Cardiology*, 87:291–301.

Zhang, Y., Dong, D., Yang, B. (2011). Atrial remodeling in atrial fibrillation and association between microRNA network and atrial fibrillation. *Science China. Life Science*, 54(12):1097-1102.

APPENDIX

Oligonucleotide name	Target sequence (5'-3')
hsa-miR-1	UGGAAUGUAAAGAAGUAUGUAU
hsa-miR-133a-3p	UUUGGUCCCCUUCAACCAGCUG
hsa-miR-133b	UUUGGUCCCCUUCAACCAGCUA
hsa-miR-21-5p	UAGCUUAUCAGACUGAUGUUGA
hsa-miR-29a-3p	UAGCACCAUCUGAAAUCGGUUA
hsa-miR-29b-3p	UAGCACCAUUUGAAAUCAGUGUU
hsa-miR-30c-5p	UGUAAACAUCCUACACUCUCAGC
hsa-miR-328-3p	CUGGCCCUCUCUGCCCUUCCGU
hsa-miR-590-5p	GAGCUUAUUCAUAAAAGUGCAG
hsa-miR-499a	UUAAGACUUGCAGUGAUGUUU
hsa-miR-208a-3p	AUAAGACGAGCAAAAAGCUUGU
hsa-miR-208b-3p	AUAAGACGAACAAAAGGUUUGU

List of oligonucleotide names and target sequences (miRCURY LNA^{TM} PCR primers set).

This part is included in the abstract *"Comparison of different methods to extract RNA from cardiac tissue for miRNA profiling by qRT-PCR"* by **L. Avogaro**, M. Grasso, E. D´ Amato, F. Tessarolo, S. Sinelli, M. Masè, A. Graffigna, M. A. Denti, F. Ravelli published on EUROPEAN BIOPHYSICS JOURNAL WITH BIOPHYSICS LETTERS; 42 (1)). Springer-Verlag, 2013, p. 191-191.

ABSTRACT

Despite the growing interest in cardiac miRNA expression profiling, having high quality and yield in RNA extraction from cardiac tissue is still challenging. Different methods of tissue homogenization and total RNA extraction from pig cardiac tissue aimed at miRNAs expression profiling were compared. Small biopsies of right atrial appendages were obtained from pig hearts and treated according to four different protocols: no homogenization (P1) and homogenization by manual (P2) or automatic (P3 and P4) methods, followed by Proteinase K digestion (PKD) except in P4. Total RNA was extracted using miRNeasy mini kit, assessing RNA yield and quality by Nanodrop. cDNA synthesis and qRT-PCR were performed using TaqMan MicroRNA Assay. Homogenization was crucial to obtain high yield of pure total RNA. Automatic methods displayed higher yield (0.27 μg RNA/mg tissue in P3) than manual (0.06 μg RNA/mg tissue in P2), with better performance without PKD step (0.38μg RNA/mg tissue in P4). RNA from P4 was suitable for miRNA expression profiling, as demonstrated by qRT-PCR on miR-21 and miR-29. These results suggest the efficacy of an automatic homogenization to extract RNA suitable for miRNA expression profiling.

METHODS

Tissue processing

Small biopsies of the right atrial appendage were obtained from a pig heart. Samples were immediately frozen on liquid nitrogen and subsequently treated according to different protocols (Figure 1).

Synthetic protocols' description:

Protocol n°1 (P1): samples without any grinding processing were incubated with Proteinase K for 20 minutes at 55°C;
Protocol n°2 (P2): samples were pulverized with a pre-chilled mortar and pestle and incubated with Proteinase K for 20 minutes at 55°C;
Protocol n°3 (P3): samples were homogenized at half speed with a rotor stator system (*Omni TH, Omni International*) in a tube containing 1 ml of QIAzol reagent (*Qiagen)* on ice. Samples were incubated with Proteinase K at RT for 10 minutes and subsequently centrifuged at 10,000x g for 3 minutes at RT. Finally 100% ethanol was added to clear the lysate;

Protocol n°4 (P4): samples were homogenized at half speed with a rotor stator system (*Omni TH, Omni International*) in a tube containing 1 ml of QIAzol reagent (*Qiagen*) on ice.

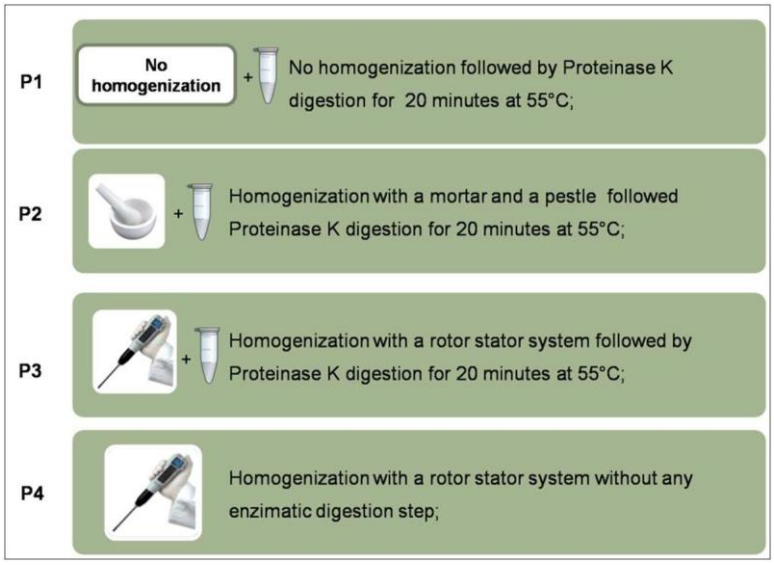

Figure 1: Summary of the protocols used for tissue RNA extraction.

Total RNA was extracted using *miRNeasy mini kit*, assessing RNA yield and quality by Nanodrop. cDNA synthesis and qRT-PCR were performed using *TaqMan MicroRNA Assay* (*Applied Biosystems, Life Technologies*).

RESULTS

	Tissue weight (mg)	Concentration (ng/µl)	$A_{260:280}$	$A_{260:230}$
Protocol 1	46,6	20,12	1,55	-0,05
Protocol 2	50,6	111,2	1,96	0,89
Protocol 3	45	404,8	2,11	1,24
Protocol 4	65	822,4	2,08	1,74

Table 1: Total RNA concentration, $A_{260:}A_{280}$ and $A_{260:230}$ ratios determined by the Nanodrop.

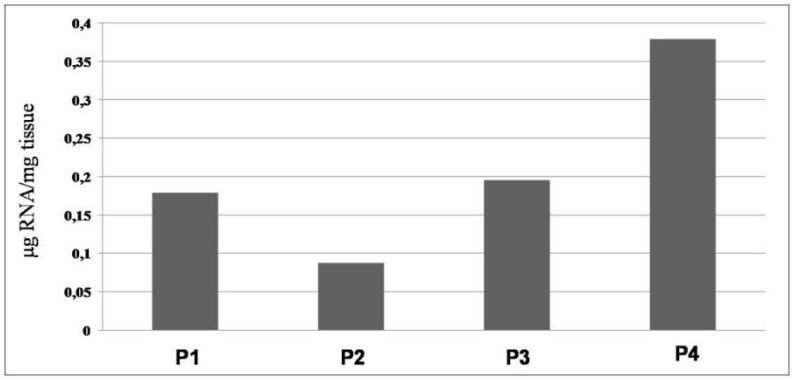

Figure 2: Total RNA yield for every protocol tested express as µg RNA/mg of tissue.

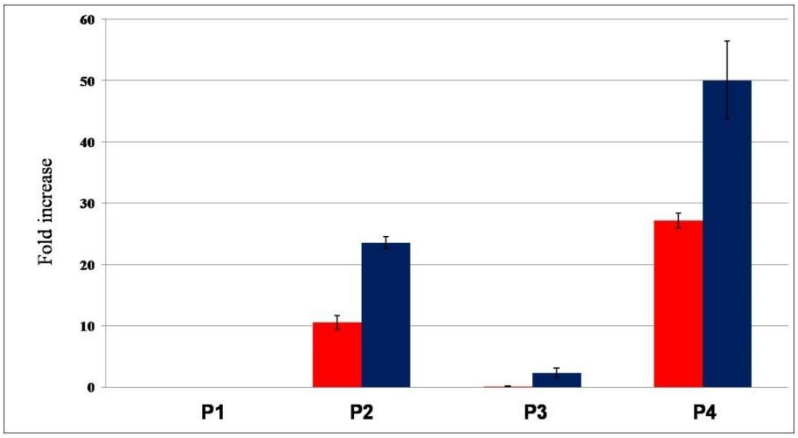

Figure 3: qRT-PCR on miR-21 and miR-29a on samples relative at each protocols tested.

CONCLUSION

Cardiac tissue homogenization with an automated method without any enzimatic digestion allows to obtain good yield and high quality RNA, which is suitable for miRNAs profiling. Preliminary results suggests the protocol suitable for applications in human heart tissue samples.

ACKNOWLEDGEMENTS

I would like to thank my tutor, Prof. Michela Denti and my advisor Dr. Flavia Ravelli, for the opportunity to take part in this challenging project, thus helping me to grow up both professionally and personally. A special thank goes to Michela Masè for her excellent support and helpful suggestions during these years, especially in the final part of my PhD project. My gratitude goes also to Elvira, Margherita and Alessandro for the technical support in the laboratory.

I would like to extend my thanks also to Prof. Thomas Thum and in particular to Dr. Claudia Bang, for providing the excellent support and help during my period in Hannover.

Finally, I would like to thanks all the people that support me during these hard 4 years. Special thanks to my parents, Ivana and Antonio, my sister Linda (as "Knutina"), my grandparents, Sofia and Zefferino, and my uncle Renzo for their unconditional love.

Thanks to all the "historical" and also to the new friends, I've encountered and supported me in these latest years. A special thank to the fantastic "Power girls", Vilma and Mary, for all the unforgettable moments spent together. Thanks to Luca, Filippo, Natascia, Cristiano, Nik, Silvia, Sabrina, for "adopt" me into the Biotech group. Thanks to Barbara, Lara, Marco and Tiziano, for…neaver leaving me alone.

Finally, I would like to express my deepest gratitude to my "Angel", Tony. Without his support, unconditional patience and understanding this thesis may have never been completed.

Sincerely,

Laura